Investigation of factors involved in late stages of homologous recombination

Vom Fachbereich Biologie der Technischen Universität Darmstadt

zur

Erlangung des akademischen Grades

eines Doctor rerum naturalium
(Dr. rer. nat.)

genehmigte Dissertation von

M. Sc. Anja Waizenegger
aus Tuttlingen

1. Referent: Prof. Dr. Paul Layer
2. Referentin: Prof. Dr. Cristina Cardoso
Tag der Einreichung: 01.06.2016
Tag der mündlichen Prüfung: 04.08.2016

Darmstadt 2016
D17

Ehrenwörtliche Erklärung

Ich erkläre hiermit ehrenwörtlich, dass ich die vorliegende Arbeit entsprechend den Regeln guter wissenschaftlicher Praxis selbstständig und ohne unzulässige Hilfe Dritter angefertigt habe. Sämtliche aus fremden Quellen direkt oder indirekt übernommenen Gedanken sowie sämtliche von Anderen direkt oder indirekt übernommenen Daten, Techniken und Materialien sind als solche kenntlich gemacht. Die Arbeit wurde bisher bei keiner anderen Hochschule zu Prüfungszwecken eingereicht.

Darmstadt, den 9. September 2016

Index

1 List of abbreviations

ADD	ATRX-DNMT3-DNMT3L
ALT	alterantive lengthening of telomeres
ATP	adenosine triphosphate
ATRX	Alpha-thalassemia mental retardation X-linked
BER	base excision repair
BIR	break induced replication
BLM	Bloom syndrome protein
Bp	base pair
BRCA2	breast cancer 2
BrdU	5-Bromo-2'-desoxy-uridine
BSA	bovine serum albumine
CDKs	cycline-dependent kinases
Chk1	checkpoint kinase 1
Chk2	checkpoint kinase 2
co-IP	co-immunoprecipitation
CtIP	CtBP-interacting protein
DAXX	death-associated protein 6
DDR	DNA damage response
DHJ	double Holliday junction
D-loop	displacement loop
DMEM	Dulbecco's minimal essential medium
DNA	desoxyribonucleic acid
Dna2	DNA replication ATP-dependent helicase/nuclease DNA2
DSB	double-strand break
dsDNA	double-stranded DNA
EdU	5-Ethylene-2'-desoxy-uridine

Exo1	Exonuclease1
EZH2	enhancer of zeste homolog 2
FCS	fetal calf serum
G4	guanine quadruplex
Gy	gray
HelQ	PolQ-like helicase
HD	helical domain
HR	homologous recombination
HP1α	heterochromatin protein 1α
ICL	interstrand crosslink
IR	ionizing radiation
IRIF	irradiation induced foci
kDa	kilodalton
KO	knockout
MeCP2	methyl CpG binding protein 2
MMC	mitomycin C
MMS	methyl methanesulfonate
Mre11	meiotic recombination 11
MRN	Mre11/Rad50/Nbs1 complex
NEAA	non-essential amino acids
Nek	NIMA-related protein kinase
NER	nucleotide excision repair
NHEJ	non-homologous end-joining
NIMA	never in mitosis A-related kinase
NLS	nuclear localization signal
NuMa	nuclear mitotic apparatus
PAGE	polyacrylamide gelelectrophoresis

PARP	poly(ADP-ribose) polymerase
PBS	phosphate buffered saline
PCNA	proliferating cell nuclear antigen
PHD	plant homeodomain
PIP	PCNA interacting protein
PML-NBs	promyelocytic nuclear bodies
Pol	polymerase
Rad	radiation repair protein
RFC	replication factor C
RNA	ribonucleic acid
ROS	reactive oxygen species
RPA	replication factor A
RT	room temperature
S572	serine 572
SDS	sodium dodecyl sulfate
SDSA	synthesis-dependent strand annealing
SNF	sucrose non-fermenting
SSB	single strand break
ssDNA	single-stranded DNA
SWI	switch
TopoIIIα	topoisomerase IIIα
UV	ultraviolet
XRCC1	X-ray repair cross-complementing protein 1
WB	Western Blot
WT	wildtype

2 Summary/ Zusammenfassung

2.1 Summary

Homologous recombination (HR) is an important mechanism to maintain genomic stability, as it is involved in the repair of double-strand breaks (DSBs) and the stabilization of replication forks. To initiate HR, the DNA ends at the break site are resected, generating single-stranded DNA (ssDNA) which is then covered by Rad51 molecules and represents the nucleoprotein filament. During a process called synapsis, this nucleoprotein filament performs homology search and strand invasion within the undamaged sister chromatid. To allow recombination-associated DNA synthesis, using the homologous DNA sequence as a template for repair, Rad51 molecules need to be removed from the DNA. This removal is promoted by the motor protein Rad54, which actively translocates along the heteroduplex DNA and permits subsequent binding of the polymerase to finalize HR.

The enzymatic steps and proteins involved in early HR are well established, but later steps of recombination are yet less defined. In this study two new factors, Nek1 and ATRX, were identified which are involved in these late steps of HR, thereby contributing to a better understanding of this important repair pathway.

In the publication "*Nek1 Regulates Rad54 to Orchestrate Homologous Recombination and Replication Fork Stability*", the never in mitosis A related kinase 1 (Nek1) was shown to regulate the function of Rad54 by phosphorylation at serine 572. This phosphorylation allows removal of Rad51 in late G2 phase, which is necessary to proceed with subsequent HR steps. In S phase however, Rad54 is not phosphorylated and thereby not enabled to remove Rad51 from replication forks, as Rad51 functions in the protection of stalled replication forks from nucleolytic degradation. Nek1 depletion or expression of an unphosphorylatable form of Rad54 (Rad54-S572A) resulted in a G2-specific HR repair defect due to persisting Rad51 molecules on the DNA. In contrast, expression of a phosphomimic form of Rad54 (Rad54-S572E) did not impair HR in G2, but promoted undesired removal of Rad51 from stalled replication forks in S phase. Therefore, Nek1 is a crucial factor for the regulation of Rad54 during the cell cycle, contributing to replication fork stability in S phase and HR functionality in G2 phase.

Another novel HR factor was identified in the manuscript "*Involvement of ATRX in Homologous Recombination Repair".* Alpha-thalassemia mental retardation X-linked protein (ATRX) was shown here to function during post-synaptic steps of HR. Depletion of ATRX resulted in reduced HR-frequencies in reporter assays, increased numbers of unrepaired DSBs in G2 at late times after irradiation (IR), and the absence of IR-induced sister chromatin exchanges (SCEs). The formation of Rad51 foci as a readout for ongoing HR repair was not affected in ATRX depleted cells compared to control cells and also the removal at late times was almost normal. This indicated an involvement of

ATRX downstream of Rad54-dependent Rad51 removal. Furthermore we could show that ATRX interacts with the DNA clamp protein PCNA (proliferating cell nuclear antigen), which is known to be involved in the subsequent step of DNA-synthesis. Strikingly, we identified a PIP box within the ATRX amino acid sequence, which potentially mediates the interaction with PCNA. Therefore, we discovered a function for ATRX besides its established role during replication in S phase and could establish, that ATRX functions in G2-phase during HR, where it interacts with PCNA.

2.2 Zusammenfassung

Die Homologe Rekombination (HR) ist ein wichtiger Prozess für den Erhalt der genomischen Integrität, da dieser sowohl für die Reparatur von Doppelstrangbrüchen (DSBs) als auch die Stabilisierung von arretierten Replikationsgabeln essentiell ist. Zu Beginn der HR werden die DSB Enden resektiert, wobei einzelsträngige DNA (ssDNA) entsteht, die anschließend von Rad51 gebunden wird und das sogenannte Nukleoproteinfilament bildet. Dieses Filament ist essentiell für den Vorgang der Homologiesuche im Schwesterchromatid, was letztendlich zur Stranginvasion führt. Um nachfolgend die DNA-Reparatursynthese einzuleiten, wobei die homologe, unbeschädigte Sequenz als Vorlage für die Reparatur verwendet wird, muss Rad51 zunächst von der DNA entfernt werden. Diese Aufgabe erfüllt das Motorprotein Rad54, indem es aktiv auf der DNA transloziert und Rad51 Moleküle ablöst. Dadurch kann im nächsten Schritt die Rekrutierung der DNA-Polymerase und somit die DNA-Synthese eingeleitet werden.

Während die frühen Schritte der HR und die dabei involvierten Proteine bereits gut erforscht sind, sind die späten Schritte bislang weniger gut verstanden. Im Rahmen dieser Dissertation wurden zwei neue Faktoren identifiziert, die bei den späten Schritten der HR jeweils eine wichtige Rolle spielen und somit zu einem besseren Verständnis dieses Reparaturweges beitragen.

In der Veröffentlichung "*Nek1 Regulates Rad54 to Orchestrate Homologous Recombination and Replication Fork Stability*" konnte gezeigt werden, dass die Kinase Nek1 (*Never-in-mitosis A related protein kinase 1*) die Funktion von Rad54 reguliert, indem diese Rad54 am Serin 572 phosphoryliert. Diese Phosphorylierung ermöglicht das Entfernen von Rad51 in der späten G2-Phase, was notwendig ist, um die nachfolgenden Schritte der HR einzuleiten. Während der S-Phase hingegen liegt Rad54 stets unphosphoryliert vor, was ein Entfernen von Rad51 von den Replikationsgabeln verhindert und somit gewährleistet dass Rad51 arretierte Replikationsgabeln vor Degradierung durch Nukleasen schützt. Die Depletion von Nek1 sowie die Expression der nicht-phosphorylierbaren Form von Rad54 (Rad54-S572A) resultierten in einem G2-Phase spezifischen HR-Reparaturdefekt, da Rad51-Moleküle unter diesen Umständen an der DNA persistieren. Die Expression einer dauer-phosphorylierten Form von Rad54 (Rad54-S572E) hingegen führte zu keiner Beeinträchtigung der HR in der G2-Phase,

allerdings konnte in diesen Zellen ein unerwünschtes Entfernen von Rad51 an arretierten Replikationsgabeln und eine damit verbundene Degradierung während der S-Phase festgestellt werden. Nek1 ist somit ein wichtiger Faktor um die Aktivität von Rad54 zu regulieren, wodurch zum einen bei Replikationsstress die Replikationsgabeln in der S-Phase geschützt werden und zum anderen die HR-Reparatur während der G2-Phase effizient ablaufen kann.

Ein weiterer neuer HR-Faktor wurde im Manuskript "*Involvement of ATRX in Homologous Recombination Repair"* identifiziert. Es konnte hierbei gezeigt werden, dass ATRX (*Alpha-Thalassemia mental Retardation X-linked)* in post-synaptische Schritte der HR involviert ist. Die Depletion von ATRX führte zu einer verringerten HR-Frequenz in Reporter-Assays, einer erhöhten Anzahl unreparierter DSBs in G2 zu späten Zeiten nach Bestrahlung (IR) und dem Ausbleiben IR-induzierter Schwesterchromatid-Austausche (SCEs). In diesen Zellen war die Ausbildung von Rad51-Foci vergleichbar mit Kontrollzellen und auch das Entfernen von Rad51-Molekülen von der DNA mit voranschreitender HR war kaum beeinträchtigt. Dies deutete darauf hin, dass ATRX erst nach der Entfernung von Rad51 durch Rad54 in die HR involviert ist. Es konnte weiterhin gezeigt werden, dass ATRX mit PCNA (*proliferating cell nuclear antigen*) interagiert, welches bekanntermaßen am nachfolgenden Schritt der DNA-Synthese beteiligt ist. Desweiteren konnte eine *PIP box* innerhalb der Proteinstruktur von ATRX nachgewiesen werden, welche möglicherweise die Interaktion mit PCNA vermittelt. Zusammengefasst wurde eine neue Funktion von ATRX entdeckt, welche unabhängig von bereits beschriebenen Aufgaben während der Replikation in der S-Phase ist. ATRX ist in die HR-Reparatur von DSBs in der G2-Phase involviert und interagiert hierbei mit PCNA.

3 Introduction

3.1 Maintenance of Genome Stability

Maintaining genome integrity is essential, as the main objective of each organism is to deliver intact genetic material to the next generation. Throughout a lifetime, endogenous and exogenous factors constantly assault the DNA and therefore eukaryotic cells have evolved mechanisms to sense DNA damage and initiate cellular responses (Jackson and Bartek, 2009). This so called DNA damage response (DDR) includes cell cycle control, programmed cell death and DNA repair, operating collectively depending on the extent and type of damage (Sancar et al., 2004). Inducing cell cycle checkpoints allows more time to repair damaged DNA, however, if extensive damage occurs, apoptotic cell death can be initiated as a last resort to prevent genomic instability (de la Torre-Ruiz and Lowndes, 2000; Polo and Jackson, 2011). Sources of endogenous damage are for example reactive oxygen species (ROS), a metabolic by-product of respiration, or replication errors like DNA mismatches. Chemicals, UV or ionizing radiation (IR) are the main sources of exogenous damage, leading to a variety of modifications within the DNA. Different pathways exist to overcome base alterations like alkylation or oxidation and also to repair DNA single- or double-strand breaks (SSB, DSB) (Ciccia and Elledge, 2010; Jeggo and Lobrich, 2007). Imbalanced DDR or mutations in DDR genes endangers cellular homeostasis and can cause disease progression, senescence or even tumorigenesis. However, proteins of the DDR machinery also represent a target for tumor therapy, as genomic instability is a hallmark of cancer and tumor cells strongly depend on DNA damage repair (Lord and Ashworth, 2012; O'Connor, 2016). As a consequence, the inhibition of certain repair pathways in tumor cells can increase the efficacy of radio-/chemotherapy and result in cell death. This inhibitory approach is already applied in a subset of tumors, e.g. PARP-1 (poly(ADP-ribose) polymerase 1) inhibition in BRCA-1/2 deficient breast cancer cells results in the accumulation of DNA damage, as homologous recombination (HR) and base excision repair (BER) pathways are non-functional (Kelley et al., 2014).

3.2 DNA Double-strand Breaks

DSBs symbolize the most harmful type of DNA lesion, as one DNA strand can separate and information might get lost during chromosome segregation. Furthermore, DSBs represent obstacles for transcription, replication and chromosome segregation. Misrepair of DSBs can cause mutations, leading to genome rearrangements and potentially drive carcinogenesis. Two main pathways exist for the repair of DSBs, the error-prone non-homologous end-joining (NHEJ) and the error-free homologous recombination (HR) (Branzei and Foiani, 2008; van Gent et al., 2001). NHEJ can

function independently of the cell cycle phase, and DSB ends are directly ligated, contributing to its fast repair kinetic. HR on the other hand, requires a sister chromatid as a template for repair and can therefore only occur during S or G2 phase. As this pathway is much more complex than NHEJ, its repair kinetic is relatively slow. Although HR is considered to be an error-free pathway, the majority of radiation-induced DSBs is repaired via NHEJ and only 20% of the DSBs are repaired via HR in G2 phase (Beucher et al., 2009; Riballo et al., 2004). Furthermore, the 20% of DSBs which are repaired by HR were shown to localize especially to heterochromatin (Goodarzi et al., 2008).

3.3 Homologous Recombination

Homologous recombination is a highly conserved biological process which is found in eukaryotes, prokaryotes and even viruses (Krejci et al., 2012). Some bacteria and viruses use HR for horizontal gene transfer to exchange genetic material (Lawrence and Retchless, 2009). HR is not only restricted to the repair of two-ended DSBs or interstrand crosslinks (ICL) in mitotic dividing cells, but plays important roles during meiosis, replication and telomere maintenance (Heyer et al., 2010). During meiosis, recombination allows the exchange of DNA within homologous chromosomes which leads to genetic variation, and crossover products are formed, a similar process to HR during DSB repair when recombination occurs between sister chromatids (Moynahan and Jasin, 2010). During replication, HR proteins stabilize the replication fork and HR processes are crucial for the recovery of stalled or broken replication forks, allowing faithful duplication of the genome. Furthermore HR is involved in the maintenance of telomere length in a recombination-based process called alternative lengthening of telomeres (ALT), which is found in a subset of cancer cells (Lydeard et al., 2010).

HR can be divided into three main sub-pathways, which process DSBs in a different manner, depending on the type of DSB. The Double Holliday junction (DHJ) model and synthesis-dependent strand annealing (SDSA) are responsible for the repair of two-ended DSBs, break-induced replication (BIR) coordinates the repair of one-ended DSBs (San Filippo et al., 2008; Sung and Klein, 2006). These so called one-ended DSBs can occur when a replication fork collapses or runs into a single-strand break during replication (Ensminger et al., 2014). BIR includes the formation of a D-loop and eventually results in a functional replication fork, allowing replication to be re-initiated at the end of this repair process (Symington and Gautier, 2011). DHJ and SDSA are similar in the first few steps, however they diverge after DNA synthesis has occurred (Figure 1). SDSA is the predominant pathway in mitotic cells, the DHJ pathway on the other hand is mainly used during meiosis (Andersen and Sekelsky, 2010; Chapman et al., 2012; Heyer et al., 2010).

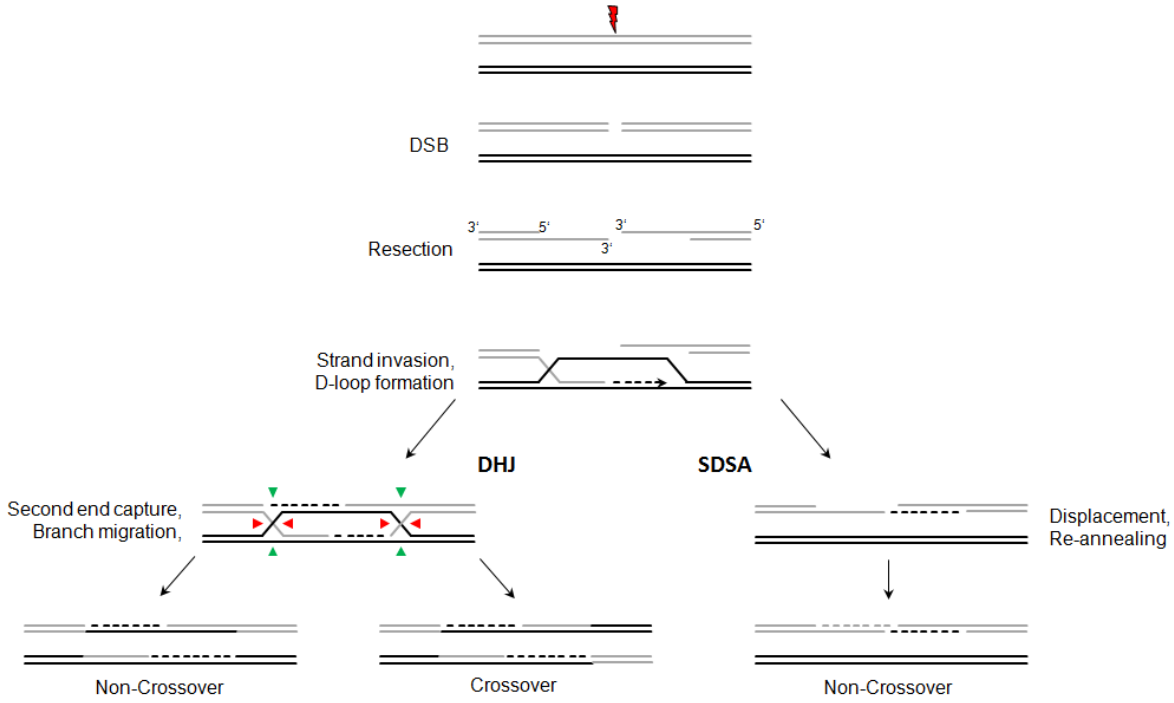

Figure 1: Sub-pathways of homologous recombination. If a DSB occurs, DSB end-resection generates 3'-overhangs for homology search within the sister chromatid. Subsequently strand invasion and D-loop formation proceeds and the two sub-pathways of DHJ and SDSA diverge after the DNA synthesis step. During DHJ the double Holliday junctions are processed by dissolution or resolution and Crossover or Non-crossover products arise. Green and red arrows indicate cutting points for resolution of DHJ. If cutting occurs horizontally at red arrows, non-crossover products are formed, if cutting occurs at one red pair of arrows and one green pair of arrows, crossover products are formed. During SDSA, the invading ssDNA is displaced from the D-loop after DNA synthesis and re-anneals with the opposite end of the original DSB. DNA synthesis occurs again to fill the gaps, resulting in non-crossover products.

When a DSB is induced, the MRN complex (Mre11, Rad50, Nbs1) directly binds to the DNA on both break ends (Figure 2). Then resection of the 5'-end is initiated to generate a suitable substrate for subsequent homology search. First, MRN and CtIP cut up to 300 bp away from the break site and resect in 3'→5' direction, additionally Exo1 or a complex of Dna2 and BLM proceed with long-range resection a few thousand bp in 5'→3' direction (Bolderson et al., 2010; Sartori et al., 2007). The generated 3'-overhangs are loaded with RPA to protect the ssDNA from degradation. Next, BRCA2 and other proteins are recruited and mediate the replacement of RPA with Rad51 (Ting and Lee, 2004; Yang et al., 2002). This so called nucleoprotein filament, consisting of Rad51 bound to ssDNA, can then perform homology search and invade the sister chromatid, representing an essential and probably the most complex step of HR (Figure 3) (Baumann et al., 2014).

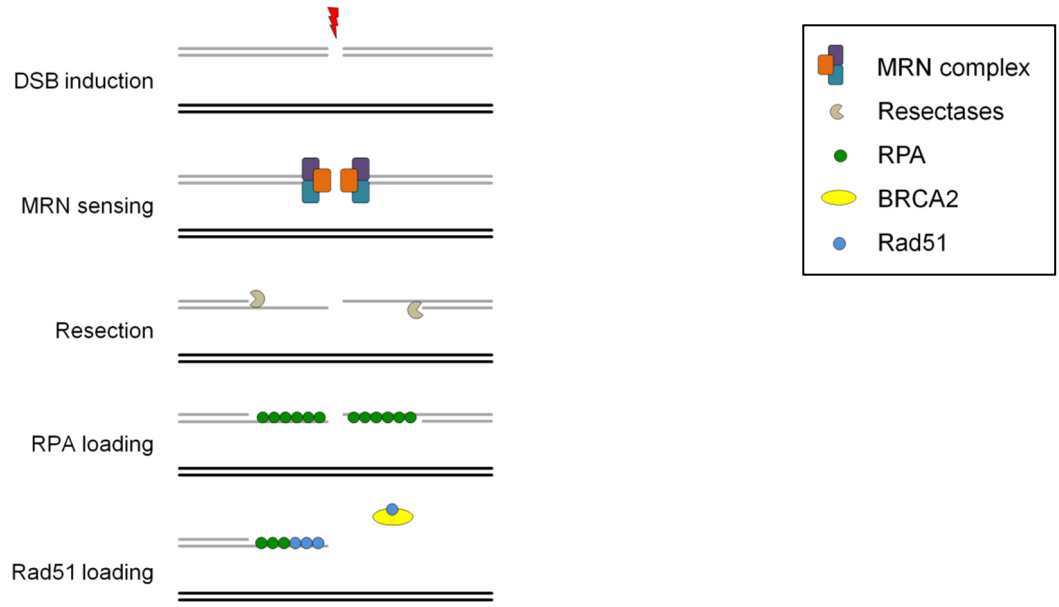

Figure 2: Enzymatic steps and proteins involved in early stages of homologous recombination. After DSB induction, the MRN complex binds to the break ends and subsequent resection occurs. The resulting 3'-ssDNA overhangs are first protected by RPA, then BRCA2 replaces RPA with Rad51 to allow homology search.

As soon as probing for homologous sequences was successful, a D-loop is formed and maintained, which likely facilitates the accessibility to the DNA and the recruitment of additional HR factors. To allow recombination-associated DNA synthesis to copy the genetic information from the sister chromatid, Rad51 has to be removed from the dsDNA, which is mediated by Rad54 and HelQ (Adelman et al., 2013; Terasawa et al., 2007). In yeast, it was shown that the following steps involve either loading of PCNA by the replication factor C (RFC) and subsequent recruitment of polymerase δ (Pol δ), or alternatively DNA synthesis can occur in a PCNA-independent manner involving the translesion polymerase η (Pol η) (Li et al., 2009; Wang et al., 2004). The second 3'-overhang, which was not involved in strand invasion, forms another Holliday junction with the displaced strand, a process called second end capture. To finalize HR, these double Holliday junctions are converted into recombination products by dissolution or resolution (Liu and West, 2004). The process of dissolution involves BLM and TopoIIIα, which promote branch migration and decatenation of the DHJ, leading to non-crossover products (Figure 1). During resolution, the nucleases Mus81-Eme1 and Gen1 can cut the DHJ in different ways, resulting in crossover or non-crossover products (Matos and West, 2014; Wu and Hickson, 2003).

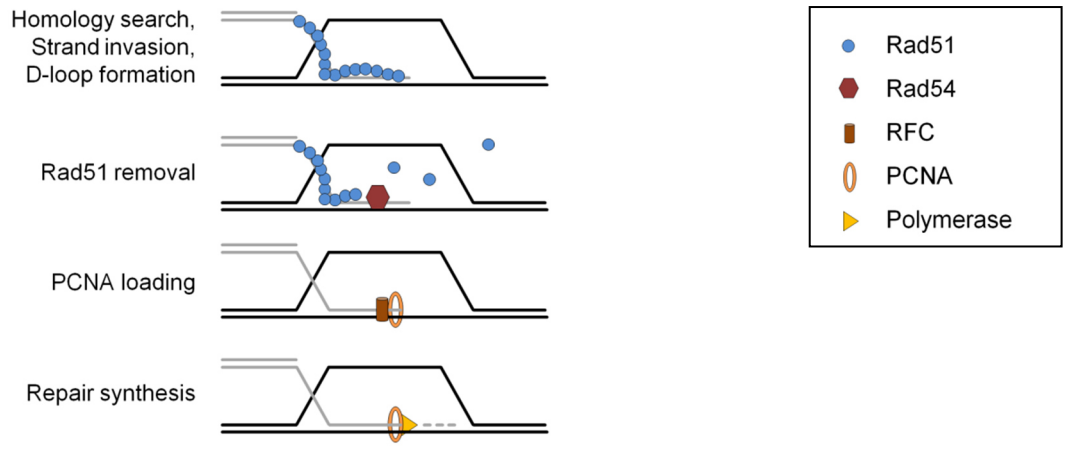

Figure 3: Enzymatic steps and proteins involved in late stages of homologous recombination. The Rad51 nucleoprotein filament performs homology search within the sister chromatid, followed by strand invasion and D-loop formation. Rad51 is removed by Rad54 to allow DNA repair synthesis and thereby copy the missing DNA sequence for genomic integrity.

In SDSA, the newly synthesized DNA strand is displaced from the D-loop and re-anneals to the 3'-overhang of the opposite DBS end. DNA synthesis is subsequently initiated to fill the gaps and after ligation this process is finalized without the occurrence of crossover products (Figure 1).

3.4 Nek1

Nek1 belongs to the Nek kinase family, represented by 11 members in mammals. The kinase domain within all family members is highly conserved and separates them from the two other big families of mitotic kinases, Polo and Aurora. Nek family members mainly localize to cilia or centrosomes, being involved in their organization and regulation (Feige et al., 2006; Hildebrandt and Otto, 2005; Moniz et al., 2011). The Nek1 protein structure exhibits an N-terminal kinase domain which allows phosphorylation of target proteins (Figure 4). Additionally a nuclear localization signal (NLS) is present, which mediates translocation into the nucleus after DNA damage induction, where Nek1 then forms IR-induced foci (Polci et al., 2004). It was shown, that Nek1 protein expression is up-regulated upon IR and also its kinase function is then activated (Polci et al., 2004). How this activation occurs remains elusive, however an auto-phosphorylation is very likely due to a high number of serin/threonin residues within the protein sequence (Hilton et al., 2009; Surpili et al., 2003).

Figure 4: Structure of the human Nek1 protein. The human Nek1 gene encodes a protein of 1258 aa with an N-terminal kinase domain allowing protein phosphorylation.

In humans, Nek1-deficiency is embryonically lethal due to a syndrome called Short-Rib Polydactyly Type Majewski. This syndrome is characterized by skeletal abnormalities, kidney failure, facial and genital dysmorphism. In mice, Nek1 deficiency is not lethal, but leads to a sever phenotype with polycystic kidney disease, dwarfism, reduced lifespan and sterility in males. Both phenotypes are caused by cilia dysfunction, as Nek1 is normally responsible for cilia formation and stability (Thiel et al., 2011; Upadhya et al., 2000; White and Quarmby, 2008; Yoder, 2007). These severe consequences of cilia dysfunction are due to the fact, that cilia are very important organelles in higher eukaryotes, functioning during development, cell division and DNA damage response and besides Nek1 several other DNA repair proteins are localized to centrosomes or cilia.

Besides its described role in cilia maintenance, Nek1 was reported to be directly involved in several DDR pathways like cell cycle control, cell death and DNA repair. Initially, it was discovered that cells with Nek1-defiency fail to efficiently activate the G1/S or G2/M checkpoint, as the checkpoint kinases Chk1 and Chk2 cannot be phosphorylated and are thereby not active (Chen et al., 2008; Pelegrini et al., 2010). Later, the Nek1 kinase was found to be responsible for phosphorylation of ATR, which in turn phosphorylates Chk1, leading to a cell cycle arrest (Liu et al., 2013). Nek1 was furthermore shown to be an anti-apoptotic factor, as Nek1-dependent phosphorylation of a voltage-dependent anion channel in the membrane of mitochondria prevents cytochrome C efflux into the cytoplasm. If this efflux occurs, caspases are subsequently activated which then induce apoptosis (Chen et al., 2009, 2014; Polci et al., 2004). With regards to DNA repair, cells with Nek1 deficiency display an increased level of γH2AX foci 24 h after IR and it was additionally reported, using different cellular assays, that the repair of DSBs in such cells is impaired (Chen et al., 2008; Pelegrini et al., 2010). This effect was also observed in *S. cerevisiae*, where a knockout of the Nek1 homolog Kin3 results in an increased sensitivity towards MMS, UV or cisplatin (Moura et al., 2010). However, it was not yet uncovered in which DSB repair pathway Nek1 is involved.

3.5 Rad54

Rad54 is a member of the SWI2/SNF2 (switch/sucrose non-fermenting) family of chromatin remodelers and can translocate along dsDNA in an ATP-dependent manner. Structurally, Rad54 exhibits 7 highly conserved SNF2-specific motifs, which form the motor domain of the protein and allow ATP hydrolysis (Figure 5) (Heyer et al., 2006). These ATPase domains lie within two RecA-like lobes, which also contain SNF2-specific helical domains (HD1, HD2). The bi-lobal domain structure of Rad54 is typical for the SF2 superfamily of helicases, to which SNF2-remodelers belong. ATPase activity is also needed for remodeling of specific protein-DNA complexes, however Rad54 and all other SWI2/SNF2 proteins do not display helicase activity *in vitro* (Mazin et al., 2003; Thomä et al., 2005). The N-terminal domain of Rad54 contains the interacting region for its partner protein Rad51, the C-terminal domain includes a zinc-coordinating motif, which might stabilize the overall protein structure (Clever et al., 1997).

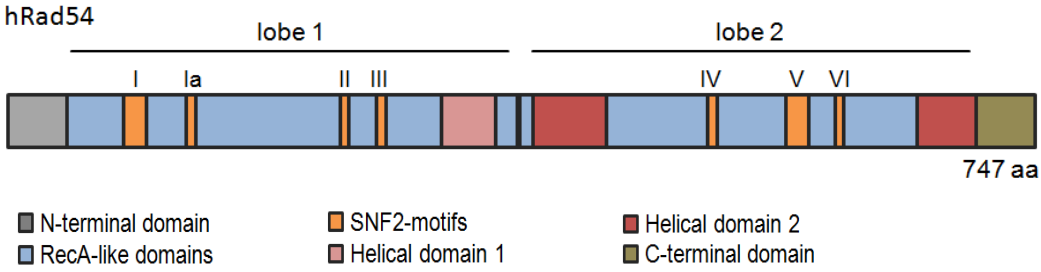

Figure 5: Structure of the human Rad54 protein. The human Rad54 gene encodes a protein of 747 aa with two RecA-like lobes, including highly conserved SNF2-specific motifs and helical domains.

Rad54 was classified as a member of the Rad52 epistasis group in *S. cerevisiae*, which encodes core proteins for the HR machinery in eukaryotes. Together with Rad51 and Rad52, Rad54 displays the most IR-sensitive single mutant in *S. cerevisiae*, all three mutants also show increased sensitivity towards alkylating agents (MMS), crosslinking agents (MMC) or other DSB-inducing agents (Heyer et al., 2006). Rad54 and its homologs have been identified in all eukaryotes and the human and yeast version of Rad54 share 66% similarity, however there are no known Rad54 homologs in bacteria (Ceballos and Heyer, 2011; Thomä et al., 2005). Yeast Rad54 mutants grow normal without DNA damage, but suffer severely from DSB induction. The phenotypes of Rad54 and Rad51 mutants in yeast are very similar in mitotic cells with regards to damage sensitivity and recombination ability, however the effects on meiotic cells are very different. Rad51 mutants are not able to form viable meiotic products, whereas Rad54 mutants produce up to 60% viable spores. This might be due to the fact that in yeast a Rad54 paralog (Rdh54) exists, which has redundant roles to Rad54 during meiosis.

A double depletion of Rad54 and Rdh54 showed a comparable phenotype to Rad51 mutants (Pâques and Haber, 1999; Shinohara et al., 1997; Symington, 2002). In mice, the situation is different than in yeast, as a Rad51 knockout is embryonically lethal and cells even fail to proliferate in cell culture. Rad54 knockout mice are viable, but mouse embryonic stem cells show increased sensitivity towards IR or MMS. However, Rad54 seems to be most important during early development, as adult Rad54$^{-/-}$ mice are no more IR-sensitive than wildtype mice (Essers et al., 2000, 2002; Tsuzuki et al., 1996). This is explicable, as NHEJ is the predominant repair pathway for DSBs in mammals and can therefore compensate for the IR sensitivity.

As a core factor of HR, Rad54 was implicated at multiple stages (pre-synapsis, synapsis, post-synapsis) during HR in eukaryotes, with the main focus on the physical interaction with Rad51. The following ATP-dependent and independent functions have been described:

First of all, in mouse and yeast Rad54 participation was shown during the replacement of RPA with Rad51 molecules, where Rad54 can stabilize the Rad51 nucleoprotein filament in an ATP-independent manner (Agarwal et al., 2011; Mazin et al., 2010). *In vivo* mouse studies even revealed that Rad54 is essential for the formation of Rad51 foci after IR and subsequent stabilization of the nucleoprotein filament (Agarwal et al., 2011; Tan et al., 1999). Notably, this function for Rad54 is not observed in human cells (Heyer et al., 2006).

During synapsis, when the Rad51 nucleoprotein filament performs homology search, Rad54 was shown to stimulate the D-loop formation in *S. cerevisiae*. This stimulation is ATP-dependent and also requires physical interaction with Rad51. Rad54 actively translocates along dsDNA, performing nucleosome remodeling, which then facilitates D-loop formation. *In vitro* studies with purified yeast Rad54 even showed that Rad51 requires Rad54 for efficient D-loop formation, and thereby influences the process of homology search (Sigurdsson et al., 2002; Solinger et al., 2002).

As soon as homologous sequences as a template for repair have been found, Rad51 needs to be removed from the heteroduplex DNA to proceed with the subsequent steps of HR. This ATP-consuming process displays a common function of Rad54 during HR in yeast, mice and humans. The interaction with Rad51 during this process stimulates the ATPase activity of Rad54 up to 6-fold (Li et al., 2007; Renkawitz et al., 2014). It was shown *in vitro,* that a yeast Rad54 multimer binds to the 3'-end of the invading DNA strand and actively translocates with up to 300 bp/sec away from the end, producing a Rad51-free substrate for the recruitment of DNA polymerases. The removal of Rad51 is the main ATP-dependent function of Rad54 and it was also shown *in vivo*, that Rad54 deficient cells display increased Rad51 foci levels, indicating a defect in Rad51 removal (Amitani et al., 2006; Kirshner et al., 2009; Li et al., 2009; Terasawa et al., 2007).

To initiate recombination-associated DNA synthesis as the next step of HR, PCNA is recruited and loaded onto the DNA by RFC (Sebesta et al., 2013; Sneeden et al., 2013). An interaction between Rad54 and PCNA was shown in *S. cerevisiae* indicating a post-synaptic function for Rad54 however, the exact physiological relevance of this interaction remains unclear (Burgess et al., 2013).

Furthermore, in yeast and humans Rad54 was found to possess a high affinitiy for Holliday junctions *in vitro*, where it is thought to promote the ATP-dependent process of branch migration along the DNA axis (Bugreev et al., 2006). Within the last step of HR, where the Holliday junctions are resolved, an interaction of Rad54 and Mus81 was observed. Rad54 stimulates the endonuclease activity of Mus81-Eme1, creating crossover or non-crossover recombination products (Matulova et al., 2009; Mazina and Mazin, 2008).

Besides its diverse roles during the repair of DSBs, Rad54 and its main partner protein Rad51 have also been implicated in maintaining replication fork stability. After replication stress, Rad51 binds to and promotes the formation of so called chicken foot structures, a type of Holliday junctions, which represent an intermediate state before the replication fork can be restored (Bugreev et al., 2006; Zellweger et al., 2015). Furthermore, Rad51 protects these structures from degradation by specific endonucleases like Mre11. Rad54 has no direct protective function at chicken foot structures, but might mediate fork regression and restoration by its branch migration activity (Henry-Mowatt et al., 2003; Schlacher et al., 2011). In summary, Rad54 has multiple reported functions during different steps of HR, which vary in their extent between yeast, mice and humans. However, the most physiological relevant function of Rad54 in humans is to remove Rad51 from the heteroduplex DNA after strand invasion.

3.6 ATRX

ATRX is like Rad54 a member of the SWI2/SNF2 family of chromatin remodeling proteins. The SNF2 protein was originally identified in yeast, as a gene involved in the regulation of mating type switching (Swi) and sucrose fermentation (Sucrose non-fermenting). It was then found to be the catalytical subunit of the SWI/SNF complex, which can modify chromatin structure. All SNF2-like proteins exhibit highly conserved ATPase/helicase motifs, however with no helicase activity (Dürr et al., 2006; Flaus et al., 2006). The ATRX gene encodes two major isoforms, a full-length protein of 280 kDa and a truncated version of 180 kDa, both are exclusively found within the nucleus. In addition to the SNF2-specific ATPase motifs, it contains a plant homeodomain (PHD)-like zinc finger region, which is most closely related to that of the DNMT3 family of DNA methyltransferases and therefore named ADD (ATRX-DNMT3-DNMT3L) domain (Figure 6). Between the N-terminal ADD domain and the C-terminal ATPase domain specific interacting regions for heterochromatin protein 1

(HP1α), the death associated protein 6 (DAXX), the methyl CpG binding protein 2 (MeCP2) and the polycomb protein EZH2 have been identified (Cardoso et al., 2000; Ratnakumar and Bernstein, 2013). The ADD domain of ATRX is very important for its localization to heterochromatin, as it forms a binding pocket for trimethylated lysine 9 at histone 3 (H3K9me3), and lysine 4 at histone 3 (H3K4me0), which are found at heterochromatic regions (Conte et al., 2012). Together with DAXX, ATRX functions as a histone chaperone complex to facilitate the incorporation of the histone 3 variant H3.3 into heterochromatin (Goldberg et al., 2010; Mito et al., 2007). The presence at heterochromatin and the interaction with DAXX, HP1, MeCP2 and EZH2 further indicate a role for ATRX in heterochromatin maintenance and transcriptional regulation (Tang et al., 2004; Voon and Wong, 2016).

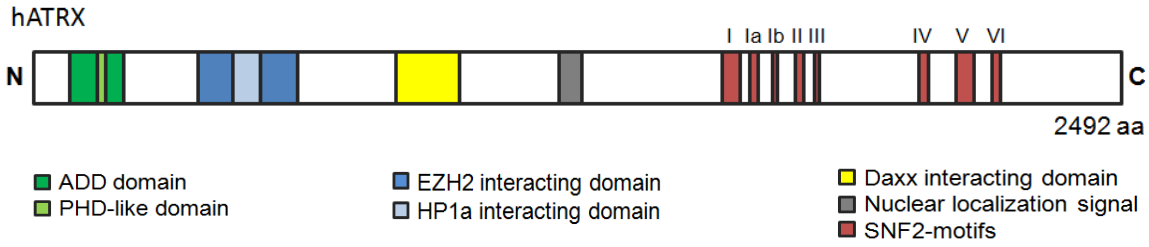

Figure 6: Structure of the human ATRX protein. The human ATRX gene encodes a protein of 2492 aa with an N-terminal ADD domain, several interacting regions for protein interaction and highly conserved SNF2-motifs.

The ATPase domain of ATRX shows high similarity to that of Rad54, and allows ATP-dependent triple helix displacement activity (Xue et al., 2003). Via its zinc finger domain, ATRX can directly bind to dsDNA *in vitro* (Cardoso et al., 2000; Law et al., 2010), using ATP hydrolysis to translocate along the DNA and remodel DNA-protein interactions (Kingston et al., 1996; Xue et al., 2003). Several studies showed that ATRX is prevalent at centromeres, telomeres and guanine-quadruplexes (G4), where it might be involved in facilitating replication and/or the proper organization of these structures. Of note, ATRX was also found in promyelocytic leukaemia nuclear bodies (PML-NBs), which have proposed functions in heterochromatin remodeling and DNA repair (Dellaire and Bazett-Jones, 2004; Luciani et al., 2006; Yeung et al., 2012).

In humans, mutations within ATRX lead to a severe phenotype accompanied by mental retardation, facial dysmorphism, urogenital dysfunctions, skeletal defects and α-thalassemia. As ATRX is encoded on the X chromosome, this condition is only found in males whereas female carriers do not display any symptoms (Gibbons et al., 2000). Most of the syndrome-causing mutations were identified within the ADD and ATPase domain of the protein (Gibbons et al., 1995; Villard et al., 1997). The impact of

the mutation or disruption of the protein varies according to the extent and timing. If mutations result in an inactivation of the protein and occur during early development, they are likely embryonically lethal. If the activity of ATRX is only diminished and such a mutation occurs at later developmental stages, this leads to the described, and above mentioned ATRX phenotype (Watson et al., 2013). Somatic inactivating mutations of ATRX appear to drive cancer progression, particularly in the central nervous system and ATRX is therefore proposed to function as a tumor suppressor. Loss of ATRX was found in the majority of cancers with no telomerase activity, which can then switch to the ALT pathway to prevent telomere shortening (Clynes et al., 2015; Lovejoy et al., 2012). In mice, mutations of ATRX or a conditional knockout results in a progeroid-like phenotype with endocrine and metabolic abnormalities (Watson et al., 2013). Both phenotypes indicate an important and versatile role for ATRX in the maintenance of genomic integrity, however the single cellular functions are yet not completely understood. Further on, several studies showed that ATRX is involved in proper replication, where it aids in fork stabilization, progression and reactivation upon fork stalling. As a chromatin remodeler, it can bind and modify complex DNA structures like G4 structures, which also occur at telomeres and facilitate their replication or transcription (Clynes et al., 2014; Leung et al., 2013; Watson et al., 2013). In this context, ATRX was described as a transcriptional regulator, as DNA methylation patterns are altered and changes in gene expression profiles were observed in ATRX deficient cells (Clynes and Gibbons, 2013; Law et al., 2010).

Furthermore, ATRX is needed for the activation of Chk1 after replication stress and thereby ATRX is involved in cell cycle control, but it remains unclear how this is achieved (Leung et al., 2013). During mitosis, ATRX assures accurate cell division with two identical sets of chromosomes, as it is present at kinetochores and thereby influences chromosome alignment and separation (Ritchie et al., 2008). Additionally, ATRX is an anti-apoptotic factor, and the induced cell death after ATRX depletion is mediated by a p53-dependent pathway (Conte et al., 2012; Iwase et al., 2011; Watson et al., 2013). In line with these observations, ATRX contributes to cell survival after several genotoxic agents and localizes to sites of DNA damage (Leung et al., 2013). In summary, ATRX is involved in several important cellular processes of the DNA damage response, which are known to contribute to genome stability. However, the exact mechanisms behind the involvement of ATRX remain partially unclear and to date, a direct participation of ATRX in DNA repair pathways was not reported.

3.7 Aim of the dissertation

Homologous Recombination is a very complex and finely regulated DSB repair pathway. Until now, not all stages are completely understood, and most certainly some factors which are involved are still unknown. Early stages of HR, such as the resection of DSB ends or the process of homology search performed by the key HR factor Rad51 are relatively well explored and their regulation has been unraveled. The basic mechanism of homology search and the participation of the motor protein Rad54 during this process have been characterized intensively in different organisms or *in vitro* systems. Also very late post-synaptic steps like the dissolution or resolution of formed Holliday junctions are already well explored. However, steps between homology search and the dissolution or resolution of Holliday junctions are poorly understood and only little is known about the regulation of steps like D-loop extension and recombination-associated DNA synthesis.

The aim of this dissertation was to investigate some of these post-synaptic steps with a focus on the identification of new HR factors involved. Understanding the precise mechanism of every stage of this important DSB repair pathway and to identify novel factors involved in the core repair process or in its regulation will help to exploit this pathway with regards to cancer therapy and is therefore of great potential.

4 Manuscript: Nek1 Regulates Rad54 to Orchestrate Homologous Recombination and Replication Fork Stability (published: June 16th 2016, Mol. Cell)

Nek1 Regulates Rad54 to Orchestrate Homologous Recombination and Replication Fork Stability

Julian Spies[1], Anja Waizenegger[1], Olivia Barton[1], Michael Sürder[1], William D. Wright[2], Wolf-Dietrich Heyer[2], Markus Löbrich[1]

GRAPHICAL ABSTRACT:

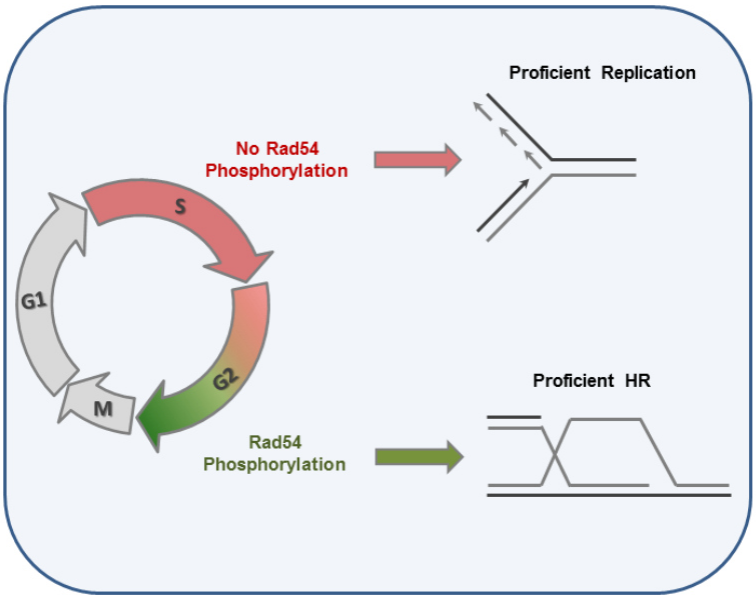

[1]Darmstadt University of Technology, Darmstadt, Germany

[2]University of California, Davis, USA

Running title:

Nek1 Regulates Homologous Recombination

Keywords:

Nek1; Rad51; Rad54; Homologous Recombination; Replication Fork Stability

4.1 Summary

Never-in-mitosis A related kinase 1 (Nek1) has established roles in apoptosis and cell cycle regulation. We show that human Nek1 regulates homologous recombination (HR) by phosphorylating Rad54 at Ser572 in late G2 phase. Nek1 deficiency as well as expression of unphosphorylatable Rad54 (Rad54-S572A) causes unresolved Rad51 foci and confers a defect in HR. Phospho-mimic Rad54 (Rad54-S572E), in contrast, promotes HR and rescues the HR defect associated with Nek1 loss. Although expression of phospho-mimic Rad54 is beneficial for HR, it causes Rad51 removal from chromatin and degradation of stalled replication forks in S phase. Thus, G2-specific phosphorylation of Rad54 by Nek1 promotes Rad51 chromatin removal during HR in G2 phase and its absence in S phase is required for replication fork stability. In summary, Nek1 regulates Rad51 removal to orchestrate HR and replication fork stability.

4.2 Introduction

Two main pathways exist for the repair of two-ended DSBs, non-homologous end-joining (NHEJ) and homologous recombination (HR), the latter operating during S and G2 phase when the sister chromatid is available as a template for repair (van Gent et al., 2001; Lukas and Lukas, 2013). HR is initiated by resection of the 5'-end and Rad51 loading to single-stranded DNA (ssDNA). Later stages of HR involve homology search, DNA strand invasion and repair synthesis to copy the missing sequence information at the break site from the donor sister chromatid (Mazón et al., 2010; Renkawitz et al., 2014). HR is finalized by the dissolution or resolution of the formed Holliday junctions (Matos and West, 2014).

In contrast to two-ended exogenously induced DSBs which can be efficiently repaired by HR and NHEJ, HR is the predominant pathway for dealing with one-ended DSBs that arise at the replication fork (Chapman et al., 2012; Moynahan and Jasin, 2010). Such DSBs occur at appreciable frequencies endogenously when replication forks encounter spontaneous base damages and/or single-strand breaks but also arise from agents which induce such single-stranded lesions (Ensminger et al., 2014; Jeggo and Löbrich, 2015). In addition to their role in repairing one-ended DSBs, HR factors also exert important functions in protecting stalled replication forks and their absence leads to degradation of newly synthesized DNA (Branzei and Foiani, 2010; Schlacher et al., 2012). The timely completion of replication is important as its failure can lead to the occurrence of under-replicated DNA regions which give rise to chromosome breakage during mitosis (Naim et al., 2013; Ying et al., 2013).

The motor protein Rad54 has multiple roles in HR-mediated DSB repair. A critical role is thought to occur after homology search is complete, to transform the synaptic complex containing three homologously aligned DNA strands (ssDNA:Rad51:dsDNA) into heteroduplex DNA. During this

process promoted by Rad54's ATPase activity, Rad51 is removed from DNA which allows 3'-end access and subsequent repair synthesis by DNA polymerases to enable the completion of HR (Agarwal et al., 2011; Ceballos and Heyer, 2011; Wright and Heyer, 2014). In the absence of Rad54, Rad51 is not removed and HR cannot be completed. Besides its role in HR, Rad51 also functions to protect stalled replication forks from degradation (Hashimoto et al., 2010; Schlacher et al., 2011). It is unclear whether fork protection is endowed by Rad51 bound to ssDNA, dsDNA, or the synaptic complex. Notably, Rad54 is not required for fork protection (Schlacher et al., 2011), suggesting that Rad51 is not removed from stalled replication forks. This raises the conceptual question of how Rad54 is differentially regulated to remove Rad51 from DNA during HR but not during replication fork stalling.

We have previously observed that gene expression of never-in-mitosis A related kinase 1 (Nek1), a member of the mammalian Nek family with highly conserved serine/threonine (Ser/Thr) and tyrosine kinase motives (Meirelles et al., 2014), is significantly up-regulated in cells exposed to ionizing radiation (IR) (Grudzenski et al., 2010). The few reports available for Nek family members explored the roles of Nek8 and Nek11 at the replication fork and during checkpoint activation, respectively (Choi et al., 2013; Melixetian et al., 2009). Nek1 is also implicated in the DNA damage response by its roles during apoptosis and cell cycle regulation (Chen et al., 2008, 2009, 2011a, 2014). More recently, Nek1 was shown to be required for proper ATR activation (Liu et al., 2013). Although Nek1-deficient cells display elevated chromosome breaks following DNA damaging agents (Chen et al., 2008), it is unclear if this phenotype results from its established role in cell cycle checkpoint regulation or represents a genuine function in a DSB repair process.

Here, we show that Nek1 phosphorylates Rad54 specifically in the G2 phase of the cell cycle. This promotes Rad51 removal from chromatin and allows the completion of HR. The absence of Rad54 phosphorylation during S phase prevents removal of Rad51 from stalled replication forks and ensures fork protection.

4.3 Results

Nek1 Functions during the DNA Damage Response and Serves to Maintain Genomic Stability

To explore the function of Nek1 during the DNA damage response, we first analyzed fibroblasts from a patient with the human disorder short-rib polydactyly syndrome (SRPS) type Majewski that harbors a nonsense mutation in Nek1 (Thiel et al., 2011). Such cells show proliferation defects following treatment with the DNA damaging agent methylmethane sulfonate (MMS) (Figure S1A) and exhibit pronounced chromosomal instability after treatment with low concentrations of hydroxyurea (HU) and aphidicolin (APH), which also induce DNA damage (Figure 1A). Since these primary cells were

poorly growing, we generated Nek1-deficient HeLa cells by shRNA technology. Using these cells, we observed substantially diminished colony formation after MMS and Olaparib (PARP inhibitor) treatment, and a more modest reduction after X-rays (Figure 1B), consistent with earlier findings that loss of Nek1 expression confers sensitivity to genotoxic agents (Chen et al., 2011b; Polci et al., 2004). Since these agents induce DSBs, we investigated the efficiency of DSB repair in Nek1-depleted cells by analyzing γH2AX and Rad51 foci, both markers for DSBs. We pulse-labeled growing cell populations with the thymidine analog EdU and quantified foci in EdU-positive cells, which represent cells that were in S phase at the time of MMS treatment (Figure S1B). We observed high foci levels early after MMS treatment which decreased due to repair while cells progressed into G2 (Figures 1C and S1B). Nek1-deficient cells showed foci levels similar to control cells at initial time points but substantially elevated levels at later times, suggesting that Nek1 is involved in repairing DSBs. Of note, the defect was most striking for Rad51 foci which monitor the repair of resected DSBs by HR (Figure 1C). The elevated foci levels were rescued by expression of shRNA-resistant GFP-Nek1 (Figure 1C). Since MMS induces DSBs during replication, we wished to explore if Nek1 has a general role during HR (as opposed to a more specific role during replication) and investigated Rad51 removal from DSBs induced by IR outside of S phase. We synchronized cells in G2 and assessed chromatin-bound Rad51 levels by immunoblotting. Chromatin-bound Rad51 increased in control cells until 2-4 h after IR and then decreased due to repair. In Nek1-deficient cells, the increase was similar but Rad51 was not released from chromatin until at least 12 h post IR (Figures 1D and S1C). As discussed below, these data were confirmed analyzing Rad51 foci.

Nek1 Functions during DSB Repair by HR and Interacts with Rad54

The failure of Nek1-deficient cells to remove Rad51 from DSBs suggests that Nek1 has a role during HR. We therefore investigated DSB repair kinetics after IR in G1- and G2-phase cells as previously described (Löbrich et al., 2010) (Figure S2A). IR-induced DSBs are repaired by NHEJ in G1 and by NHEJ or HR in G2 (Rothkamm et al., 2003). We depleted Nek1 by siRNA and observed similar γH2AX foci levels as in control cells at all time points in G1 suggesting that Nek1 is not involved in NHEJ (Figure S2A). In G2 phase, γH2AX and Rad51 foci levels in Nek1-deficient cells were similar to control cells initially but were elevated compared to control cells at later times after IR (Figures 2A and S2A). The elevated γH2AX foci level was similar to Brca2- and Rad54-depleted cells while the elevated Rad51 foci level was similar to Rad54-deficient cells but distinct from Brca2-depleted cells (Figure 2A). This reflects the role of Brca2 in Rad51 filament formation and the function of Rad54 during Rad51 removal (Moynahan and Jasin, 2010; Shah et al., 2010). A second siRNA for Nek1 provided the same result (Figure S2B). Of note, concomitant down-regulation of Nek1 and Rad54 provided no further increase than the single Nek1 or Rad54 knock-downs (Figure S2B). Further, wild-type (WT) but not kinase-deficient Nek1 (Nek1-K33R) rescued the elevated foci level of Nek1-

depleted cells (Figure 2B). Fibroblasts from SRPS patients also showed kinetics for γH2AX foci removal distinct to NHEJ mutants but similar to HR mutants (Figure S2C), and Nek1-depleted non-transformed G2 fibroblasts exhibited elevated Rad51 foci levels, demonstrating that the repair defect is not cell line dependent (Figure S2D). Collectively, these data support the conclusion that Nek1 operates during HR.

To further substantiate this notion, we employed HeLa cells containing an integrated HR reporter with two differentially mutated GFP genes (Mansour et al., 2008). Expression of the endonuclease I-*Sce*I generates a DSB in one of the two genes which can be repaired by HR with the second gene copy serving as a template, resulting in a cell expressing functional GFP. HR frequencies assessed by the fraction of GFP-positive cells were significantly decreased after depletion of HR but not NHEJ factors. Strikingly, Nek1-depleted cells showed a reduction in GFP-positive recombinants identical to Brca2- or Rad54-depleted cells (Figures 2C and S2E). We also measured the formation of sister chromatid exchanges (SCEs) which arise due to HR. As previously described (Conrad et al., 2011a), IR in G2-phase cells induces SCEs. Nek1-depleted cells showed reduced SCE levels similar to Brca2- and Rad54-depleted cells (Figure S2F). Finally, we assessed DNA synthesis occurring during later stages of HR. For this, we quantified the incorporation of the nucleotide analog EdU following irradiation of G2-phase cells. Nuclear EdU foci arise in control cells within 8 h post IR, and depletion of HR but not NHEJ factors abolishes EdU foci formation (Beucher et al., 2009). Nek1-depleted cells exhibited the same defect as Rad54-depleted cells (Figure S2G). In summary, these data firmly establish that Nek1 is a critical HR factor.

The elevated level of unresolved Rad51 foci and the failure to perform DNA synthesis suggest that Nek1 functions after resection but before repair synthesis. This is similar to Rad54 (Essers et al., 2002) and, indeed, all assays performed in the present study provided identical results for Nek1- and Rad54-deficient cells. Therefore, we investigated if Nek1 interacts with Rad54 by co-immunoprecipitation (co-IP) experiments. We confirmed the presence of Rad51 in IPs from Rad54 (Heyer et al., 2006), and detected Rad54 but not Rad51 in IPs from Nek1 and *vice versa* (Figure 2D). The interactions were induced by IR (Figure 2D), resisted DNase treatment suggesting that they are independent of DNA, and were confirmed in another cell system (Figure S2H).

Nek1 Phosphorylates Rad54 at Serine 572 (S572) Specifically in G2 Phase

The interaction between Nek1 and Rad54 raised the possibility that Rad54 is a phosphorylation target of Nek1. To identify potential Nek1 phosphorylation sites on Rad54, we screened Rad54 for Nek1 consensus sites, Ser/Thr residues with phenylalanine at position -3 relative to Ser/Thr (Chen et al., 2009; Surpili et al., 2003). Rad54-Ser572 is such a Nek1 consensus site located in a highly conserved ATPase domain and is also surface-exposed (Thomä et al., 2005). We mutated Ser572 to the unphosphorylatable (phospho-mutant) alanine (S572A) or the potentially phospho-mimic glutamate

(S572E) (Figure 3A). First, we performed an *in vitro* kinase assay with immunoprecipitated GFP-Rad54, recombinant Nek1, and radioactive ATP. GFP-Rad54-WT but not GFP-Rad54-S572A was readily phosphorylated by Nek1 (Figure 3B). To verify Nek1-dependent Rad54 phosphorylation at Ser572 (Rad54-pS572), we employed a phospho-specific antibody which provided a signal for immunoprecipitated GFP-Rad54-WT but not GFP-Rad54-S572A proteins incubated with Nek1 and ATP (Figure 3C). Importantly, Rad54-pS572 was observed *in vivo* in whole cell extracts (WCE) of HeLa and Hek293 cells in a manner dependent on Nek1 (Figure 3D). We then investigated the time-course of Rad54 phosphorylation in nuclear cell extracts of synchronized G2-phase cells and observed strongly increased Rad54-pS572 levels at 8 h after IR, a time when Rad51 is removed from chromatin but irradiated G2-phase cells have not yet entered mitosis (Deckbar et al., 2007) (Figures 3E and S3A). We also assessed Rad54-pS572 levels in S-phase cells treated with DNA-damaging agents. Of note, Rad54-pS572 is delayed in damaged S-phase cells and does not reach its maximum level until the cells have progressed into G2 phase (Figures 3F and S3B). A slight increase in Rad54 phosphorylation from S to G2 was also observed in undamaged cells (Figure S3C). We finally aimed to assess the fraction of Rad54 which is phosphorylated by Nek1 after damage induction. We used Phos-tag™ gels which allow the visualization of phosphorylation events by band shifts. We used G2-synchronized cells and detected only minor Rad54 phosphorylation events in unirradiated cells. In contrast, about half of all Rad54 proteins were phosphorylated at 8 h after IR (Figure 3G). The fraction of phosphorylated Rad54 was reduced following phosphatase treatment or Nek1 siRNA (Figure 3G).

Nek1 Promotes HR by Phosphorylating Rad54 at Ser572

We then investigated if Rad54-pS572 is required for efficient DSB repair. Since Rad54's critical function during DSB repair involves its interaction with Rad51, we first investigated whether the three GFP-Rad54 variants differ in their ability to interact with Rad51. We transiently tansfected Hek293 cells with GFP-Rad54-WT, -S572A or -S572E constructs, immunoprecipitated Rad51 and observed similar interaction levels in all three Rad54 variants (Figure S4A). Purified Rad54-S572A and -S572E proteins also showed similar interaction levels (see Figure S7D). We then generated HeLa cell clones with stably integrated siRNA-resistant GFP-tagged Rad54-WT, Rad54-S572A or Rad54-S572E (hereafter named 54WT for a clone with Rad54-WT, 54SA for a clone with Rad54-S572A, 54SE for a clone with Rad54-S572E, and HeLa for the uncomplemented parental cells). All three clones showed physiological Rad54 expression levels by immunoblotting and formed similar numbers of IR-induced GFP-Rad54 foci which co-localized with Rad51 foci (Figure 4A and S4B). 48 h prior to all experiments, we depleted the endogenous Rad54 by siRNA. We assessed Rad51 and γH2AX foci levels in G2-irradiated cells and revealed unrepaired foci in 54SA but not in 54SE cells (Figure 4B). The magnitude of the repair defect in 54SA cells was similar to that of HeLa cells treated with siRad54 (hereafter named 54KD). Nek1 depletion by siRNA caused similarly elevated foci levels in

54WT and 54SA cells, demonstrating epistasis between Nek1 deficiency and the inability to phosphorylate Rad54 at Ser572. Nek1 depletion in 54SE cells had little effect, demonstrating that the major function of Nek1 during DSB repair by HR is to phosphorylate Rad54 at Ser572 (Figures 4B and S4C). To employ foci-independent DSB repair measurements, we assessed chromatin-bound Rad51 levels by immunoblotting in G2-sychronized cells at distinct time points after irradiation. In 54WT and 54SE cells, chromatin-bound Rad51 was increased at 4 h after IR and then decreased due to repair. In contrast, chromatin-bound Rad51 did not decrease between 4 and 10 h after IR in 54SA cells (Figure 4C and S4D). This is consistent with the Rad51 foci analysis and confirms the HR defect of cells with unphosphorylatable Rad54-S572A. We also analyzed chromatid breaks and SCEs as a measure for unrepaired DSBs and efficient HR events, respectively. 54SA and 54KD but not 54SE cells showed elevated chromatid breaks and a failure to form SCEs (Figures 4D and S4E).

To independently confirm the results with the stable cell lines, we transiently transfected cells with Rad54 constructs. We depleted endogenous Rad54 and/or Nek1 in HeLa cells, complemented them with siRNA-resistant GFP-Rad54-WT, -S572A or -S572E constructs and confirmed that they show similar expression levels (Figure S4F). First, we measured Rad51 foci in irradiated G2 cells which formed GFP-Rad54 foci of physiological intensity. Rad54-WT and Rad54-S572E but not Rad54-S572A complemented the elevated foci level of siRad54-treated cells (Figure 4E). Moreover, the elevated foci level conferred by Nek1 depletion was rescued by the Rad54-S572E mutant, demonstrating that phospho-mimic Rad54 suppresses the requirement for Nek1 function (Figure 4E). We then quantified GFP-Rad54 foci and obtained results identical as with Rad51 foci; that is, we observed elevated foci levels in Nek1-depleted cells and in cells expressing Rad54-S572A but not Rad54-WT or Rad54-S572E constructs and a rescue of the Nek1 defect by the Rad54-S572E mutant (Figure S4G). Moreover, the analysis of γH2AX foci in cells with a pan-nuclear GFP-Rad54 signal provided similar results to that of cells which formed GFP-Rad54 foci of physiological intensity (Figure S4H), demonstrating that differences in Rad54 expression levels do not substantially affect the repair capacity. Finally, we employed the HR reporter assay in cells expressing RFP-tagged Rad54 constructs and observed diminished HR frequencies in the S572A mutant and a rescue of the HR defect in Nek1-depleted cells through expression of the S572E mutant (Figure 4F). In summary, these data establish that Nek1 promotes HR by phosphorylating Rad54 at Ser572.

Rad54 Phosphorylation during S Phase Causes Rad51 Removal from Stalled Replication Forks

The finding that Rad54 is regulated by a specific phosphorylation event raises the possibility that permanent phosphorylation of Rad54, although being beneficial for HR, could be detrimental under specific conditions. The observation that Rad54-pS572 occurs specifically in G2 further suggests that Rad54 phosphorylation might be detrimental during S phase. To explore this possibility, we analyzed HeLa cells with the stably integrated Rad54 variants after exposure to high doses of HU which are

known to cause replication fork stalling. Since Rad54-pS572 promotes Rad51 removal during late stages of HR, we speculated that it might also remove Rad51 from stalled replication forks where Rad51 is required to prevent fork degradation (Hashimoto et al., 2010; Schlacher et al., 2011). We first employed immunoblotting and observed diminished levels of chromatin-bound Rad51 after HU treatment in 54SE cells, suggesting that Rad54-pS572 removes Rad51 from stalled forks (Figure 5A). Also Hek293 cells over-expressing Rad54-S572E, but not cells over-expressing Rad54-WT or Rad54-S572A, showed diminished levels of chromatin-bound Rad51 after HU treatment (Figure S5A). We then assessed the level of chromatin-bound Rad51 by immunofluorescence microscopy. Rad51 bound to stalled replication forks co-localizes with newly synthesized DNA but does not form clear Rad51 foci (Petermann and Helleday, 2010; Zellweger et al., 2015). We therefore applied an extraction procedure to remove Rad51 that is not bound to chromatin and measured the total nuclear Rad51 intensity in EdU-positive S-phase cells. 54WT and 54SA cells showed an increase in Rad51 intensity after HU treatment suggesting that Rad51 binds to stalled replication forks (Figure 5B). Of note, HU-induced Rad51 binding was absent in 54SE cells (Figure 5B). We also analyzed Rad51 foci and did not detect an increase in foci number under these treatment conditions, consistent with the observation that Rad51 bound to stalled replication forks does not form foci (Petermann and Helleday, 2010; Zellweger et al., 2015) (Figure S5B). This control experiment confirms that the differences in the HU-induced total nuclear Rad51 intensity between 54WT/54SA and 54SE are not affected by differences in foci number.

To gain further insight into the processes of how untimely phosphorylation of Rad54 during S phase causes removal of Rad51 from chromatin, we applied iPOND technology (Sirbu et al., 2011). We observed that Rad54 as well as Rad51 bind to stalled replication forks, with the level of Rad54/Rad51 binding increasing with increasing periods of fork stalling. Interestingly, despite the increased abundance of Rad54 at stalled forks, Rad51 was not removed (Figure 5C), consistent with the interpretation that WT Rad54 does not remove Rad51 from chromatin during S phase. This is supported by the observation that Rad54 is not phosphorylated at Ser572 during prolonged periods of replication fork stalling (Figure S5C). We then investigated how the different Rad54 variants bind to stalled replication forks and observed that Rad54-S572E has significantly higher occupancy at stalled forks than Rad54-WT or Rad54-S572A. Importantly, the enhanced presence of Rad54-S572E lead to removal of Rad51 from stalled forks, consistent with the interpretation that phosphorylated Rad54 promotes removal of Rad51 from chromatin (Figure 5D). Thus, untimely phosphorylation of Rad54 during S phase leads to Rad51 removal from stalled replication forks.

Rad54 Phosphorylation during S Phase Causes Degradation of Stalled Replication Forks

We next investigated if Rad51 removal from stalled replication forks in 54SE cells causes fork degradation. We applied the DNA fiber assay and used conditions which were described to cause fork

degradation in cells with destabilized Rad51 (4 mM HU for 5 h) (Schlacher et al., 2011). Of note, 54SE cells but not 54WT or 54SA cells exhibited degradation of newly synthesized DNA (Figure 6A). The extent of degradation in 54SE cells was similar to that of HeLa cells treated with siRad51 whereas cells treated with siRad54 (54KD cells) did not exhibit fork degradation (Figure S6A). Moreover, 54SE cells treated with siRad51 did not show more extensive degradation than HeLa cells treated with siRad51 or 54SE cells without siRad51, demonstrating an epistatic relationship between Rad51 depletion and Rad54-S572E expression for replication fork degradation (Figure S6B). We also quantified the fraction of forks that failed to restart after HU withdrawal (Petermann et al., 2010). HeLa cells treated with siRad51 and 54SE cells showed a defect in the ability to restart stalled replication forks (Figure 6B). Finally, fork degradation in 54SE cells was suppressed by Mre11 siRNA or treatment with the Mre11 nuclease inhibitor Mirin, which was previously shown to suppress fork degradation in Brca2-deficient cells (Schlacher et al., 2011), but was unaffected by DNA2 siRNA (Figure 6C and S6C). Collectively, these findings demonstrate that untimely Rad54 phosphorylation during S phase phenocopies the loss of Rad51 and severely compromises the ability to stabilize stalled replication forks.

To gain further insight into the process of fork degradation by Rad54 phosphorylation, we performed the fiber assay under conditions that were described to cause degradation of stalled forks even in control cells (4 mM HU for 8 h) (Thangavel et al., 2015). Consistent with this study, we observed that this degradation in 54WT cells is diminished after DNA2 siRNA but unaffected by Mre11 siRNA (Figure 6D). Of note, fork degradation in 54SE cells was purely dependent on Mre11; i.e. Mirin but not DNA2 siRNA treatment abolished the degradation (Figure 6D). Thus, we obtained fundamentally different results with 54WT and 54SE cells. 54WT cells showed fork degradation only after 8 h HU (and not after 5 h) which is dependent on DNA2. 54SE cells showed fork degradation already after 5 h which is dependent on Mre11, and the degradation after 8 h remained dependent on Mre11. Since the DNA2-dependent fork degradation in control cells has been suggested to occur at chicken foot structures which arise after prolonged periods of replication fork stalling (Thangavel et al., 2015), our data suggest that 54SE cells fail to form such structures and remove Rad51 from stalled replication forks before these convert into chicken foot structures. This interpretation is in line with the finding that Rad51 is essential for the conversion from stalled forks into chicken foot structures (Zellweger et al., 2015).

Cells with Unregulatable Rad54 Show Genomic Instability

Cells with unphosphorylatable Rad54-S572A fail to efficiently repair DSBs by HR while cells with phospho-mimic Rad54-S572E fail to protect stalled replication forks. We therefore reasoned that both cell types might be unable to cope with replication stress which requires that cells minimize the generation of lesions at stalled replication forks and repair DSBs which inevitably arise. To explore

this possibility, we initially exposed 54SA or 54SE cells to low concentrations of APH and assessed the level of γH2AX foci in mitotic cells. 54SA cells show elevated foci levels in prophase cells compared to 54SE and 54WT cells, both with and without APH treatment, likely reflecting the inability of 54SA cells to repair DSBs by HR (Figure 7A). Of note, the treatment conditions applied are known to cause under-replicated DNA regions which result during mitotic chromatin condensation in an increase in γH2AX foci numbers when cells progress from prophase to metaphase (Glover, 2006; Ying et al., 2013). We therefore also assessed foci levels in metaphase cells and observed that 54SE but not 54SA or 54WT cells show a substantial increase in γH2AX foci numbers between prophase and metaphase, both with and without APH treatment (Figure 7A). Together, this demonstrates that both cell variants with unregulatable Rad54 exhibit a diminished ability to cope with replication stress. We also quantified 53BP1 bodies in G1-phase cells, which are known to arise from under-replicated DNA regions (Lukas et al., 2011). 54SE cells show increased 53BP1 bodies after APH treatment, suggesting that Rad54 phosphorylation during S phase causes under-replicated DNA regions. 54SA cells, in contrast, show elevated 53BP1 bodies already in untreated cells (Figure 7B), consistent with the interpretation that unrepaired γH2AX foci in prophase lead to 53BP1 bodies in G1 phase. Finally, we studied the survival of cells with unregulatable Rad54 after agents inducing DSBs as well as other lesions which interfere with replication. Compared to 54WT cells, both 54SA and 54SE cells show diminished colony formation after MMS, Olaparib or X-rays, confirming that regulation of Rad54 phosphorylation is important for maintaining genomic stability (Figure 7C).

4.4 Discussion

We have discovered that Rad54 is phosphorylated at Ser572 and generated stable cell lines expressing either unphosphorylatable Rad54-S572A or phospho-mimic Rad54-S572E protein (54SA or 54SE cells, respectively). 54SA cells fail to resolve Rad51 foci during DSB repair by HR while 54SE cells repair DSBs by HR as efficiently as control cells with WT Rad54 (54WT cells). Strikingly, although Rad54-S572E is beneficial for HR, it is detrimental for the protection of stalled replication forks. This latter effect is associated with removal of Rad51 from stalled forks which leads to fork degradation similar to what is observed in cells lacking Rad51. In contrast, 54SA cells are able to protect stalled replication forks (Figure 6A). Thus, Rad54 phosphorylation exerts cell cycle phase-specific positive or negative effects and hence needs to be finely tuned dependent on the cell cycle requirements. The necessity to regulate Rad54 phosphorylation is further demonstrated by the observation that both 54SA and 54SE cells show elevated DNA damage and decreased survival if exposed to agents that induce replication fork stalling as well as DSBs (Figure 7A-C).

The Ser572 phosphorylation site of Rad54 is positioned within one of 7 highly conserved ATPase domains (Ceballos and Heyer, 2011; Thomä et al., 2005) and phosphorylation events have been reported to enhance the activity of other ATPases (Alzamora et al., 2010). It is therefore tempting to speculate that Ser572 phosphorylation stimulates Rad54's ATPase function. To test the possibility that Rad54-Ser572 phosphorylation directly affects the ATPase activity of Rad54 or its ability to promote critical HR reactions, we purified WT and mutant Rad54 proteins (Figure S7A). Surprisingly, the Rad51-stimulated ATPase activity of the Rad54-S572E mutant and its D-loop formation ability were substantially lower than those of Rad54-WT or the Rad54-S572A mutant (Figure S7B and C), although it retained the ability to interact with Rad51 and bind dsDNA (Figure S7D and E). Also contrary to expectation, the Rad54-S572A mutant protein was proficient in stimulating Rad51-mediated D-loop formation, even better than Rad54-WT under the tested conditions (Figure S7C), and displayed near WT ATPase activity on dsDNA (Figure S7B). Lack of a defect in Rad54-S572A might suggest an alternative view that there is a factor which restrains unphosphorylated Rad54 activity *in vivo*. The activity of Rad54-S572E, though reduced, appears sufficient *in vivo* when coupled to the change effected by the phospho-mimic. The inability to pinpoint biochemical differences to explain the cellular phenotypes suggests that yet unknown factors are missing in the *in vitro* reactions. One possibility is the Rad54 paralog Rad54B, which shows highly similar biochemical activity and partially overlapping *in vivo* functions. Thus, the precise mechanism of how Rad54 phosphorylation promotes Rad51 removal from chromatin awaits clarification.

Rad54 removes Rad51 from DNA when the synaptic complex of ssDNA:Rad51:dsDNA is transformed into heteroduplex DNA (Solinger et al., 2002; Wright and Heyer, 2014). We observed that 54WT, 54KD, 54SA and 54SE cells form Rad51 foci at early time points post IR with equal efficiency (Figure 4B), implying that the presence of Rad54 or its phosphorylation does not affect Rad51 binding to ssDNA at resected DSBs. Moreover, purified Rad54 does not exhibit ATPase activity on ssDNA *in vitro* (Swagemakers et al., 1998) and is not stimulated by Rad51 on ssDNA (Figure S7F). The observation that Rad54 phosphorylation removes Rad51 from stalled replication forks might therefore suggest that the protective role of Rad51 at stalled forks involves the presence of a synaptic complex (Figure 7D). How might a synaptic complex arise during replication fork stalling? The prevailing evidence suggests that chicken foot structures arise during prolonged periods of replication fork stalling (Thangavel et al., 2015). Thus, it might be possible that Rad51 is initially loaded onto ssDNA by Brca2 but then promotes, *via* homology search, the formation of a synaptic complex which serves to stabilize the stalled replication fork until it can be converted into a chicken foot structure, or directly aids in this process (Figure 7D). In either case, Rad51 is not removed during this process (Sirbu et al., 2011), consistent with our iPOND data (Figure 5C) and the observation that Rad54 is not phosphorylated at Ser572 during replication (Figure S5C).

We have shown that Rad54 phosphorylation following DNA damage induction is restricted to late G2 phase irrespective of the position in the cell cycle when the damage is induced. This cell cycle-specific modulation of Rad54 allows for the timely removal of Rad51 prior to the onset of mitosis and complements previous studies by others showing that nucleases such as Mus81-Eme1 and Gen1 are under cell cycle-specific regulation to resolve late HR intermediates during mitosis (Matos and West, 2014a; Ying et al., 2013). Moreover, it was described that DNA lesions which arise from replication stress can be repaired by HR uncoupled from replication in the following G2 phase and it was further suggested that such repair is promoted by cell cycle-specific kinases (González□Prieto et al., 2013; Karras and Jentsch, 2010). Our discovery of the G2-specific activation of Rad54 closes the gap between damage processing that starts during S phase and is completed in mitosis and thus represents both the missing link and a mechanistic explanation for these previous findings. Collectively, our work, together with published findings, establishes that the process of HR is finely regulated during the cell cycle such that the required factors are activated when they are most needed and the least harmful. The concept that a synchronization process underlies HR has precedent from meiosis, where defined steps of HR occur at defined stages during meiotic progression (Baudat et al., 2013). However, it has to be considered that the process of HR synchronization with cell cycle progression may be lesion dependent (DSBs, gaps, stalled forks) as double Holiday junctions can be resolved by the BLM–TopoIIIα–RMI1–RMI2 (BTR) complex during S phase (Matos and West, 2014a; Sarbajna et al., 2014).

In summary, our work shows that the process of HR is regulated during the cell cycle by restricting Rad54 phosphorylation to late G2 phase. On one hand, this limits Rad54 function during replication and allows Rad51 to protect stalled replication forks; on the other hand, it promotes Rad51 removal prior to the onset of mitosis and the completion of HR (Figure 7D). We identified Nek1 as the kinase regulating Rad51 removal and orchestrating HR with replication fork stability.

4.5 Experimental Procedures

ShNek1 or shCtrl cells were generated by viral transduction. Stable cell lines expressing GFP-Rad54 variants were generated by transfection with plasmids carrying a G418 resistance cassette. SiRNA and plasmid transfections were carried out using HiPerFect and MATra-A reagents, respectively. For foci analysis, cells were categorized at the microscope in G1-, G2- or S-phase cells by their DAPI content and EdU intensity. Foci were enumerated manually. Intensity measurements of chromatin-bound Rad51 using IF microscopy involved pre-extraction using ice cold methanol.

The EdU incorporation assay, preparation of chromosome spreads, SCE analysis and clonogenic survival assays were carried out as described (Beucher et al., 2009; Conrad et al., 2011a; Nikolova et

al., 2010). For the HR reporter assay, HeLa pGC cells were siRNA treated, transfected with RFP-Rad54 and I-*Sce*I plasmids (Mansour et al., 2008), and GFP-positive cells were counted at the microscope. For DNA fiber analysis, cells were labeled with CldU for 30 min, treated with 4 mM HU for 5 or 8 h, incubated with IdU for 30 min, harvested and prepared for DNA fiber spreading as described (Schlacher et al., 2011).

Isolation of nuclear cell extracts and chromatin or soluble protein fractions, protein analysis by SDS-PAGE and immunoblotting were performed as described (Barton et al., 2014). For *in vitro* kinase assays, constitutively active Nek1 protein was pre-incubated with ^{32}P ATP or with unlabeled ATP before immunoprecipitated Rad54 was added. Phosphorylation signals were detected by auto-radiography or with a custom made antibody for Rad54-pSer572. Detailed descriptions of all assays including co-IP and iPOND experiments are provided in the Extended Experimental Procedures.

P-values were obtained by student's t-test and represent a comparison of all cells analyzed in the indicated cell populations (for all foci and chromosomal experiments) or a comparison of the data mean (for the HR reporter, colony formation and the DNA fiber assays and for Rad51 intensity measurements); *, $p < 0.05$; **, $p < 0.01$; ***, $p < 0.001$. For each experiment protein expression levels were controlled by immunoblotting and are displayed in the corresponding figures.

AUTHOR CONTRIBUTIONS

J.S. and M. L. designed the study and wrote the paper with input from W.D.W. and W.-D.H.; J.S., A.W., O.B., W.D.W., W.-D.H, and M.L. analyzed and interpreted the data. J.S., A.W., O.B., M.S. and W.D.W. conducted the experiments

ACKNOWLEDGEMENTS

We thank Jochen Dahm-Daphi, Jörg Kobarg, Roland Kanaar, and Christian Thiel for sharing cell lines and DNA plasmids and Helle Ulrich, Cristina Cardoso, David Chen, Junjie Chen, Dale Wigley, and the M.L. lab for critical discussions. We further thank Bettina Basso, Christel Braun, and Cornelia Schmitt for technical assistance and Jessica Sneeden for pilot experiments. This work was supported by the Deutsche Forschungsgemeinschaft (GRK 1657 to M.L.), the Bundesministerium für Bildung und Forschung (02NUK037C to M.L.), and the NIH (GM58015 to W.D.-H.).

4.6 References

Agarwal, S., van Cappellen, W. a, Guénolé, A., Eppink, B., Linsen, S.E. V, Meijering, E., Houtsmuller, A., Kanaar, R., and Essers, J. (2011). ATP-dependent and independent functions of Rad54 in genome maintenance. J. Cell Biol. *192*, 735–750.

Alzamora, R., Thali, R.F., Gong, F., Smolak, C., Li, H., Baty, C.J., Bertrand, C.A., Auchli, Y., Brunisholz, R.A., Neumann, D., et al. (2010). PKA Regulates Vacuolar H+-ATPase Localization and Activity via Direct Phosphorylation of the A Subunit in Kidney Cells. J. Biol. Chem. *285* , 24676–24685.

Barton, O., Naumann, S.C., Diemer-Biehs, R., Künzel, J., Steinlage, M., Conrad, S., Makharashvili, N., Wang, J., Feng, L., Lopez, B.S., et al. (2014). Polo-like kinase 3 regulates CtIP during DNA double-strand break repair in G1. J. Cell Biol. *206* , 877–894.

Baudat, F., Imai, Y., and de Massy, B. (2013). Meiotic recombination in mammals: localization and regulation. Nat Rev Genet *14*, 794–806.

Beucher, A., Birraux, J., Tchouandong, L., Barton, O., Shibata, A., Conrad, S., Goodarzi, A.A., Krempler, A., Jeggo, P.A., and Löbrich, M. (2009). ATM and Artemis promote homologous recombination of radiation-induced DNA double-strand breaks in G2. EMBO J. *28*, 3413–3427.

Branzei, D., and Foiani, M. (2010). Maintaining genome stability at the replication fork. Nat Rev Mol Cell Biol *11*, 208–219.

Ceballos, S.J., and Heyer, W.-D. (2011). Functions of the Snf2/Swi2 family Rad54 motor protein in homologous recombination. Biochim. Biophys. Acta - Gene Regul. Mech. *1809*, 509–523.

Chapman, J.R., Taylor, M.R.G., and Boulton, S.J. (2012). Playing the End Game: DNA Double-Strand Break Repair Pathway Choice. Mol. Cell *47*, 497–510.

Chen, Y., Chen, P.-L., Chen, C.-F., Jiang, X., and Riley, D.J. (2008). Never-in-mitosis related Kinase 1 functions in DNA damage response and checkpoint control. Cc *7*, 3194–3201.

Chen, Y., Craigen, W.J., and Riley, D.J. (2009). Nek1 regulates cell death and mitochondrial membrane permeability through phosphorylation of VDAC1. Cc *8*, 257–267.

Chen, Y., Chen, C.-F., Chiang, H.-C., Pena, M., Polci, R., Wei, R.L., Edwards, R. a, Hansel, D.E., Chen, P.-L., and Riley, D.J. (2011a). Mutation of NIMA-related kinase 1 (NEK1) leads to chromosome instability. Mol. Cancer *10*, 5.

Chen, Y., Chen, C.-F., Riley, D.J., and Chen, P.-L. (2011b). Nek1 kinase functions in DNA damage response and checkpoint control through a pathway independent of ATM and ATR. Cell Cycle *10*, 655–663.

Chen, Y., Chen, C., Polci, R., Wei, R., Riley, D.J., and Chen, P. (2014). Increased Nek1 expression in Renal Cell Carcinoma cells is associated with decreased sensitivity to DNA-damaging treatment. *1*.

Choi, H.J.C., Lin, J.-R., Vannier, J.-B., Slaats, G.G., Kile, A.C., Paulsen, R.D., Manning, D.K., Beier, D.R., Giles, R.H., Boulton, S.J., et al. (2013). NEK8 links the ATR-regulated replication stress response and S phase CDK activity to renal ciliopathies. Mol. Cell *51*, 423–439.

Conrad, S., Künzel, J., and Löbrich, M. (2011). Sister chromatid exchanges occur in G 2 -irradiated cells. Cell Cycle *10*, 222–228.

Deckbar, D., Birraux, J., Krempler, A., Tchouandong, L., Beucher, A., Walker, S., Stiff, T., Jeggo, P., and Löbrich, M. (2007). Chromosome breakage after G2 checkpoint release. J. Cell Biol. *176*, 749–755.

Ensminger, M., Iloff, L., Ebel, C., Nikolova, T., Kaina, B., and Löbrich, M. (2014). DNA breaks and chromosomal aberrations arise when replication meets base excision repair. J. Cell Biol. *206* , 29–43.

Essers, J., Houtsmuller, A.B., van Veelen, L., Paulusma, C., Nigg, A.L., Pastink, A., Vermeulen, W., Hoeijmakers, J.H.J., and Kanaar, R. (2002). Nuclear dynamics of RAD52 group homologous recombination proteins in response to DNA damage. EMBO J. *21*, 2030–2037.

van Gent, D.C., Hoeijmakers, J.H.J., and Kanaar, R. (2001). Chromosomal stability and the DNA double-stranded break connection. Nat Rev Genet *2*, 196–206.

Glover, T.W. (2006). Common fragile sites. Cancer Lett. *232*, 4–12.

González-Prieto, R., Muñoz-Cabello, A.M., Cabello-Lobato, M.J., and Prado, F. (2013). Rad51 replication fork recruitment is required for DNA damage tolerance. EMBO J. *32*, 1307–1321.

Grudzenski, S., Raths, A., Conrad, S., Rübe, C.E., and Löbrich, M. (2010). Inducible response required for repair of low-dose radiation damage in human fibroblasts. Proc. Natl. Acad. Sci. U. S. A. *107*, 14205–14210.

Hashimoto, Y., Chaudhuri, A.R., Lopes, M., and Costanzo, V. (2010). Rad51 protects nascent DNA from Mre11-dependent degradation and promotes continuous DNA synthesis. Nat Struct Mol Biol *17*, 1305–1311.

Heyer, W.-D., Li, X., Rolfsmeier, M., and Zhang, X.-P. (2006). Rad54: the Swiss Army knife of homologous recombination? Nucleic Acids Res. *34* , 4115–4125.

Jeggo, P.A., and Löbrich, M. (2015). How cancer cells hijack DNA double-strand break repair pathways to gain genomic instability. Biochem. J. *471*, 1–11.

Karras, G.I., and Jentsch, S. (2010). The RAD6 DNA Damage Tolerance Pathway Operates Uncoupled from the Replication Fork and Is Functional Beyond S Phase. Cell *141*, 255–267.

Liu, S., Ho, C.K., Ouyang, J., and Zou, L. (2013). Nek1 kinase associates with ATR-ATRIP and primes ATR for efficient DNA damage signaling. Proc. Natl. Acad. Sci. U. S. A. *110*, 2175–2180.

Löbrich, M., Shibata, A., Beucher, A., Fisher, A., Ensminger, M., Goodarzi, A.A., Barton, O., and Jeggo, P.A. (2010). γH2AX foci analysis for monitoring DNA double-strand break repair: Strengths, limitations and optimization. Cc *9*, 662–669.

Lukas, J., and Lukas, C. (2013). Shielding Broken DNA for a Quick Fix. Science (80-.). *339*, 652–653.

Lukas, C., Savic, V., Bekker-Jensen, S., Doil, C., Neumann, B., Solvhoj Pedersen, R., Grofte, M., Chan, K.L., Hickson, I.D., Bartek, J., et al. (2011). 53BP1 nuclear bodies form around DNA lesions generated by mitotic transmission of chromosomes under replication stress. Nat Cell Biol *13*, 243–253.

Mansour, W.Y., Schumacher, S., Rosskopf, R., Rhein, T., Schmidt-Petersen, F., Gatzemeier, F., Haag, F., Borgmann, K., Willers, H., and Dahm-Daphi, J. (2008). Hierarchy of nonhomologous end-joining, single-strand annealing and gene conversion at site-directed DNA double-strand breaks. Nucleic Acids Res. *36*, 4088–4098.

Matos, J., and West, S.C. (2014). Holliday junction resolution: Regulation in space and time. DNA Repair (Amst). *19*, 176–181.

Mazón, G., Mimitou, E.P., and Symington, L.S. (2010). SnapShot: Homologous Recombination in DNA Double-Strand Break Repair. Cell *142*, 648.e1–e648.e2.

Meirelles, G.V., Perez, A.M., de Souza, E.E., Basei, F.L., Papa, P.F., Melo Hanchuk, T.D., Cardoso, V.B., and Kobarg, J. (2014). "Stop Ne(c)king around": How interactomics contributes to functionally characterize Nek family kinases. World J. Biol. Chem. *5*, 141–160.

Melixetian, M., Klein, D.K., Sorensen, C.S., and Helin, K. (2009). NEK11 regulates CDC25A degradation and the IR-induced G2/M checkpoint. Nat Cell Biol *11*, 1247–1253.

Moynahan, M.E., and Jasin, M. (2010). Mitotic homologous recombination maintains genomic stability and suppresses tumorigenesis. Nat Rev Mol Cell Biol *11*, 196–207.

Naim, V., Wilhelm, T., Debatisse, M., and Rosselli, F. (2013). ERCC1 and MUS81–EME1 promote sister chromatid separation by processing late replication intermediates at common fragile sites during mitosis. Nat Cell Biol *15*, 1008–1015.

Nikolova, T., Ensminger, M., Löbrich, M., and Kaina, B. (2010). Homologous recombination protects mammalian cells from replication-associated DNA double-strand breaks arising in response to methyl methanesulfonate. DNA Repair (Amst). *9*, 1050–1063.

Petermann, E., and Helleday, T. (2010). Pathways of mammalian replication fork restart. Nat Rev Mol Cell Biol *11*, 683–687.

Petermann, E., Orta, M.L., Issaeva, N., Schultz, N., and Helleday, T. (2010). Hydroxyurea-Stalled Replication Forks Become Progressively Inactivated and Require Two Different RAD51-Mediated Pathways for Restart and Repair. Mol. Cell *37*, 492–502.

Polci, R., Peng, A., Chen, P., Riley, D.J., and Chen, Y. (2004). NIMA-Related Protein Kinase 1 Is Involved Early in the Ionizing Radiation-Induced DNA Damage Response. 8800–8803.

Renkawitz, J., Lademann, C.A., and Jentsch, S. (2014). Mechanisms and principles of homology search during recombination. Nat Rev Mol Cell Biol *15*, 369–383.

Riballo, E., Kühne, M., Rief, N., Doherty, A., Smith, G.C.M., Recio, M.-J., Reis, C., Dahm, K., Fricke, A., Krempler, A., et al. (2004). A Pathway of Double-Strand Break Rejoining Dependent upon ATM, Artemis, and Proteins Locating to γ-H2AX Foci. Mol. Cell *16*, 715–724.

Rothkamm, K., Krüger, I., Thompson, L.H., and Löbrich, M. (2003). Pathways of DNA Double-Strand Break Repair during the Mammalian Cell Cycle. Mol. Cell. Biol. *23*, 5706–5715.

Sarbajna, S., Davies, D., and West, S.C. (2014). Roles of SLX1–SLX4, MUS81–EME1, and GEN1 in avoiding genome instability and mitotic catastrophe. Genes Dev. *28* , 1124–1136.

Schlacher, K., Christ, N., Siaud, N., Egashira, A., Wu, H., and Jasin, M. (2011). Double-Strand Break Repair-Independent Role for BRCA2 in Blocking Stalled Replication Fork Degradation by MRE11. Cell *145*, 529–542.

Schlacher, K., Wu, H., and Jasin, M. (2012). A Distinct Replication Fork Protection Pathway Connects Fanconi Anemia Tumor Suppressors to RAD51-BRCA1/2. Cancer Cell *22*, 106–116.

Shah, P.P., Zheng, X., Epshtein, A., Carey, J.N., Bishop, D.K., and Klein, H.L. (2010). Swi2/Snf2-related translocases prevent accumulation of toxic Rad51 complexes during mitotic growth. Mol. Cell *39*, 862–872.

Sirbu, B.M., Couch, F.B., Feigerle, J.T., Bhaskara, S., Hiebert, S.W., and Cortez, D. (2011). Analysis of protein dynamics at active, stalled, and collapsed replication forks. Genes Dev. *25* , 1320–1327.

Solinger, J. a, Kiianitsa, K., and Heyer, W.-D. (2002). Rad54, a Swi2/Snf2-like recombinational repair protein, disassembles Rad51:dsDNA filaments. Mol. Cell *10*, 1175–1188.

Surpili, M.J., Delben, T.M., and Kobarg, J. (2003). Identification of Proteins That Interact with the Central Coiled-Coil Region of the Human Protein Kinase NEK1†. Biochemistry *42*, 15369–15376.

Swagemakers, S.M.A., Essers, J., de Wit, J., Hoeijmakers, J.H.J., and Kanaar, R. (1998). The Human Rad54 Recombinational DNA Repair Protein Is a Double-stranded DNA-dependent ATPase. J. Biol. Chem. *273* , 28292–28297.

Thangavel, S., Berti, M., Levikova, M., Pinto, C., Gomathinayagam, S., Vujanovic, M., Zellweger, R., Moore, H., Lee, E.H., Hendrickson, E.A., et al. (2015). DNA2 drives processing and restart of reversed replication forks in human cells. J. Cell Biol. *208* , 545–562.

Thiel, C., Kessler, K., Giessl, A., Dimmler, A., Shalev, S. a., Von Der Haar, S., Zenker, M., Zahnleiter, D., Stöss, H., Beinder, E., et al. (2011). NEK1 mutations cause short-rib polydactyly syndrome type majewski. Am. J. Hum. Genet. *88*, 106–114.

Thomä, N.H., Czyzewski, B.K., Alexeev, A. a, Mazin, A. V, Kowalczykowski, S.C., and Pavletich, N.P. (2005). Structure of the SWI2/SNF2 chromatin-remodeling domain of eukaryotic Rad54. Nat. Struct. Mol. Biol. *12*, 350–356.

Wright, W.D., and Heyer, W.-D. (2014). Rad54 Functions as a Heteroduplex DNA Pump Modulated by Its DNA Substrates and Rad51 during D Loop Formation. Mol. Cell *53*, 420–432.

Ying, S., Minocherhomji, S., Chan, K.L., Palmai-Pallag, T., Chu, W.K., Wass, T., Mankouri, H.W., Liu, Y., and Hickson, I.D. (2013). MUS81 promotes common fragile site expression. Nat Cell Biol *15*, 1001–1007.

Zellweger, R., Dalcher, D., Mutreja, K., Berti, M., Schmid, J.A., Herrador, R., Vindigni, A., and Lopes, M. (2015). Rad51-mediated replication fork reversal is a global response to genotoxic treatments in human cells. J. Cell Biol. *208*, 563–579.

4.7 Figure legends

Figure 1. Nek1 Functions during the DNA Damage Response and Serves to Maintain Genomic Stability

(A) Chromosome spreads of human fibroblasts. Chromatid breaks were analyzed in Nek1-deficient (ERDA1) and control (HSF1) cells both spontaneously (NT: not treated) and after a 20 h exposure to HU or APH. Mean ± SEM (n=3).

(B) Clonogenic survival of Nek1-deficient cells. Two independent shNek1 HeLa cell clones were generated by genomic shRNA insertion. Non-silencing shRNA was used as a control. DNA damage was induced by MMS (for 1 h), Olaparib (permanent), or X-rays. Mean ± SEM (n=3).

(C) γH2AX and Rad51 foci in Nek1-depleted and GFP-Nek1-complemented cells. Asynchronous cells were co-treated with MMS and EdU for 1 h. γH2AX and Rad51 foci were enumerated in EdU-positive cells (see Figure S1B). Mean ± SEM (n=3); spontaneous foci were subtracted.

(D) Chromatin fraction of Rad51 in Nek1-depleted cells. Synchronized cells were X-irradiated in G2 (see Figure S1C) and chromatin fractions were analyzed for Rad51 by immunoblotting. H3 and αTubulin signals demonstrate the efficiency of chromatin fractionation (sol.: soluble fraction).

Figure 2. Nek1 Functions during DSB Repair by HR and Interacts with Rad54

(A) γH2AX and Rad51 foci in Nek1-, Rad54- and Brca2-depleted cells. HeLa cells were treated with siRNAs, EdU labeled, and X-irradiated. γH2AX and Rad51 foci were analyzed in EdU-negative G2-phase cells (see Figure S2A). Mean ± SEM (n=3); spontaneous foci were subtracted.

(B) γH2AX foci in catalytically-deficient Nek1 cells. HeLa cells were treated with siNek1, transfected with siRNA resistant plasmids, X-irradiated and γH2AX foci were enumerated 8 h post 2 Gy in G2-phase cells identified as in panel A. Mean ± SEM (n=3); spontaneous foci were subtracted.

(C) GFP-based HR reporter assay with Nek1-, Rad54-, Brca2-, and Ku80-depleted cells. HeLa pGC cells were treated with siRNAs and transfected with an I-*Sce*I plasmid. The number of GFP-positive cells was analyzed by IF microscopy. Mean ± SEM (n=4).

(D) Physical interaction between Nek1, Rad54 and Rad51 in HeLa cells. Proteins were immunoprecipitated from nuclear cell extracts at 5 h post irradiation and interactions were tested by immunoblotting.

Figure 3. Nek1 Phosphorylates Rad54 at Ser572 Specifically in G2 Phase

(A) Schematic diagram showing the position of Ser572 within ATPase domain V of Rad54. GFP-Rad54 plasmids with point mutations S572A and S572E were generated by site-directed mutagenesis.

(B) Detection of Rad54 phosphorylation using autoradiography. GFP-coupled Rad54-WT or Rad54-S572A was obtained from transfected Hek293 cells by IP. The *in vitro* kinase assay was performed

with radioactive ATP and constitutively active recombinant Nek1. The presence of Rad54 in the reaction was controlled by immunoblotting. Arrows indicate phosphorylated GFP-Rad54 and autophosphorylated Nek1.

(C) Detection of Rad54 phosphorylation using a phospho-specific antibody. The *in vitro* kinase assay was performed as in panel B and Rad54 phosphorylation at Ser572 (Rad54-pS572) was analyzed with a phospho-specific antibody.

(D) Detection of Rad54 phosphorylation *in vivo*. HeLa and Hek293 cells were treated with siRNAs prior to X-irradiation. Cell extracts were obtained at 4 h post 10 Gy and analyzed by immunoblotting using the antibody against Rad54-pS572.

(E) Time course of Rad54 phosphorylation in G2-irradiated cells. HeLa cells were synchronized in G2 (see Figure S3A), X-irradiated, and Rad54-pS572 in nuclear cell extracts was analyzed by immunoblotting.

(F) Time course of Rad54 phosphorylation in S- and G2-irradiated cells. HeLa cells were synchronized in S or G2 (see Figure S3A and B), X-irradiated, and Rad54-pS572 in nuclear cell extracts was analyzed by immunoblotting.

(G) Analysis of the phosphorylated fraction of Rad54 in G2-irradiated cells. HeLa cells were synchronized in G2, X-irradiated, and Rad54 phosphorylation was analyzed on Phos-tag™ gels via immunoblotting. GAPDH and Nek1 were analyzed on a regular acrylamide gel. Phosphatase treatment was applied to control phospho-specific band shifts.

Figure 4. Nek1 Promotes HR by Phosphorylating Rad54 at Ser572

(A) Generation of GFP-Rad54 mutants. HeLa clones with stably integrated siRNA-resistant and GFP-tagged Rad54-WT, Rad54-S572A or Rad54-S572E were generated (named 54WT, 54SA, and 54SE) and treated with siRad54. IF images show cells with GFP-Rad54 and Rad51 foci at 2 h post 2 Gy.

(B) Rad51 and γH2AX foci in Rad54 mutants. HeLa clones were treated with siRNAs, X-irradiated and Rad51 and γH2AX foci were analyzed in G2-phase cells that were identified as in Figure 2A. Mean ± SEM (n=3); spontaneous foci numbers were subtracted. 54KD: HeLa cells treated with siRad54.

(C) Chromatin fraction of Rad51 in Rad54 mutants. HeLa clones were treated with siRad54, synchronized, irradiated with 10 Gy in G2, and chromatin fractions were analyzed by immunoblotting. The soluble fractions served as controls.

(D) SCEs and chromatid breaks in Rad54 mutants. HeLa clones were treated with siRad54, EdU labeled, and X-irradiated. SCEs and chromatid breaks were analyzed in EdU-negative mitotic spreads from G2-irradiated cells (see Figure S4E). Mean ± SEM (n=3); spontaneous SCEs and breaks were subtracted.

(E) Rad51 foci in transiently transfected HeLa cells. Cells were treated with siRNAs, transfected with siRNA-resistent Rad54 plasmids and X-irradiated. Rad51 foci were counted in G2-phase cells (identified as in Figure 2A) which formed GFP-Rad54 foci (~30% of all transfected cells). Mean ± SEM (n=4).

(F) GFP-based HR reporter assay with transiently transfected HeLa pGC cells. Cells were treated with siRNAs and transfected with RFP-Rad54 and I-*Sce*I plasmids. The ratio between RFP-positive cells which were also positive for GFP and all RFP-positive cells was assessed by IF microscopy. Note that the impact of a deficiency in HR, exemplified by cells treated with siBrca2, is less pronounced than in Figure 2C, likely due to the modified experimental setup involving the dual transfection of I-*Sce*I and RFP-Rad54 plasmids. Mean ± SEM (n=4).

Figure 5. Rad54 Phosphorylation during S Phase Causes Rad51 Removal from Stalled Replication Forks

(A) Chromatin fraction of Rad51 in Rad54 mutants. HeLa clones were treated with siRad54 prior to HU treatment (4 mM for 5 h), and chromatin fractions were analyzed by immunoblotting. The soluble fractions served as controls.

(B) Chromatin-bound Rad51 in Rad54 mutants. HeLa clones were treated with siRad54, co-treated with HU (0.5 mM for 2 h) and EdU, and chromatin-bound Rad51 levels were analyzed by IF microscopy in EdU-positive nuclei. Rad51 showed a distribution of intensities with signals in the gray value range between 20 and 55 representing non-foci signals and intensities between 150 and 250 representing foci signals. The analysis was restricted to signals between 20 and 55. The mean ± SEM for each intensity is shown (n=4)

(C) Analysis of proteins bound to stalled replication forks using iPOND. Hek293 cells were labeled with EdU, followed by different times of HU treatment. H3 signals were used to control the pull-down efficiency of EdU-labeled chromatin.

(D) Analysis of proteins bound to stalled replication forks in Rad54 mutants using iPOND. HeLa clones were treated with siRad54 prior to EdU labeling and HU treatment. H3 signals were used to control the pull-down efficiency of EdU-labeled chromatin.

Figure 6. Rad54 Phosphorylation during S Phase Causes Degradation of Stalled Replication Forks

(A) DNA degradation at stalled forks in Rad54 mutants analyzed by the DNA fiber assay. CldU was added to siRad54-treated HeLa clones, followed by HU treatment and an IdU pulse. CldU-positive DNA fibers were analyzed and categorized according to size. The mean ± SEM for each category separately and for all categories together are shown (n=5).

(B) Replication fork recovery in Rad54 mutants. HeLa clones were treated with siRad54 and HeLa cells with siCtrl, siRad54 or siRad51 prior to the experiment which was performed as in panel A. CldU-positive fibers without a flanking IdU signal were scored (indicated by arrow). Mean ± SEM (n=5).

(C) DNA degradation at stalled forks in the 54SE mutant analyzed by the DNA fiber assay. CldU was added to siRNA-treated 54SE cells, followed by HU treatment and an IdU pulse. The analysis was performed as in panel A. Mean ± SEM (n=3).

(D) DNA degradation at stalled forks in 54WT or 54SE cells analyzed by the DNA fiber assay. HeLa clones were treated with siRNAs and/or Mirin. CldU was added, followed by HU treatment and an IdU pulse. The analysis was performed as in panel A. Mean ± SEM (n=3).

Figure 7. Cells with Unregulatable Rad54 Show Genomic Instability

(A) γH2AX foci in mitotic Rad54 mutants. HeLa clones were treated with siRad54 and exposed to low concentrations of APH (0.3 μM) for 20 h. γH2AX foci were quantified in pH3-positive pro- and metaphases. Mean ± SEM (n=3).

(B) 53BP1 bodies in Rad54 mutants in G1 phase. HeLa clones were treated with siRad54, exposed to low concentrations of APH (0.3 μM) for 24 h, and EdU labeled. 53BP1 bodies were counted in EdU-negative G1-phase cells. Mean ± SEM (n=3).

(C) Clonogenic survival of Rad54 mutants. SiRad54-treated HeLa clones were treated with MMS (for 1 h), Olaparib (permanent), or X-rays. Mean ± SEM (n=3).

(D) Model: Effects of timely phosphorylation of Rad54 (box 1 and 3): The absence of Rad54 phosphorylation during S phase stabilizes Rad51 at stalled replication forks to prevent degradation of newly synthesized DNA. The presence of Rad54 phosphorylation in G2 phase promotes Rad51 removal and the completion of HR. Consequences of untimely phosphorylation of Rad54 (box 2 and 4): Rad54 phosphorylation during S phase destabilizes Rad51 at stalled replication forks causing degradation of newly synthesized DNA. The absence of Rad54 phosphorylation in G2 phase prevents Rad51 removal and the completion of HR.

4.8 Supplemental information

SUPPLEMENTAL EXPERIMENTAL PROCEDURES

Cell Culture

Primary human fibroblasts used were HSF1 (control), HSC62 (Brca2 deficient), 180BR (LigIV deficient) and ERDA1 (Nek1 deficient); immortalized and transformed cell lines used were 82-6 hTert (control), HeLa, HeLa pGC (clone 2), HeLa shNek1-1, HeLa shNek1-2, HeLa GFP-Rad54 clones and

Hek293. HeLa and Hek293 cells were cultured in DMEM supplemented with 10% FCS and 1% NEAA. ERDA1 cells in DMEM supplemented with 15% FCS and 1% NEAA. HSF1 cells in MEM supplemented with 10% FCS and 1% NEAA. All other cell lines were cultured in MEM supplemented with 20% FCS and 1% NEAA. All cells were maintained at 37°C in a 5% CO_2 incubator.

Generation of Stable Cell Lines

Lentiviral transduction of a pTRIPZ vector was used to generate shNek1-expressing HeLa cell lines following the manufacturer´s protocol (ThermoFisher Scientific). pTRIPZ vectors carried shRNA against Nek1 (shNek1-1: AAT CTA CGA AGT ATT TCT C; shNek1-2: TAA ATA ATT GCT GTA TTT C) or a non-silencing control sequence (shCtrl: CTT ACT CTC GCC CAA GCG AGA G) and a puromycin resistance cassette. Nek1-depletion was induced by addition of 2 µg/ml doxycycline to the media for at least 4 days. Positive clones were identified by immunoblotting. Stable cell lines expressing GFP-Rad54 variants were generated by transfecting GFP-Rad54 plasmids into HeLa cells followed by G418 treatment for selection. Clonal cell lines were identified and analyzed by immunoblotting.

RNA Interference

SiRNA transfection of HeLa and 82-6 hTert cells was carried out using HiPerFect Transfection Reagent following the manufacturer's instructions (Qiagen). Brca2, Rad54, Rad51 and Nek1 siRNAs were used at a final concentration of 25 nM (20 nM for Ku 80). Cells were transfected immediately after cell seeding. A second transfection was performed 24 h after the first transfection. SiRNA sequences were as follows: siBrca2 (TTG GAG GAA TAT CGT AGG TAA); siRad54 (GAA CTC CCA TCC AGA ATG ATT); siRad51 (AAG GGA ATT AGT GAA GCC AAA); siNek1-1 (AAG GAG AGA AGT TGC AGT ATT); siNek1-2 (AAG GGA AGC TAT GCA GAA TAA); siKu80 (AAG ACA GAC ACC CTT GAA GAC); siMre11 (AAG AAA GGC TCT ATC GAA TGT); siDNA2 (AAA TAG CCA GTA GTA TTC GAT); siCtrl (AAT TCT CCG AAC GTG TCA CGT).

Plasmid Transfection

pEGFP-Rad54-WT-N1 and pDsRed-Nek1-C1 were kindly provided by Roland Kanaar and Jörg Kobarg, respectively. Silent mutations in the siRNA targeting regions and at amino acid positions S572 (for Rad54) and K33 (for Nek1) were generated by site directed mutagenesis. Primers used were: CTT TGT CTT CAT GCT GGC CAG CAA AGC TGG GG (forward for Rad54-S572A), CCC CAG CTT TGC TGG CCA GCA TGA AGA CAA AG (reverse for Rad54-S572A); CTT TGT CTT CAT GCT GGA GAG CAA AGC TGG GG (forward for Rad54-S572E), CCC CAG CTT TGC TCT CCA GCA TGA AGA CAA AG (reverse for Rad54-S572E), GCC AAT ACT GCA CCT CAC GCC TTG ATT CTT CTC (forward for Nek1-K33R), GGC AGA CAG TAT GTT ATC AGG GAA ATT AAC

ATC TCA AGA ATG (reverse for Nek1-K33R). Rad54-WT, Rad54-S572A and Rad54-S572E inserts were excised from pEGFP-Rad54-N1 and cloned into a ptagRFP-N vector using *SnaB*I and *Age*I. Nek1-WT and Nek1-K33R inserts were excised from pDsRed-Nek1-C1 and cloned into a pEGFP-C1 vector using *BamH*I and *Sal*I. 24 - 48 h after cell seeding DNA plasmids were magnet-assisted-transfected into HeLa or Hek293 cells using MATra-A reagent (IBA) following the manufacturer's protocol.

Antibodies

Two different customized Nek1 antibodies (rabbit) and a phosphospecific Rad54-pS572 antibody (rabbit) were purchased from ThermoFischer Scientific. Other antibodies used were purchased from Abcam: rat anti-BrdU (ab6326), rabbit anti-DNA2 (ab96488), mouse anti-Rad51 (ab213), rabbit anti-Rad51 (ab63801), mouse anti-H3 (ab10799); Abgent: rabbit anti-Nek1 (AP80723); Becton Dickinson: mouse anti-BrdU (347580); Biocat: rabbit anti-RFP (AB233); Cell Signaling Technology: rabbit anti-Brca2 (9012), mouse anti-pH3 (9706), mouse anti-Chk1 (2360), rabbit anti-Ku80 (2180S); Epitomics rabbit anti-γH2AX (2212-1); Roche: mouse anti-GFP (11814460001); Santa Cruz Biotechnology: rabbit anti-GAPDH (sc-25778), rabbit anti-GFP (sc-8334), mouse anti-Rad54 (sc-163370), goat anti-Rad54 (sc-34199), mouse anti-αTubulin (sc-8035); Millipore: mouse anti-53BP1 (05-726), rabbit anti-pH3 (06-570), mouse anti-γH2AX (05-636); Novus Biologicals: rabbit anti-Mre11 (NB100-142).

DNA Damage Induction

X-irradiation was performed at 90 kV and 19 mA (37 mA for doses of 10 Gy) with an aluminium filter at a dose rate of 2,9 Gy/min or 5,2 Gy/min respectively. To induce DSBs during S phase, cells were pulse-treated for 1 h with different concentrations of MMS or Olaparib. For induction of replication stress, cells were treated with HU (Sigma) (1 µM for 20 h, 0.5 mM for 2 h, or 4 mM for 4 h, 5 h, or 8 h) or APH (0.2 or 0.3 µM for 20 or 24 h).

Immunofluorescence

Cells were fixed with 2.5% formaldehyde in PBS for 15 min, washed three times in PBS, permeabilised in 0.5% TritonX100 (PBS/1% FCS) for 10 min at 4°C, and washed thrice in PBS/1% FCS. Samples were blocked for 30 min in 5% BSA (PBS/1% FCS), incubated with primary antibodies over night at 4°C, washed thrice in PBS/1% FCS and incubated for 1 h at room temperature (RT) with Alexa Fluor 488- or Alexa Fluor 594-conjugated secondary antibodies (Invitrogen). EdU staining was carried out with ClickIT® EdU Imaging Kit following the manufacturer's protocol (Invitrogen). Cells were then washed again in PBS, stained with DAPI (Sigma), and embedded in Vectashield mounting medium (Vector Laboratories). For the EdU-incorporation assay, cells were pre-extracted 5 min with 0.5% TritonX100 (PBS) prior to fixation. All cells were examined using a Zeiss microscope and

Metasystems software (Metasystems). For intensity measurements of chromatin-bound Rad51, cells were pre-extracted with 100% methanol for 12 min at -20°C. EdU-positive nuclei were captured using a Zeiss microscope and analyzed with the histogram function of ImageJ software. At least 40 nuclei were evaluated per experiment.

Cell Cycle-specific DSB Repair

For S-phase labeling and to analyze the repair of DSBs in a cell cycle-specific manner, 10 µM EdU was added to the cells 30 min prior to irradiation. Additionally, 100 ng/ml nocodazole was added immediately after irradiation to prevent G2 phase cells from progressing into G1 during repair incubation. After fixation and staining of the cells, DAPI- and EdU-intensities were measured in the nuclei and blotted in a diagram. Populations of G1-, G2-, or S-phase cells were gated and single cells were relocated for foci evaluation (Beucher et al., 2009). For foci analysis post MMS, 10 µM EdU and MMS was pulse treated for 1 h simultaneously. At least 40 cells were relocated for foci evaluation in each experiment.

Cell Synchronization and FACS

Proliferating HeLa cells or Rad54 mutants were treated with 2 mM thymidine for 16 h, released in thymidine-free medium for 10 h and again treated with thymidine for 14 h. Cells were again released in fresh medium not supplemented with thymidine and irradiated with 10 Gy (or treated with 1 mM MMS for 1 h) at different times post release. Cell synchronization was controlled by propidium iodide FACS as described previously (Ensminger et al., 2014b).

Immunoblotting

Whole cell extracts, nuclear cell extracts, soluble or chromatin-bound protein fractions were generated as described previously (Barton et al., 2014). Protein extracts were prepared for SDS-PAGE or Phos-tag™ gels (Wako) in Laemmli buffer. Separated proteins were transferred to PVDF or nitrocellulose membranes. The membranes were blocked for 1 h in 5% BSA or low fat milk and incubated with antibodies at 4°C over night. Membranes were incubated with HRP-conjugated secondary antibody (Santa Cruz Biotechnology) for 1 h at RT, washed and chemiluminescence signals were detected with a Chemi-Smart system (Vilber Lourmat).

Co-Immunoprecipitation

4 µg antibodies and 25 µl Dynabeads™ ProteinG (Invitrogen) were incubation at 4°C over night. Antibodies were cross-linked to Dynabeads™ using 1 ng/µl disuccinimidyl suberate (AppliChem). Protein precipitation was carried out in lysis buffer (20 mM Tris, 150 mM NaCl, 1% Triton, pH 8.2) supplemented with protease and phosphatase inhibitors (Complete and PhosSTOP, Roche). DNAse-

treated protein extracts were incubated with antibody-Protein G complexes at 4°C over night. Precipitated immune complexes were washed thrice in lysis buffer, boiled in SDS sample buffer and loaded onto SDS-PAGE. Separated proteins were immunoblotted as described above.

In Vitro Phosphorylation and Dephosphorylation

Hek293 cells were transiently transfected with various GFP-Rad54 constructs or with an empty GFP vector. GFP-tagged proteins were obtained by IP against GFP. Recombinant Nek1 protein (0.2 µg) (Invitrogen) was diluted in 20 µl kinase buffer (25 mM Tris, 10 mM $MgCl_2$, 0.5 mM EGTA, 0.5 mM Na_3VO_4, 2.5 mM DTT, 0.01% TritonX-100, 200 µM ATP; pH 7.5) and pre-incubated at 30°C for 15 min. The kinase buffer containing constitutively active Nek1 was added to the substrates and the kinase assay was carried out in the presence of 10 µCi [^{32}P] ATP at 30°C for 30 min. Phosphorylated proteins were detected by autoradiography after SDS-PAGE and gel drying. For the detection of Rad54 phosphorylation by immunoblotting with the phospho-specific antibody, the kinase assay was carried out under the same conditions, but cold ATP was used instead of radioactive ATP. The phosphatase assay using lambda protein phosphatase (New England Biolabs) was carried out according to the manufacturer's description.

Chromosome Breaks, Cell Proliferation and Clonogenic Survival

For SCE preparation HeLa cells were treated with BrdU for 48 h. Cells were then irradiated with 2 Gy and collected in mitosis between 7 and 10 h post IR. Cells were additionally treated with EdU 30 min prior to irradiation for specific evaluation of cells irradiated in G2 phase. Preparation of chromosome spreads and EdU staining for analysis of SCEs and chromatid breaks in EdU-negative G2-phase cells was carried out as described previously (Conrad et al., 2011). For analysis of chromatid breaks in primary fibroblasts, cells were incubated with 1 µM HU or with 0.2 µM APH for 20 h prior to premature chromosome condensation in G2 phase caused by addition of 50 ng/ml calyculin A (Calbiochem) for 30 min. For each experiment at least 40 chromosome spreads were captured and analyzed using an Axioplan2 microscope (Zeiss) and Metafer software (MetaSystems). For proliferation studies, cells were treated with 0.5 mM MMS for 1 h and cell numbers were counted at day 2, 4 and 7 post MMS treatment. The clonogenic survival assay was carried out in shCtrl, shNek1-1, shNek1-2 cells or in HeLa cell clones which stably express GFP-Rad54 variants. Prior to DNA damage induction by X-rays, MMS, or Olaparib cells were treated with doxycycline to induce Nek1 depletion or siRad54 treatment to induce depletion of endogenous Rad54 protein. 24 h prior to DNA damage induction distinct numbers of cells were seeded and incubated for 10 days at 37°C and 5% CO_2 as described previously (Nikolova et al., 2010; Riballo et al., 2004).

HR Reporter Assay

HeLa pGC cells, containing a stably integrated HR substrate, were kindly provided by Jochen Dahm-Daphi. 24 h after siRNA treatment, HeLa pGC cells were transfected with ptagRFP-Rad54-N plasmids and I-*Sce*I expression vector. 48 h later cells were fixed and stained against DAPI and GFP or DAPI, GFP and RFP. All cells were analyzed using a Zeiss microscope and MetaCyte software (Metasystems). At least 15000 cells were analyzed per experiment.

iPOND

iPOND technology was carried out as previously described (Sirbu et al., 2011) with slight modifications. HeLa clones or Hek293 cells were 12 min pulse treated with 10 µM EdU. Cells were then treated with 5 mM HU for 4, 5 or 8 h and subsequently fixed using 1% formaldehyde for 15 min at RT. Cross-linking reaction was stopped with 0.125 M glycine and cells were pelleted. After washing cells with PBS cells were incubated with 0.25% TritonX-100 in PBS for 15 min at RT and again pelleted. Permeabilization was stopped with 0.5% BSA in PBS. Cells were pelleted again and washed with PBS. After centrifugation cells were resuspended with a click reaction cocktail (10 µM biotin azide, 10 mM sodium ascorbate, and 2 mM $CuSO_4$ in PBS) and incubated for 1.5 h at RT on a rotator. After centrifugation, click reaction was stopped by resuspending cells with 0.5% BSA in PBS. Cells were pelleted and washed with PBS twice. Cells were lysed in RIPA buffer and sonicated with max power in 20 s pulses with a Bandelin sonopuls GM70 sonicator. Lysates were cleared and then incubated with 70 µl of streptavidin-coupled magnetic beads over night at 4°C on a rotator. Beads were washed thrice with RIPA buffer and once with PBS. Co-precipitated proteins were analyzed by immunoblotting.

DNA Fiber Assay

HeLa cells were labeled with 30 µM CldU (Roth) for 30 min at 37°C, washed 5 times with PBS followed by exposure to 4 mM HU for 5 h or 8 h. After HU treatment cells were labeled with 225 µM IdU (Roth) for 30 min at 37°C. For experiments carried out with Mre11 inhibitor Mirin (Sigma), 75 µM Mirin was added to the media 30 min prior to CldU treatment and was also added to cells during HU treatment. Cells were then trypsinized at 4°C and dropped onto a glass slide, lysed and DNA fibers were spreaded as described by (Schlacher et al., 2011). CldU- and IdU-positive DNA tracts were stained with primary antibodies rat anti-BrdU (1:5000) and mouse anti-BrdU (1:1500). Secondary antibodies were Alexa Fluor 594 (rat) and Alexa Flour 488 (mouse). DNA fibers were imaged with Zeiss Axio Observer microscope and tract length of CldU- and IdU-positive DNA fibers were analyzed using ImageJ software. At least 200 CldU-positive fibers were evaluated per experiment.

Rad54 expression and purification

N-terminally GST-tagged Rad54-WT, -S572A, and -S572E proteins were cloned into pFastbac vectors and expressed using the Bac to Bac insect cell expression system (Invitrogen). Sf9 cells were infected with 1/10 culture volume of P3 virus at ~3 x10^6 cells/ml and were collected after 72 h. Two sets of Rad54-WT, -S572A and -S572E pFastbac expression constructs were generated independently, with and without a TEV protease recognition site between the GST tag and the start of Rad54. Cleavage with TEV protease at this site yields native Rad54 without retention of any extra amino acids, *i.e.* cleavage occurs preceding the initiating methionine. To purify Rad54 proteins followed by proteolytic removal of the GST tag, an amount of cells corresponding to 0.5 l original culture volume was lysed in 50 ml lysis buffer (50 mM Tris-HCl pH 7.5, 1 M KCl, 2 mM EDTA, 10% glycerol, and 0.5% IGEPAL CA-630, 0.5 mM TCEP and protease inhibitors) with stirring for about 1.5 h. All steps were carried out at 4°C. The cell lysate was cleared by ultracentrifugation in a Ti 70 rotor at 45,000 rpm for 45 min. The cleared lysate was batch bound to 3 ml pre-equilibrated glutathione agarose beads (Pierce) for 2 h with agitation. Beads were briefly pelleted by centrifugation at 500 rpm in a swinging bucket tabletop centrifuge, resuspended in 20 ml lysis buffer and poured into a 1.5 cm diameter column (BioRAD). The column was washed extensively (~150 ml at 1ml/min) with buffer A (20 mM Tris HCl pH 7.5, 10% glycerol, 1 mM EDTA, 0.5 mM TCEP) + 1 M KCl, followed by a 30 ml wash with A/400 mM KCl. Purified GST-TEV protease (600 µg) was added and the beads resuspended with a glass rod, and digestion was allowed to occur over night. A 5 ml pool of digested material was then collected (GST-TEV protease remains bound to column) and applied to a Sephacryl S 300 column (130 ml), which was developed in A/400 mM KCl. The S300 peak fractions were pooled and concentrated to ~300 µl in a 15 ml, 30 kDa MWCO centrifugal filter device (Amicon), aliquoted and flash frozen in liquid nitrogen.

Rad54 protein preparations retaining the GST tag were carried out similarly with the following changes. The lysis buffer contained only 200 mM KCl and DNA was eliminated through passage of lysate through a 30 ml Q-sepharose column pre-equilibrated with A/200 mM KCl buffer. The flow-through was collected and the solution adjusted to 500 mM KCL with the addition of 3 M KCl solution. 10 ml pre-equilibrated glutathione agarose was then added and incubated with agitation for 2 h. The slurry was then poured into a 1.5 cm diameter column and washed with 100 ml A/500 mM KCl. Rad54 was then eluted with 30 ml of A/500 KCl/20 mM reduced glutathione. The Rad54-containing fractions were pooled and diluted with 5 volumes of buffer A and loaded onto a 1 ml monoS column, washed with buffer A/100 mM KCl and eluted with a 40 ml gradient of 0.1-0.5 M KCl. Rad54-containing fractions were flash frozen in liquid nitrogen and stored at -80°C.

D-loop assay

D-loop reaction mix contained 30 mM Tris-HCl pH 7.4, 1 mM ATP, 2 mM $MgCl_2$, 2 mM $CaCl_2$, 50 mM KCl 0.25 mg/ml BSA, 0.5 mM TCEP, 10 mM phosphocreatine, and 0.1 mg/ml phosphocreatine kinase. The ssDNA substrate was ds98-*402* (5' 98 bp dsDNA heterology, 402 nt ssDNA 3' homology to a PhiX174-derived sequence). In 20 µl total volume, Rad51 (0.2 µM) filaments were formed on ds98-*402* (0.76 µM bp/nt) for 10 min at 30°C (throughout), followed by RPA (25 nM heterotrimer) for 10 min. Next, donor plasmid and Rad54 variants were delivered together (120 nM; 30 µM bp, respectively) and incubation continued for 20 min before processing for agarose gel electrophoresis and phosphoimaging of products (for details, see Wright and Heyer, 2014).

GST pull downs/Rad51 interaction assay

GST-Rad54 variants (200 nM, 0.44 µg) or GST (2 µg) were incubated with 20 µl of a 50% slurry of pre-equilibrated glutathione agarose beads in a total volume of 60 µl of binding buffer containing 20 mM Tris acetate, pH 7.4, 100 mM (or as indicated) KCL, 10% glycerol, 1 mM EDTA, 0.1% IGEPAL CA630, 0.25 mg/ml BSA and 1 mM DTT. An air bubble of ~20 µl was introduced to facilitate mixing and prevent beads from settling as the mixtures were rocked in 0.5 ml eppendorf tubes on a nutator apparatus (Becton Dickenson). Beads were incubated in such a manner with GST-Rad54 for 30 min at RT before the addition of the indicated concentrations of 10x Rad51 in 6 µl binding buffer (bringing the total to 60 µl), and incubation continued for a further hour. Beads were pelleted by brief centrifugation and washed 3 times in 60 µl reaction buffer. All buffer was then removed from the beads and they were resuspended in 100 µl of 1.5x Laemmli buffer and promptly heated to 95°C for 5 min. 10 µl of these samples was then separated on SDS PAGE gels, stained with Sypro orange and imaged on a Storm 860 scanner.

Rad54 ATPase assay

ATPase activity was measured at 30°C using the NADH-coupled assay, which allows for continuous monitoring of ATPase activity, essentially as described previously (Wright et al., 2014). Reactions (100 µl final) contained 10 nM Rad54 variants and where indicated included Rad51 (at noted concentrations), dsDNA (pUC19 at 6 µM bp), and/or ssDNA (6 µM nt of 100 mer poly dT).

DNA binding assay

Rad54 variants were bound to DNA in a total volume of 10 µl containing 6 µM bp of *Xmn*I-linearized pBluescript DNA in a buffer containing 20 mM Tris-HCl pH 7.5, 100 mM KCl, 0.1 mg/ml BSA, 0.1% CHAPS, 1 mM EDTA, 0.5 mM TCEP at RT for 5 min. 2 µl 6X DNA load dye (1x: 2.5% ficol, 0.01% bromophenol blue, 10 mM EDTA) was then added, samples were quickly mixed and loaded in a 1%

agarose, TBE gel and electrophoresed at 80 V for 3 h. The gel was then stained with 1: 10,000 CYBR gold (Invitrogen) and imaged.

SUPPLEMENTAL FIGURE LEGENDS

Figure S1 (related to Figure 1): Nek1 Functions during the DNA Damage Response and Serves to Maintain Genomic Stability after Various DNA-damaging Agents

(A) Cell proliferation of untreated or MMS-treated (0.5 mM for 1 h) control (HSF1), Brca2-deficient (HSC62), and Nek1-deficient (ERDA1) primary human fibroblasts. Mean ± SEM (n=3). NT: not treated.

(B) S phase-specific foci analysis in control (shCtrl) and Nek1-depleted (shNek1) HeLa cells using a semi-automated microscopic approach. Asynchronous cells were co-treated with MMS and EdU for 1 h and scanned, after immunofluorescence labeling, under the microscope. The EdU signal was plotted against the DAPI signal, and S-phase cells were identified based on their EdU signal. S-phase cells were then marked in the histogram (red ovals) and automatically relocated for manual foci counting. Note that cells progress from S into G2 phase during the 10 h interval post MMS treatment.

(C) FACS analysis of synchronized control (shCtrl) and Nek1-depleted (shNek1) HeLa cells. Cells were synchronized at the G1/S border using a double thymidine block. 8 h post thymidine release, cells have progressed into G2 phase and were irradiated with 10 Gy. Cells remained in G2 phase for at least 12 h post irradiation due to G2 checkpoint induction.

Figure S2 (related to Figure 2): Nek1 Functions during DSB Repair by HR and Interacts with Rad54

(A) Upper four panels: G1- and G2-specific foci analysis in control (siCtrl) and Nek1-depleted (siNek1) HeLa cells using a semi-automated microscopic approach. Asynchronously growing cells were treated with EdU 30 min prior to X-irradiation until the end of the repair time and scanned, after immunofluorescence labeling, under the microscope. The EdU signal was plotted against the DAPI signal, and G1 cells were discriminated from G2 cells based on their DAPI signal (DNA content) and from S-phase cells by the absence of EdU. Control experiments confirmed that all G1 cells were negative and all G2 cells positive for the S/G2 marker CENP-F (Barton et al., 2014). Cells identified as G1 or G2 cells were then marked in the histogram (red ovals) and automatically relocated for manual foci enumeration. Note that the majority of irradiated G2 cells remained in G2 for at least 8 h post irradiation due to G2 checkpoint induction. To prevent that a small fraction of G2-irradiated cells progressed into G1 phase during repair incubation, nocodazole was added during the time of repair

incubation. Lower two panels: γH2AX foci kinetics in G1- and G2-phase HeLa cells treated with siRNAs 48 h prior to irradiation. Mean ± SEM (n=3); spontaneous foci numbers were subtracted.
(B) Rad51 foci analysis in G2-phase HeLa cells treated with siRNAs 48 h prior to irradiation. Co-depletion of Nek1 and Rad54 shows epistasis between Nek1 and Rad54. Mean ± SEM (n=3); spontaneous foci numbers were subtracted. The immunoblot demonstrates the siRNA efficiencies.
(C) γH2AX foci kinetics in G1- and G2-phase primary human fibroblasts (control: HSF1; Nek1-deficient: ERDA1; Brca2-deficient: HSC62; LigIV-deficient: 180BR). Elevated foci numbers in G1 phase are indicative of defective NHEJ. In G2 phase, NHEJ mutants exhibit elevated foci numbers at all time points while HR mutants are specifically defective at repair times > 4 h (Beucher et al., 2009). Mean ± SEM (n=3); spontaneous foci numbers were subtracted.
(D) Rad51 foci analysis in non-transformed G2-phase human fibroblasts (82-6 hTert) treated with siRNAs 48 h prior to irradiation. Mean ± SEM (n=3); spontaneous foci numbers were subtracted.
(E) Immunoblots demonstrating the efficiencies of Brca2, Ku80, Nek1, and Rad54 depletion in HeLa pGC cells treated with siRNAs for 48 h. IF images show GFP-positive cells (green) 48 h post I-*Sce*I transfection.
(F) SCE analysis in HeLa cells. Cells were treated with siRNAs for 48 h, labeled with EdU, and X-irradiated. SCEs were analyzed in EdU-negative mitotic spreads from G2-irradiated cells (see Figure S4E for images). Mean ± SEM (n=3); spontaneous SCEs were subtracted.
(G) Analysis of recombination-associated repair foci in HeLa cells. DNA synthesis occurs during later stages of HR and can be visualized via the incorporation of EdU at repair sites giving rise to distinct foci (Beucher et al., 2009). Cells were treated with siRNAs for 48 h, labeled for 30 min with BrdU prior to irradiation, and afterwards labeled with EdU during the entire repair period. EdU foci were enumerated in BrdU-negative G2-phase cells. Mean ± SEM (n=3).
(H) Physical interaction between Nek1, Rad54 and Rad51 in Hek293 cells. Nek1 was immunoprecipitated from nuclear cell extracts, and Rad54 and Rad51 were analyzed for co-IP by immunoblotting.

Figure S3 (related to Figure 3): Nek1 Phosphorylates Rad54 at Ser572 Specifically in G2 Phase
(A) FACS analysis of synchronized HeLa cells. Cells were synchronized at the G1/S border using a double thymidine block. 8 h post thymidine release, cells have progressed into G2 phase and were irradiated with 10 Gy. Cells remained in G2 phase for at least 8 h post irradiation due to G2 checkpoint induction.
(B) Upper panels: FACS analysis of synchronized HeLa cells. Cells were synchronized at the G1/S border using a double thymidine block. 1.5 h post thymidine release, cells have progressed to early S phase and were irradiated with 10 Gy. After irradiation, cells progressed from early S phase to late S phase (8 h post irradiation) and into G2 phase (16 h post irradiation). Lower panel: Time course of

Rad54 phosphorylation after damage induction in S phase. HeLa cells were synchronized in early S phase (1.5 h after thymidine release), irradiated or treated for 1 h with MMS, and Rad54-pS572 in nuclear cell extracts was analyzed by immunoblotting.

(C) Time course of Rad54 phosphorylation in unirradiated HeLa cells. HeLa cells were synchronized at the G1/S border by a double thymidine block, released in fresh medium and harvested at different time points post thymidine release. Rad54-pS572 signals were analyzed by immunoblotting. CyclinA and pH3 control the progression from S phase to late G2 phase/mitosis.

Figure S4 (related to Figure 4): Nek1 Promotes HR by Phosphorylating Rad54 at Ser572

(A) Physical interaction between Rad51 and the Rad54 mutants. Hek293 cells were transfected with GFP-Rad54 constructs, without siRad54 treatment, irradiated 30 h later with 10 Gy, and harvested after a 2 h repair time. Rad51 was immunoprecipitated from nuclear cell extracts and GFP-Rad54 proteins were analyzed for co-IP by immunoblotting. IgG antibody served as a control for unspecific binding.

(B) Formation of GFP-Rad54 foci in Rad54 mutants. HeLa clones were treated with siRad54 48 h prior to X-irradiation. GFP-foci numbers and the fraction of foci which co-localize with Rad51 foci were analyzed at 2 h post 2 Gy in G2-phase cells that were identified as in Figure S2A. Mean ± SEM (n=3); spontaneous foci numbers were subtracted.

(C) γH2AX foci analysis in G2-phase HeLa Rad54 mutants treated with siRad54 and siNek1 48 h prior to irradiation. Mean ± SEM (n=3); spontaneous foci numbers were subtracted. The immunoblot demonstrates the siRNA efficiencies.

(D) Upper panels: FACS analysis of synchronized HeLa Rad54 mutants. Cell clones were synchronized at the G1/S border using a double thymidine block. 8 h post thymidine release, G2-phase cells were irradiated with 10 Gy. Cells remained for at least another 10 h in G2 phase. Lower panel: The immunoblot shows the fractionation efficiency of the G2-synchronized cell clones used in Figure 4C.

(E) Representative IF images of EdU-positive and EdU-negative mitotic spreads from 54WT cells. Cells were treated with EdU directly before irradiation until mitotic spreads were prepared 10 h after irradiation. EdU-negative spreads represent G2-irradiated cells while cells irradiated in S phase will give rise to EdU-positive spreads.

(F) The immunoblot demonstrates the depletion of endogenous Rad54 and Nek1 and the expression of GFP-tagged Rad54 variants in the HeLa cells used in Figure 4E.

(G) GFP-Rad54 foci analysis in transiently transfected HeLa Rad54 mutants. Cells were treated with siRNAs 24 h prior to transfection with siRNA-resistent Rad54 plasmids. 48 h later, cells were irradiated with 2 Gy and fixed 8 h later. GFP foci were enumerated in G2-phase cells (identified as described in Figure S2A) Mean ± SEM (n=4).

(H) Analysis of γH2AX foci in the samples described in panel G. γH2AX foci were enumerated in G2-phase cells (identified as described in Figure S2A) which were either able to form GFP-Rad54 foci (~30%) or showed a strong pan-nuclear GFP-Rad54 signal (~70%). Mean ± SEM (n=4).

Figure S5 (related to Figure 5): Rad54 Phosphorylation during S Phase Causes Rad51 Removal from Stalled Replication Forks

(A) Chromatin-bound and soluble fraction of Rad51 after HU treatment. Hek293 cells were transfected with GFP-Rad54 plasmids without siRad54 treatment, 48 h later treated with 4 mM HU for 5 h, and fractions were prepared and analyzed by immunoblotting.

(B) Rad51 foci in Rad54 mutants with and without HU treatment. HeLa clones were treated with siRad54 48 h prior to 0.5 mM HU treatment for 2 h and Rad51 foci were quantified in EdU-positive S-phase cells. IF images show representative cells. Mean ± SEM (n=2).

(C) Rad54 phosphorylation in HeLa cells treated with HU in S phase or X-irradiated in G2 phase. Cells were treated with 4 mM HU for up to 8 h and analyzed immediately by immunoblotting using the antibody against Rad54-pS572; the Rad54 phosphorylation signal at 8 h after irradiation of G2-phase cells served as a positive control.

Figure S6 (related to Figure 6): Rad54 Phosphorylation during S Phase Causes Degradation of Stalled Replication Forks

(A) DNA degradation at stalled forks analyzed by the DNA fiber assay. HeLa cells were treated with siCtrl, siRad51, or siRad54 48 h prior to a CldU pulse for 30 min, followed by exposure to 4 mM of HU for 5 h and a subsequent IdU pulse for 30 min. CldU-positive DNA fibers were analyzed and categorized according to size. The means ± SEM for each category separately and for all categories together are shown (n=5). The curves serve to guide the eye. The immunoblot demonstrates the knock-down efficiency of Rad51.

(B) DNA degradation at stalled forks in 54SE cells analyzed by the DNA fiber assay. Cells were treated with siRad54 and siRad51 48 h prior to a CldU pulse for 30 min, followed by exposure to 4 mM of HU for 5 h and a subsequent IdU pulse for 30 min. CldU-positive DNA fibers were analyzed and categorized according to size. The means ± SEM for each category separately and for all categories together are shown (n=3). The curves serve to guide the eye. The immunoblot demonstrates the knock-down efficiencies of Rad54 and Rad51.

(C) DNA degradation at stalled forks in 54SE cells analyzed by the DNA fiber assay. Cells were treated with siRad54 48 h prior to a CldU pulse for 30 min, followed by exposure to 4 mM of HU for 5 h and a subsequent IdU pulse for 30 min. Mirin was added 30 min prior to and during the HU treatment. CldU-positive DNA fibers were analyzed and categorized according to size. The means ±

SEM for each category separately and for all categories together are shown (n=3). The curves serve to guide the eye.

Figure S7 (related to discussion): Biochemical Analysis of Rad54-WT, -S572A, and -S572E proteins

(A) Protein purification. Coomassie Blue stained SDS-PAGE gels of purified GST-Rad54 variants (left gel; 111 kDa; 3.5 μg/lane) or Rad54 from which the GST tag had been proteolytically removed during purification (right gel; 84.4 kDa; 8 μg/lane).

(B) Left panel: Rad54 (10 nM) ATPase activities were measured on dsDNA (6 μM bp pUC19 plasmid) continuously using an NADH absorbance-coupled assay for 8 min before addition of Rad51 (0.5 μM). ATPase activity was monitored in the presence of Rad51 for an additional 8 min. Graphed are rates of ATP hydrolysis before and after Rad51 addition. Mean ± SD (n=3). These assays revealed that Rad54-S572E exhibited about 10-fold reduced Rad51-stimulated ATPase (~600 ATP/min) compared to wild type (>6,000 ATP/min). Very similar relative levels of Rad51-stimulated ATPase were measured for the set of Rad54 preparations retaining the GST tag (data not shown). Right panel: All Rad54 variants exhibited similar instability of their Rad51-stimulated dsDNA-dependent ATPase activity at 30°C. Rad54 variants were incubated at 100 nM in a diluent (20 mM Tris acetate pH 7.4, 1 mg/ml BSA, and 0.5 mM TCEP) and reactions were initiated at 10 nM from this stock at the indicated times. These reactions contained 0.2 μM Rad51 and 6 μM bp pUC19 dsDNA. Data were normalized such that the first measurement from the Rad54 dilution made on ice was set as 100% for each replicate. Starting levels of ATPase were similar to the values presented in panels B and D. Mean ± SD of three reactions.

(C) Rad54 stimulates Rad51-mediated D-loop formation. Rad51 (0.2 μM) filaments were formed on a ds98-ss402 DNA substrate (0.76 μM bp/nt; 1 nM molecules; 402 nt homology) for 10 min, and then 25 nM RPA was added for an additional 10 min. Rad54 (120 nM) was delivered along with donor plasmid (30 μM bp) and the reaction continued for 20 min before termination. Left, representative gel. Right, quantification. Mean ± SD (n=3). These assays showed that the Rad54-S572A protein was able to stimulate D-loop formation by Rad51. The Rad54-S572E protein also stimulated D-loop formation, but to a lesser extent, as might be expected from the ATPase defect.

(D) The Rad54:Rad51 interaction is unchanged between Rad54-S572A and Rad54-S572E proteins. Sypro orange-stained SDS-PAGE gels of GST pull down reactions. Left gel: 0.2 μM of GST-Rad54-S572A, -S572E, or purified GST were incubated with glutathione agarose beads at RT for 30 min. Rad51 was then added at 0.2, 0.4 or 0.6 μM and incubation continued for 1 h. All lanes are pellet fractions except those marked "S" which are the supernatants of the next lane's reaction (equal fraction), as a control for efficient pulldown of GST-Rad54 (~1/11 reaction loaded). The amounts of Rad51 recovered in each lane are estimated below the gel (from a plot of Rad51 protein versus signal

intensities of standard protein bands also on the gel but not shown). The 1/11 volume input quantities are 40, 81 and 121 ng Rad51, and thus the majority of Rad51 is pulled down in each case. Right gel: As described above, except reactions contained 0.5 μM Rad51, and proteins were incubated in the presence of 0.1, 0.2, 0.3 or 0.5 M KCl.

(E) dsDNA binding is not qualitatively affected by Rad54-S572 mutation. Rad54 variants were titrated (0.125, 0.25, 0.5, 1 and 2 μM) and bound to 6 μM bp XmnI-linearized pBluescript DNA.

(F) All Rad54 Ser572 variants lack ssDNA-dependent ATPase activity, regardless of the presence of Rad51. The ATPase rates of Rad54 variants (10 nM) were monitored in the presence of ssDNA (6 μM nts; 100-mer poly dT) for 5 min at 30°C (rate 1). Next, Rad51 (0.2 μM) was added and the ATPase rates were measured for another 5 min (rate 2). Lastly, dsDNA (6 μM bp pUC19 plasmid) was added as a positive control for protein activity under these conditions (rate 3). Background consumption of NADH from its decay and/or that of ATP was measured under these conditions without proteins other than the ATP regeneration system present, corresponding to ~25 ATP/min on the graphed scale. This was not subtracted from the data. Mean ± SD (n=3).

4.9 Figures

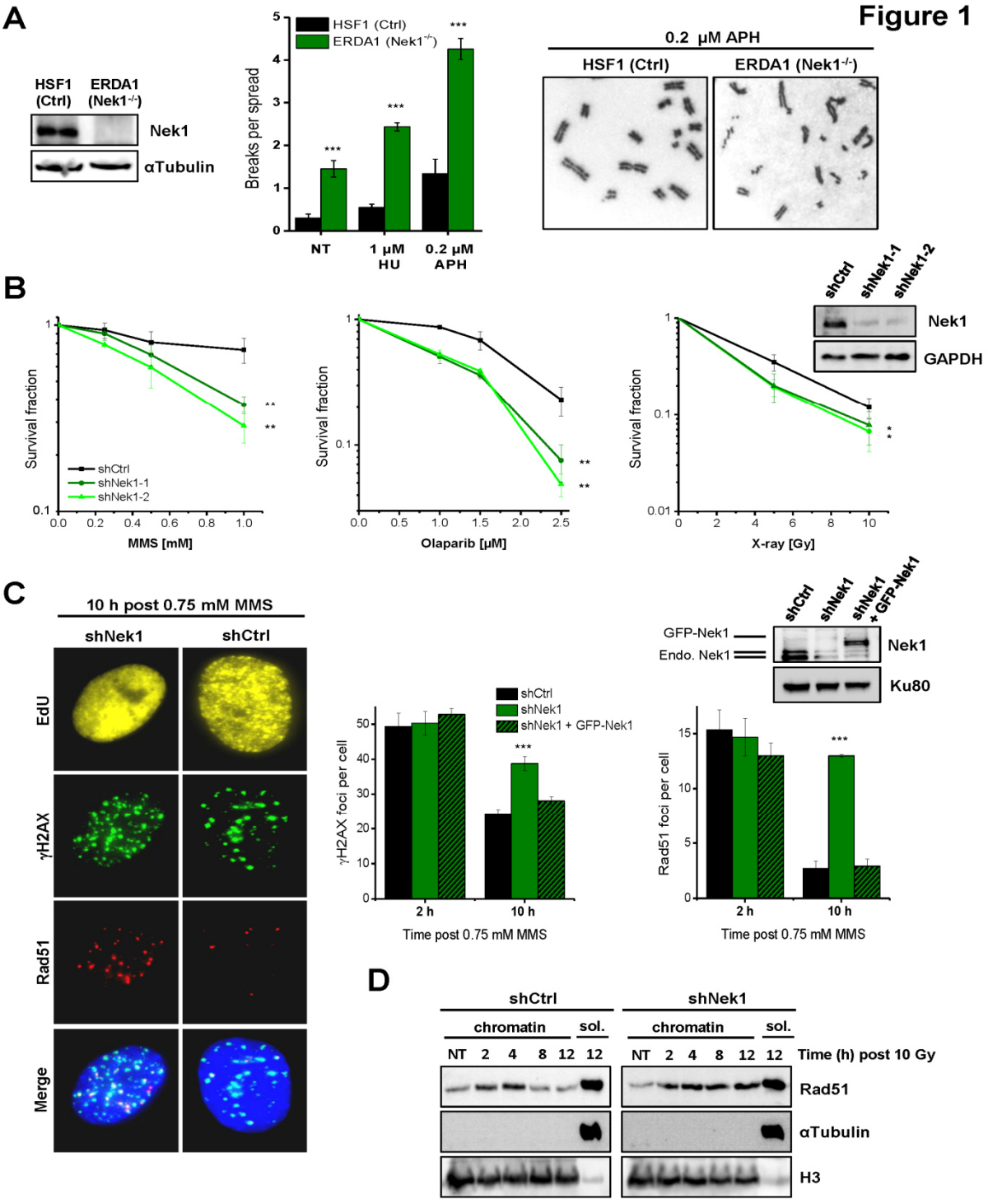
Figure 1
A
HSF1 (Ctrl)
ERDA1 (Nek1-/-)
Nek1
αTubulin
Breaks per spread
NT
1 μM HU
0.2 μM APH
0.2 μM APH
B
Survival fraction
MMS [mM]
Olaparib [μM]
X-ray [Gy]
shCtrl
shNek1-1
shNek1-2
GAPDH
C
10 h post 0.75 mM MMS
shNek1
shCtrl
EdU
γH2AX
Rad51
Merge
GFP-Nek1
Endo. Nek1
shNek1 + GFP-Nek1
Ku80
γH2AX foci per cell
Rad51 foci per cell
2 h
10 h
Time post 0.75 mM MMS
D
chromatin
sol.
Time (h) post 10 Gy
Rad51
αTubulin
H3

Figure 2

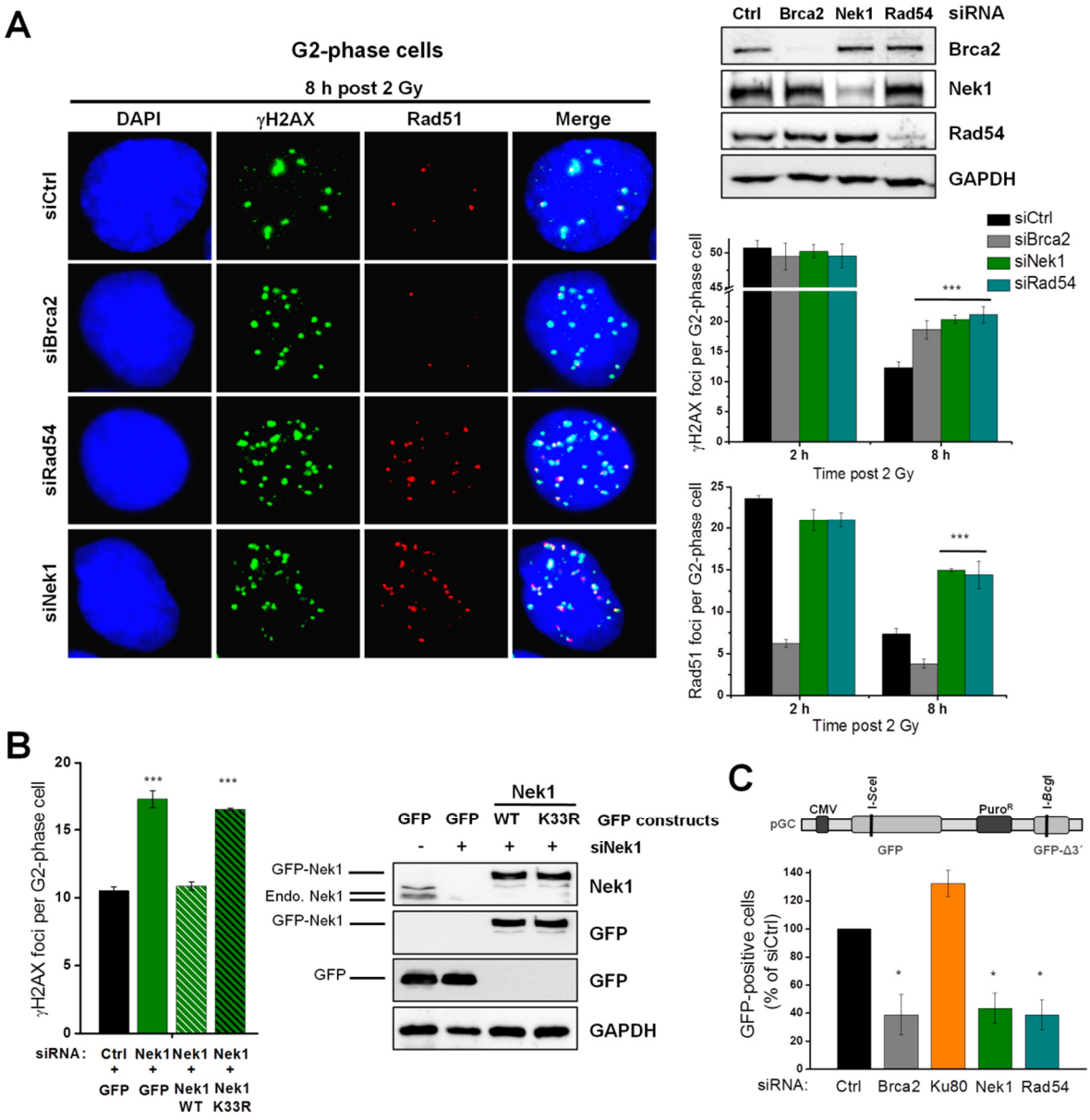
A
G2-phase cells
8 h post 2 Gy
DAPI
γH2AX
Rad51
Merge
siCtrl
siBrca2
siRad54
siNek1
Ctrl Brca2 Nek1 Rad54 siRNA
Brca2
Nek1
Rad54
GAPDH
siCtrl
siBrca2
siNek1
siRad54
γH2AX foci per G2-phase cell
2 h
8 h
Time post 2 Gy
Rad51 foci per G2-phase cell
B
γH2AX foci per G2-phase cell
siRNA: Ctrl Nek1 Nek1 Nek1
GFP GFP Nek1 WT Nek1 K33R
Nek1
GFP GFP WT K33R GFP constructs
siNek1
GFP-Nek1
Endo. Nek1
GFP-Nek1
GFP
Nek1
GFP
GFP
GAPDH
C
CMV
I-SceI
Puro^R
I-BcgI
pGC
GFP
GFP-Δ3´
GFP-positive cells (% of siCtrl)
siRNA: Ctrl Brca2 Ku80 Nek1 Rad54
D
Input
IP: Nek1
IP: IgG
Input
IP: Rad54
IP: IgG
Input
IP: Rad51
IP: IgG
10 Gy
Nek1
Rad54
Rad51

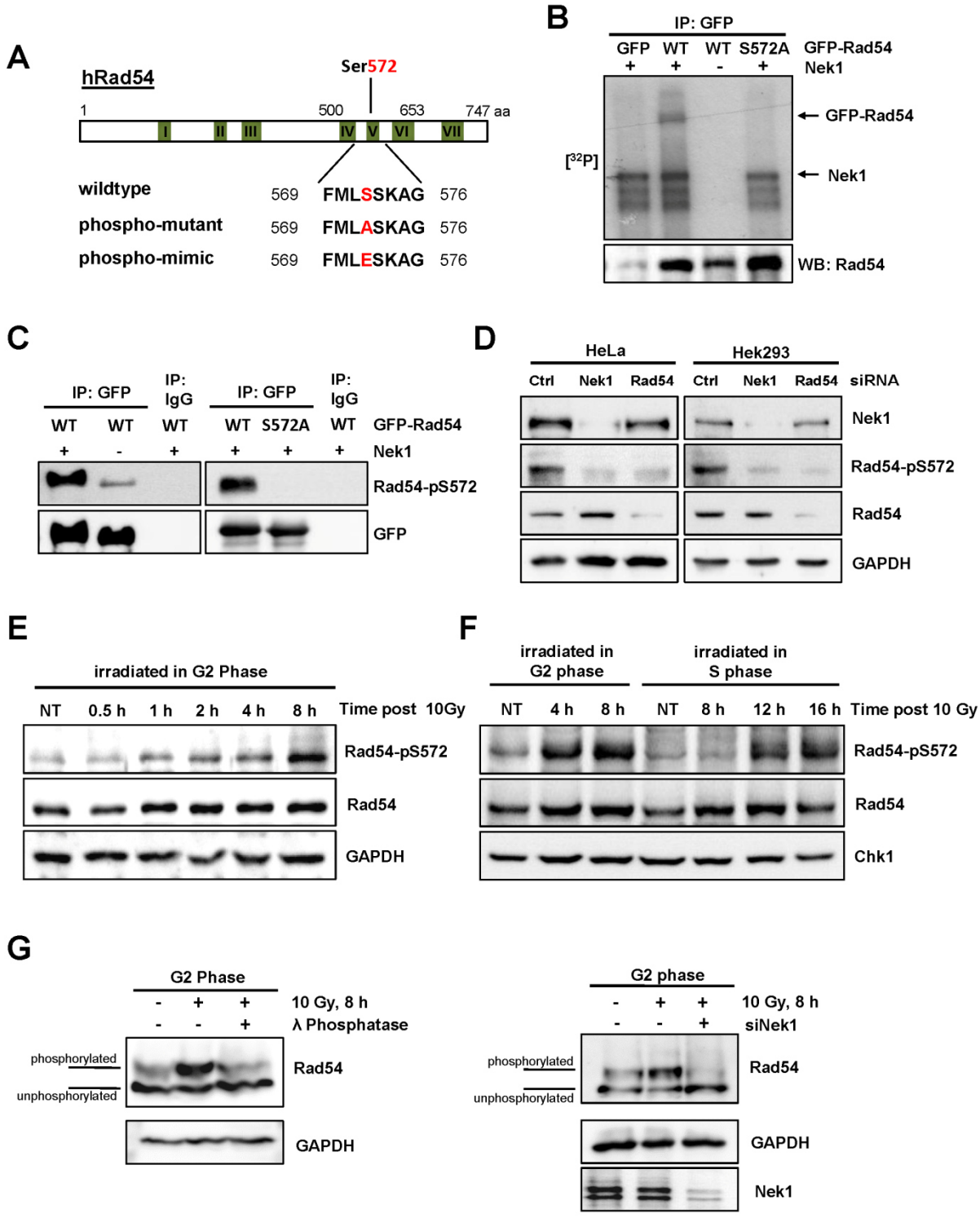
A
hRad54
Ser572
1
500
653
747 aa
I
II
III
IV
V
VI
VII
wildtype 569 FMLSSKAG 576
phospho-mutant 569 FMLASKAG 576
phospho-mimic 569 FMLESKAG 576
B
IP: GFP
GFP WT WT S572A GFP-Rad54
+ + - + Nek1
[32P]
GFP-Rad54
Nek1
WB: Rad54
C
IP: GFP
IP: IgG
IP: GFP
IP: IgG
WT WT WT WT S572A WT GFP-Rad54
+ - + + + + Nek1
Rad54-pS572
GFP
D
HeLa
Hek293
Ctrl Nek1 Rad54 Ctrl Nek1 Rad54 siRNA
Nek1
Rad54-pS572
Rad54
GAPDH
E
irradiated in G2 Phase
NT 0.5 h 1 h 2 h 4 h 8 h Time post 10Gy
Rad54-pS572
Rad54
GAPDH
F
irradiated in G2 phase
irradiated in S phase
NT 4 h 8 h NT 8 h 12 h 16 h Time post 10 Gy
Rad54-pS572
Rad54
Chk1
G
G2 Phase
- + + 10 Gy, 8 h
- - + λ Phosphatase
phosphorylated
unphosphorylated
Rad54
GAPDH
G2 phase
- + + 10 Gy, 8 h
- - + siNek1
phosphorylated
unphosphorylated
Rad54
GAPDH
Nek1

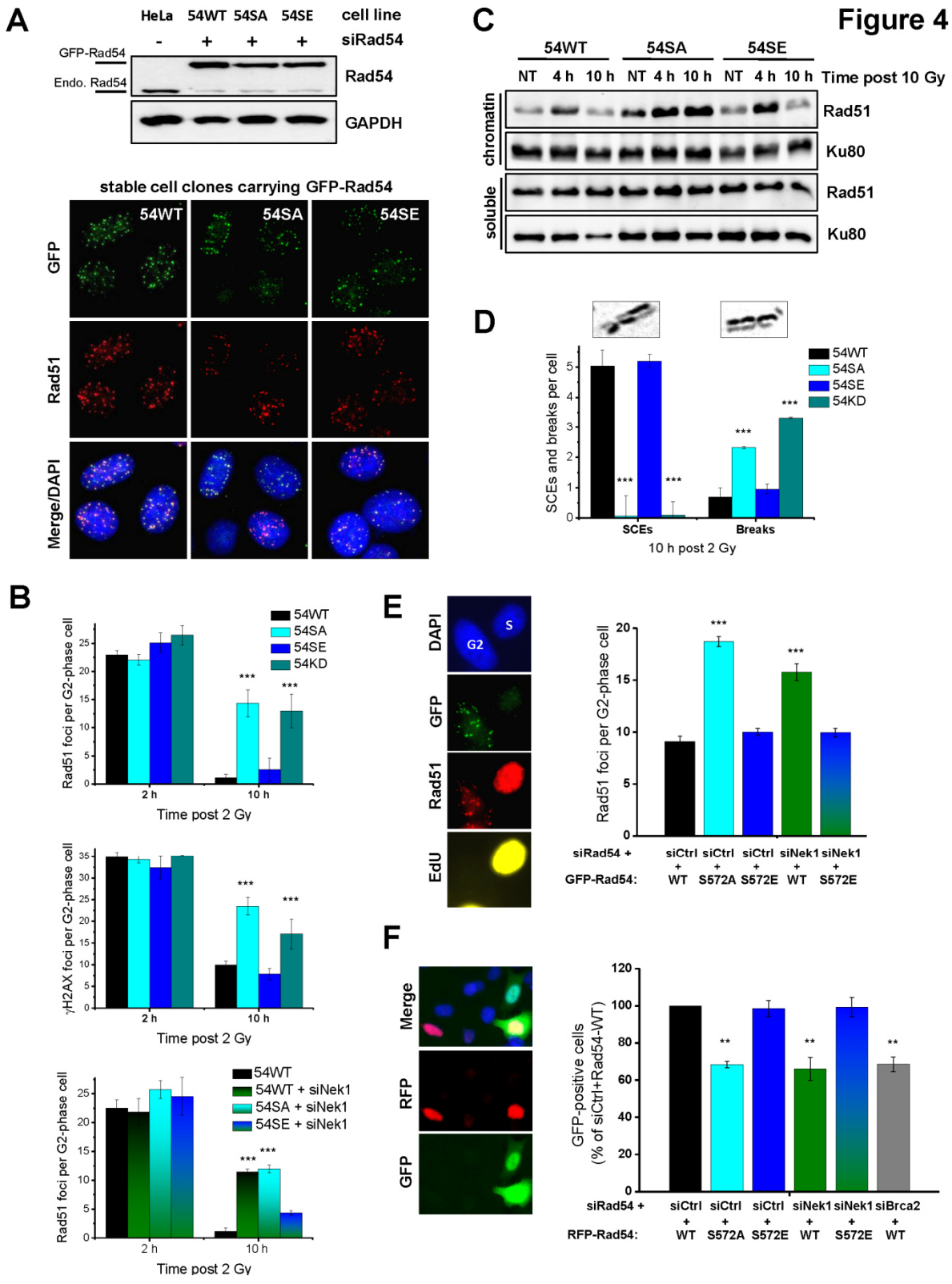
A
HeLa 54WT 54SA 54SE cell line
- + + + siRad54
GFP-Rad54
Endo. Rad54
Rad54
GAPDH
stable cell clones carrying GFP-Rad54
54WT 54SA 54SE
GFP
Rad51
Merge/DAPI
C
54WT 54SA 54SE
NT 4 h 10 h NT 4 h 10 h NT 4 h 10 h Time post 10 Gy
chromatin
soluble
Rad51
Ku80
Rad51
Ku80
D
SCEs and breaks per cell
54WT
54SA
54SE
54KD
SCEs
Breaks
10 h post 2 Gy
B
Rad51 foci per G2-phase cell
γH2AX foci per G2-phase cell
2 h
10 h
Time post 2 Gy
54WT
54SA
54SE
54KD
54WT + siNek1
54SA + siNek1
54SE + siNek1
E
DAPI
GFP
Rad51
EdU
G2
S
siRad54 +
GFP-Rad54:
siCtrl + WT
siCtrl + S572A
siCtrl + S572E
siNek1 + WT
siNek1 + S572E
F
Merge
RFP
GFP
GFP-positive cells (% of siCtrl+Rad54-WT)
siRad54 +
RFP-Rad54:
siCtrl + WT
siCtrl + S572A
siCtrl + S572E
siNek1 + WT
siNek1 + S572E
siBrca2 + WT

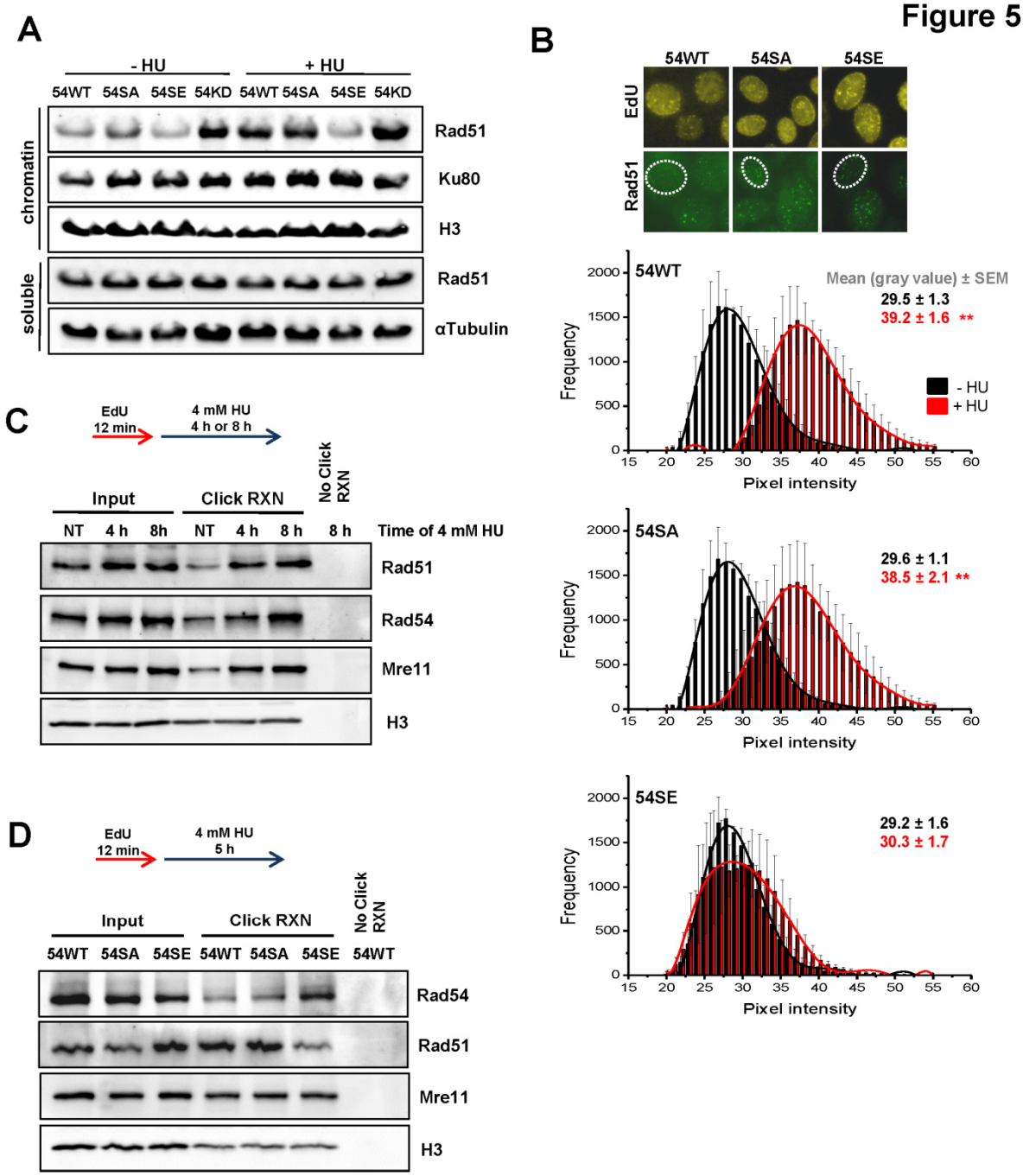
A
- HU
+ HU
54WT 54SA 54SE 54KD 54WT 54SA 54SE 54KD
chromatin
soluble
Rad51
Ku80
H3
Rad51
αTubulin
B
54WT
54SA
54SE
EdU
Rad51
54WT
Mean (gray value) ± SEM
29.5 ± 1.3
39.2 ± 1.6 **
- HU
+ HU
Frequency
Pixel intensity
54SA
29.6 ± 1.1
38.5 ± 2.1 **
54SE
29.2 ± 1.6
30.3 ± 1.7
C
EdU
12 min
4 mM HU
4 h or 8 h
No Click RXN
Input
Click RXN
NT 4 h 8h NT 4 h 8 h 8 h
Time of 4 mM HU
Rad51
Rad54
Mre11
H3
D
EdU
12 min
4 mM HU
5 h
No Click RXN
Input
Click RXN
54WT 54SA 54SE 54WT 54SA 54SE 54WT
Rad54
Rad51
Mre11
H3

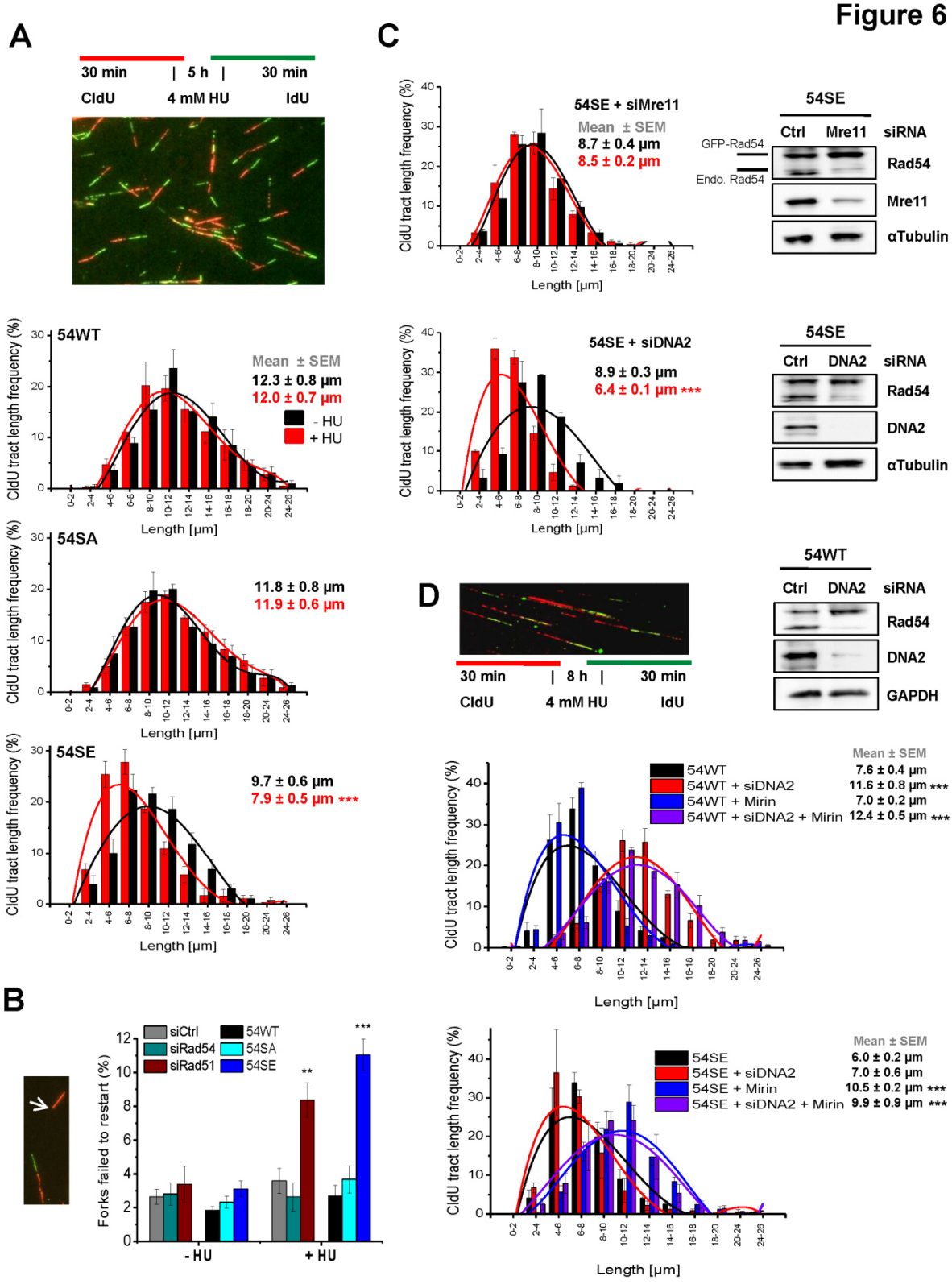
A
30 min
5 h
30 min
CldU
4 mM HU
IdU
54WT
Mean ± SEM
12.3 ± 0.8 µm
12.0 ± 0.7 µm
- HU
+ HU
54SA
11.8 ± 0.8 µm
11.9 ± 0.6 µm
54SE
9.7 ± 0.6 µm
7.9 ± 0.5 µm ***
CldU tract length frequency (%)
Length [µm]
B
siCtrl
siRad54
siRad51
54WT
54SA
54SE
Forks failed to restart (%)
- HU
+ HU
C
54SE + siMre11
Mean ± SEM
8.7 ± 0.4 µm
8.5 ± 0.2 µm
54SE
Ctrl
Mre11
siRNA
GFP-Rad54
Endo. Rad54
Rad54
Mre11
αTubulin
54SE + siDNA2
8.9 ± 0.3 µm
6.4 ± 0.1 µm ***
DNA2
D
30 min
8 h
30 min
CldU
4 mM HU
IdU
54WT
GAPDH
54WT
54WT + siDNA2
54WT + Mirin
54WT + siDNA2 + Mirin
7.6 ± 0.4 µm
11.6 ± 0.8 µm ***
7.0 ± 0.2 µm
12.4 ± 0.5 µm ***
54SE
54SE + siDNA2
54SE + Mirin
54SE + siDNA2 + Mirin
6.0 ± 0.2 µm
7.0 ± 0.6 µm
10.5 ± 0.2 µm ***
9.9 ± 0.9 µm ***

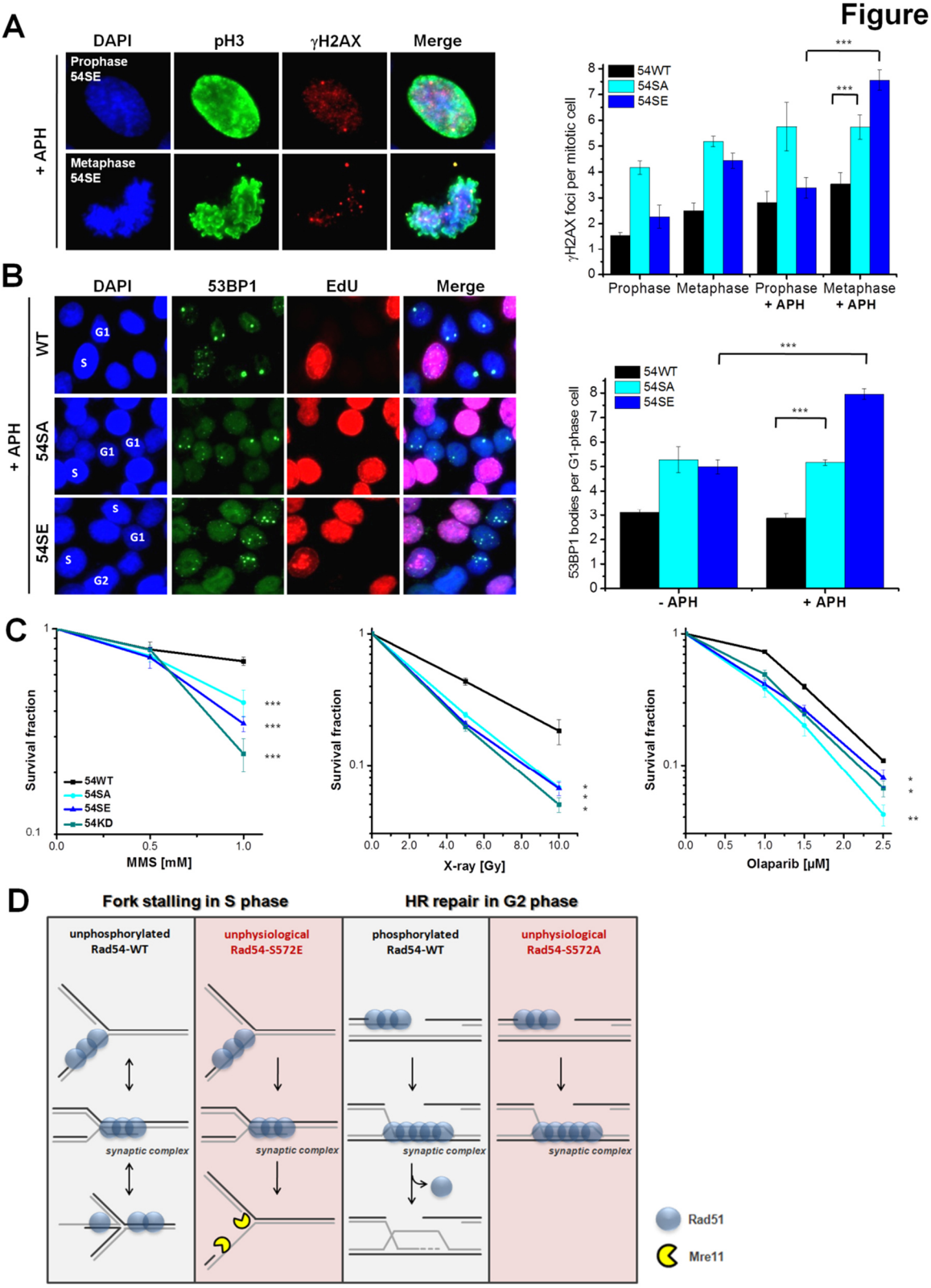
A
DAPI
pH3
γH2AX
Merge
+ APH
Prophase 54SE
Metaphase 54SE
γH2AX foci per mitotic cell
54WT
54SA
54SE
Prophase
Metaphase
Prophase + APH
Metaphase + APH
B
DAPI
53BP1
EdU
Merge
WT
54SA
54SE
G1
S
G2
53BP1 bodies per G1-phase cell
- APH
+ APH
C
Survival fraction
54WT
54SA
54SE
54KD
MMS [mM]
X-ray [Gy]
Olaparib [μM]
D
Fork stalling in S phase
HR repair in G2 phase
unphosphorylated Rad54-WT
unphysiological Rad54-S572E
phosphorylated Rad54-WT
unphysiological Rad54-S572A
synaptic complex
Rad51
Mre11

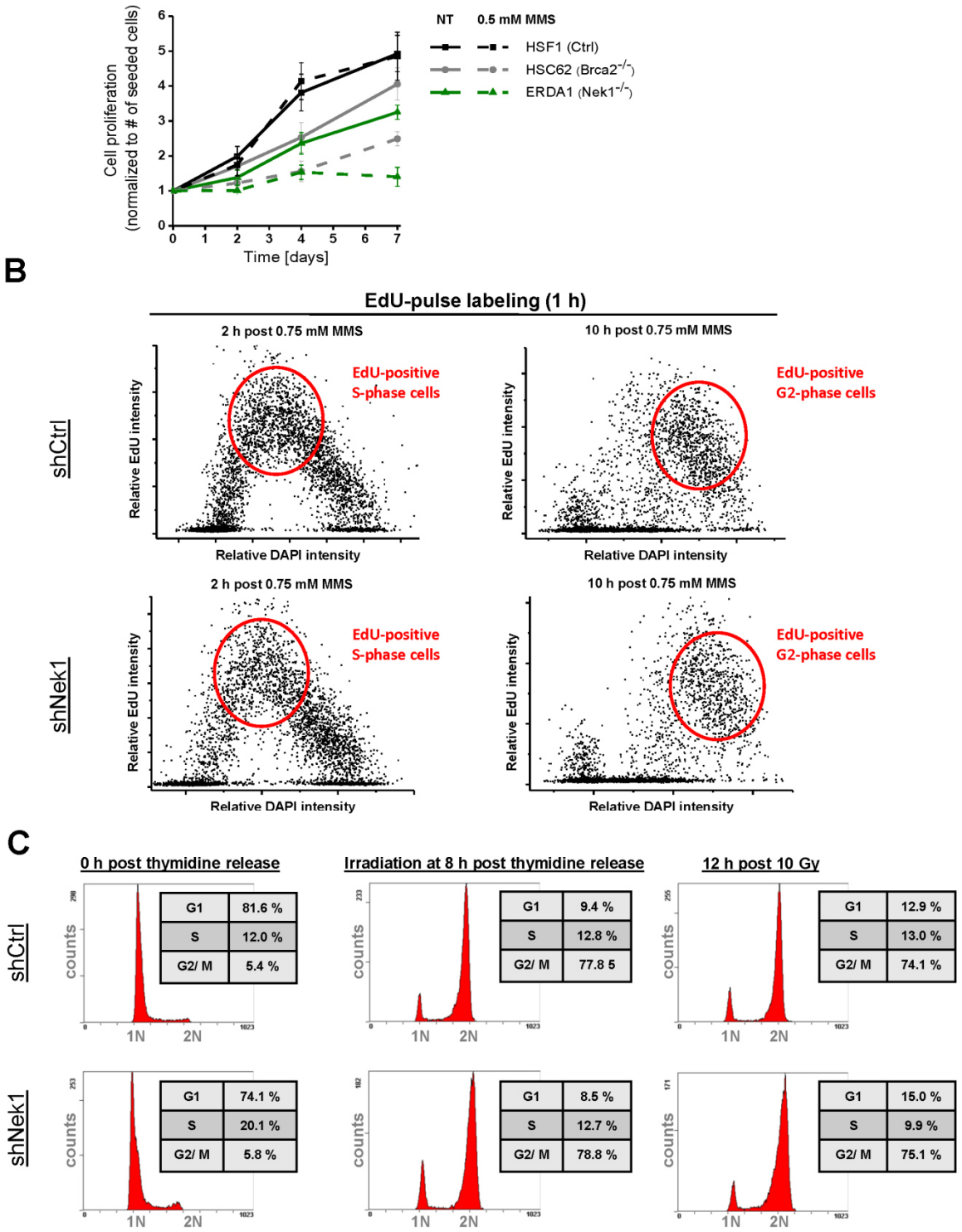
A
Cell proliferation (normalized to # of seeded cells)
Time [days]
NT
0.5 mM MMS
HSF1 (Ctrl)
HSC62 (Brca2-/-)
ERDA1 (Nek1-/-)
B
EdU-pulse labeling (1 h)
shCtrl
shNek1
2 h post 0.75 mM MMS
10 h post 0.75 mM MMS
EdU-positive S-phase cells
EdU-positive G2-phase cells
Relative EdU intensity
Relative DAPI intensity
C
0 h post thymidine release
Irradiation at 8 h post thymidine release
12 h post 10 Gy
counts
1N
2N
G1 81.6 %
S 12.0 %
G2/ M 5.4 %
G1 9.4 %
S 12.8 %
G2/ M 77.8 5
G1 12.9 %
S 13.0 %
G2/ M 74.1 %
G1 74.1 %
S 20.1 %
G2/ M 5.8 %
G1 8.5 %
S 12.7 %
G2/ M 78.8 %
G1 15.0 %
S 9.9 %
G2/ M 75.1 %

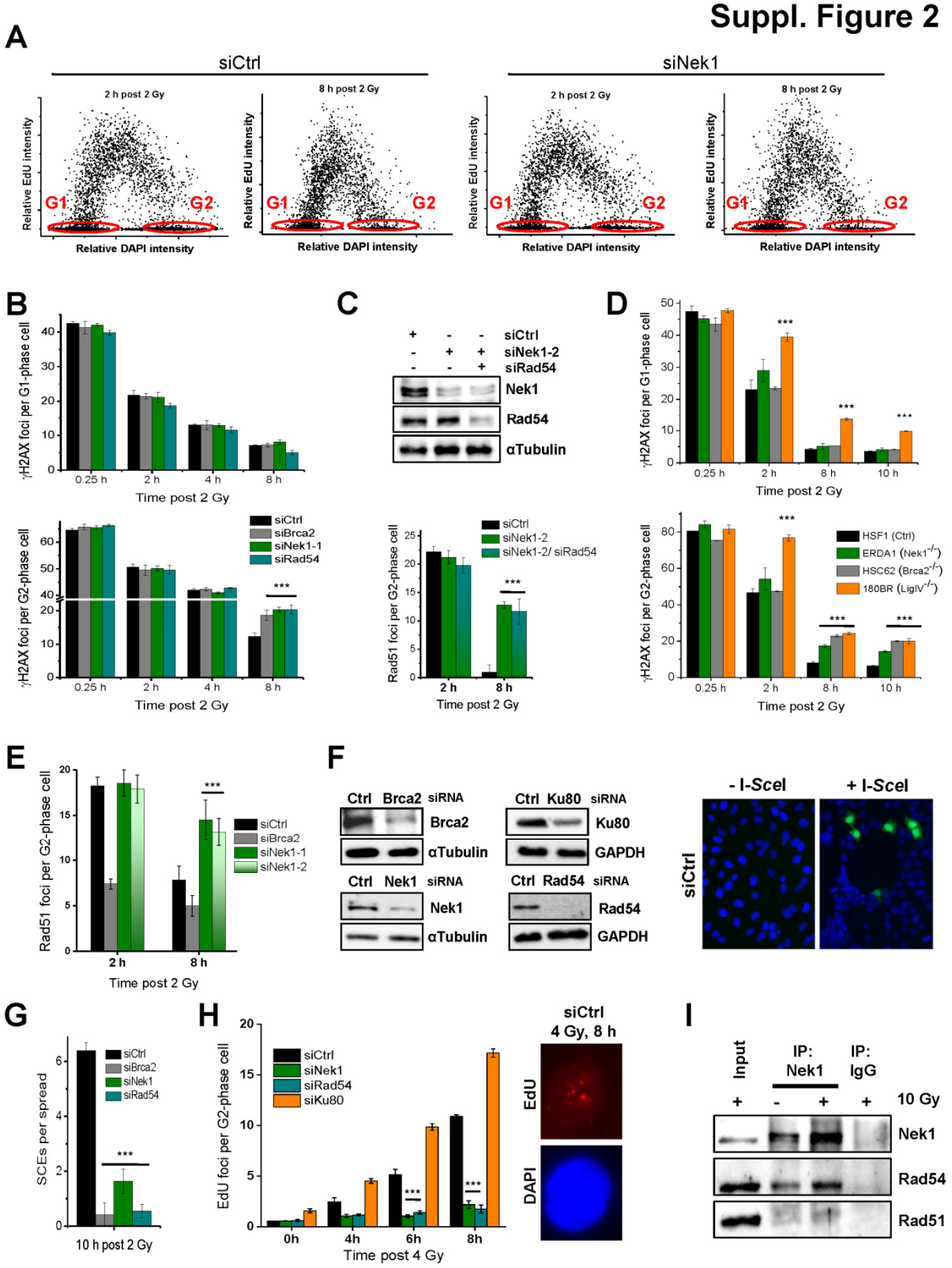
A
siCtrl
siNek1
2 h post 2 Gy
8 h post 2 Gy
Relative EdU intensity
Relative DAPI intensity
G1
G2
B
γH2AX foci per G1-phase cell
γH2AX foci per G2-phase cell
Time post 2 Gy
0.25 h
2 h
4 h
8 h
siCtrl
siBrca2
siNek1-1
siRad54
C
siCtrl
siNek1-2
siRad54
Nek1
Rad54
αTubulin
Rad51 foci per G2-phase cell
siNek1-2/ siRad54
D
10 h
HSF1 (Ctrl)
ERDA1 (Nek1-/-)
HSC62 (Brca2-/-)
180BR (LigIV-/-)
E
Rad51 foci per G2-phase cell
F
Ctrl Brca2 siRNA
Brca2
αTubulin
Ctrl Ku80 siRNA
Ku80
GAPDH
Ctrl Nek1 siRNA
Nek1
Ctrl Rad54 siRNA
Rad54
- I-SceI
+ I-SceI
siCtrl
G
SCEs per spread
10 h post 2 Gy
siNek1
siRad54
H
EdU foci per G2-phase cell
siKu80
0h
4h
6h
8h
Time post 4 Gy
siCtrl
4 Gy, 8 h
EdU
DAPI
I
Input
IP: Nek1
IP: IgG
10 Gy
Nek1
Rad54
Rad51

Suppl. Figure 3

A

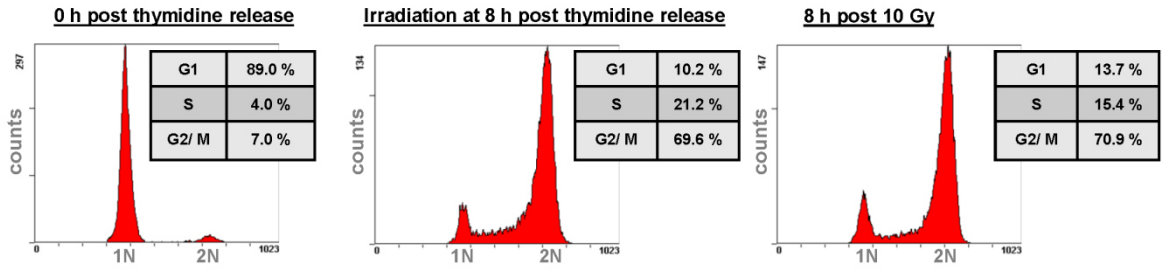

B

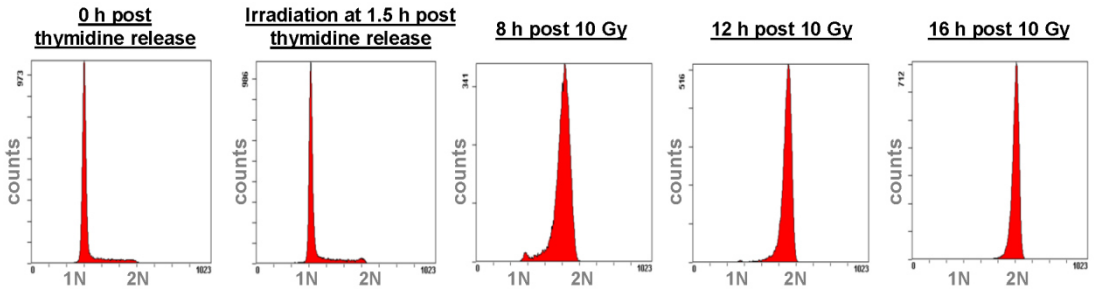

G1	78.7 %	72.1 %	2.2 %	0.9 %	0.3 %
S	17.3 %	22.0 %	70.3 %	8.5 %	3.1 %
G2/ M	4.0 %	5.9 %	17.5 %	90.6 %	96.6 %

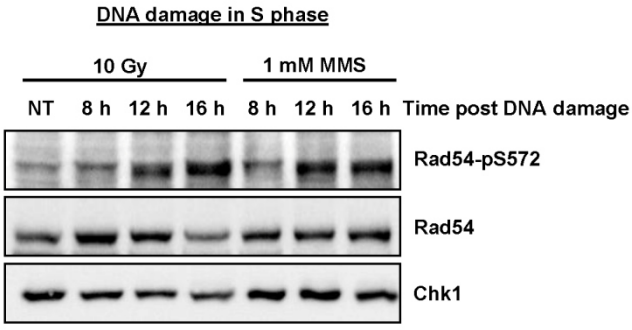

C

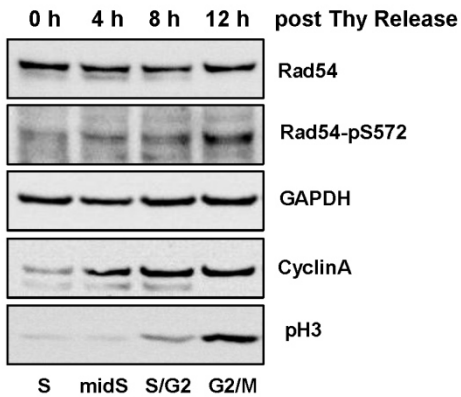

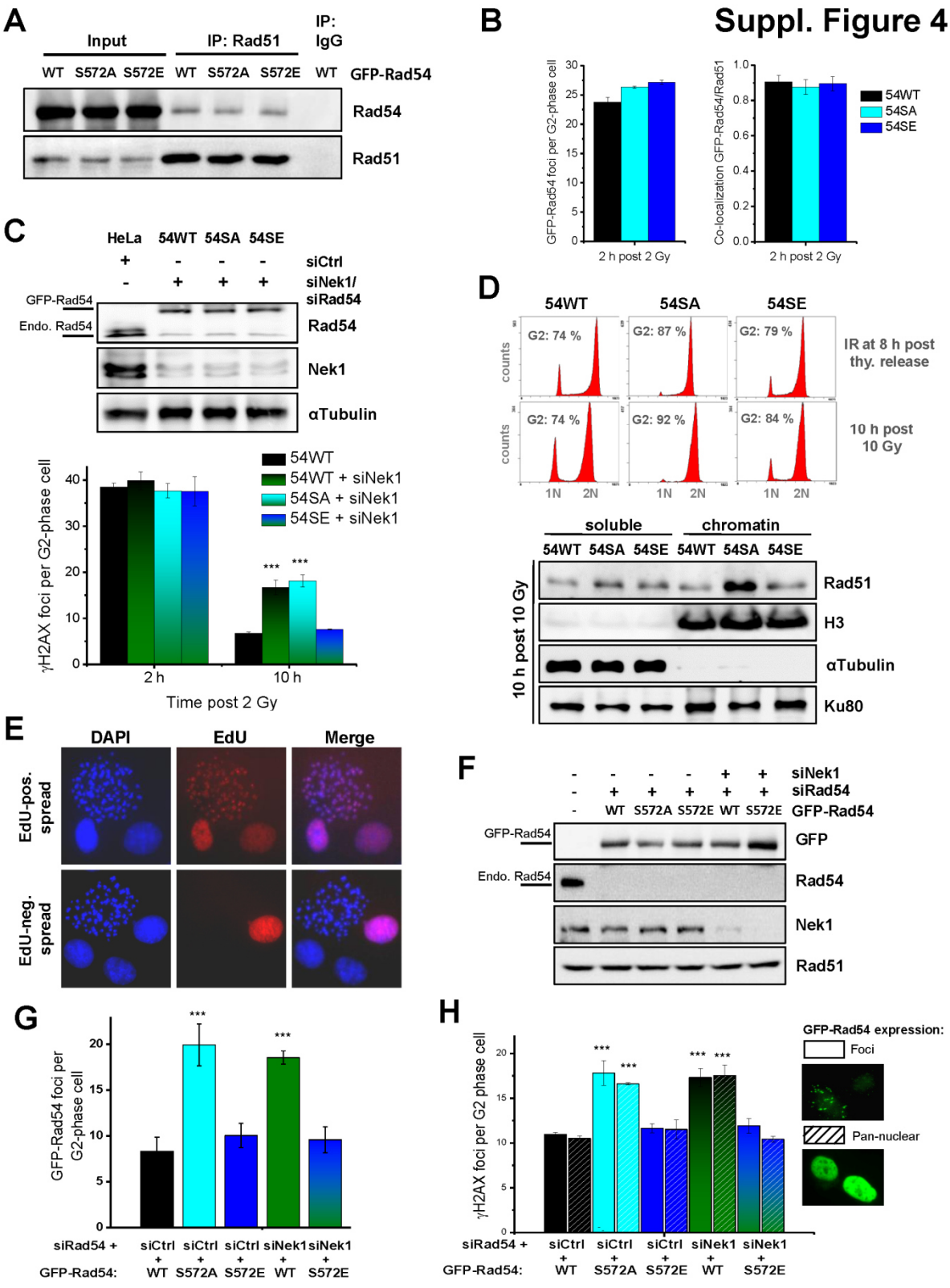
Suppl. Figure 4
A
Input
IP: Rad51
IP: IgG
WT S572A S572E WT S572A S572E WT GFP-Rad54
Rad54
Rad51
B
GFP-Rad54 foci per G2-phase cell
2 h post 2 Gy
Co-localization GFP-Rad54/Rad51
54WT
54SA
54SE
C
HeLa 54WT 54SA 54SE
siCtrl
siNek1/ siRad54
GFP-Rad54
Endo. Rad54
Rad54
Nek1
αTubulin
γH2AX foci per G2-phase cell
54WT
54WT + siNek1
54SA + siNek1
54SE + siNek1
2 h
10 h
Time post 2 Gy
D
54WT 54SA 54SE
G2: 74 %
G2: 87 %
G2: 79 %
IR at 8 h post thy. release
G2: 74 %
G2: 92 %
G2: 84 %
10 h post 10 Gy
counts
1N 2N
soluble
chromatin
54WT 54SA 54SE 54WT 54SA 54SE
10 h post 10 Gy
Rad51
H3
αTubulin
Ku80
E
DAPI
EdU
Merge
EdU-pos. spread
EdU-neg. spread
F
siNek1
siRad54
WT S572A S572E WT S572E GFP-Rad54
GFP-Rad54
Endo. Rad54
GFP
Rad54
Nek1
Rad51
G
GFP-Rad54 foci per G2-phase cell
siRad54 +
GFP-Rad54:
siCtrl + WT
siCtrl + S572A
siCtrl + S572E
siNek1 + WT
siNek1 + S572E
H
γH2AX foci per G2 phase cell
GFP-Rad54 expression:
Foci
Pan-nuclear

Suppl. Figure 5

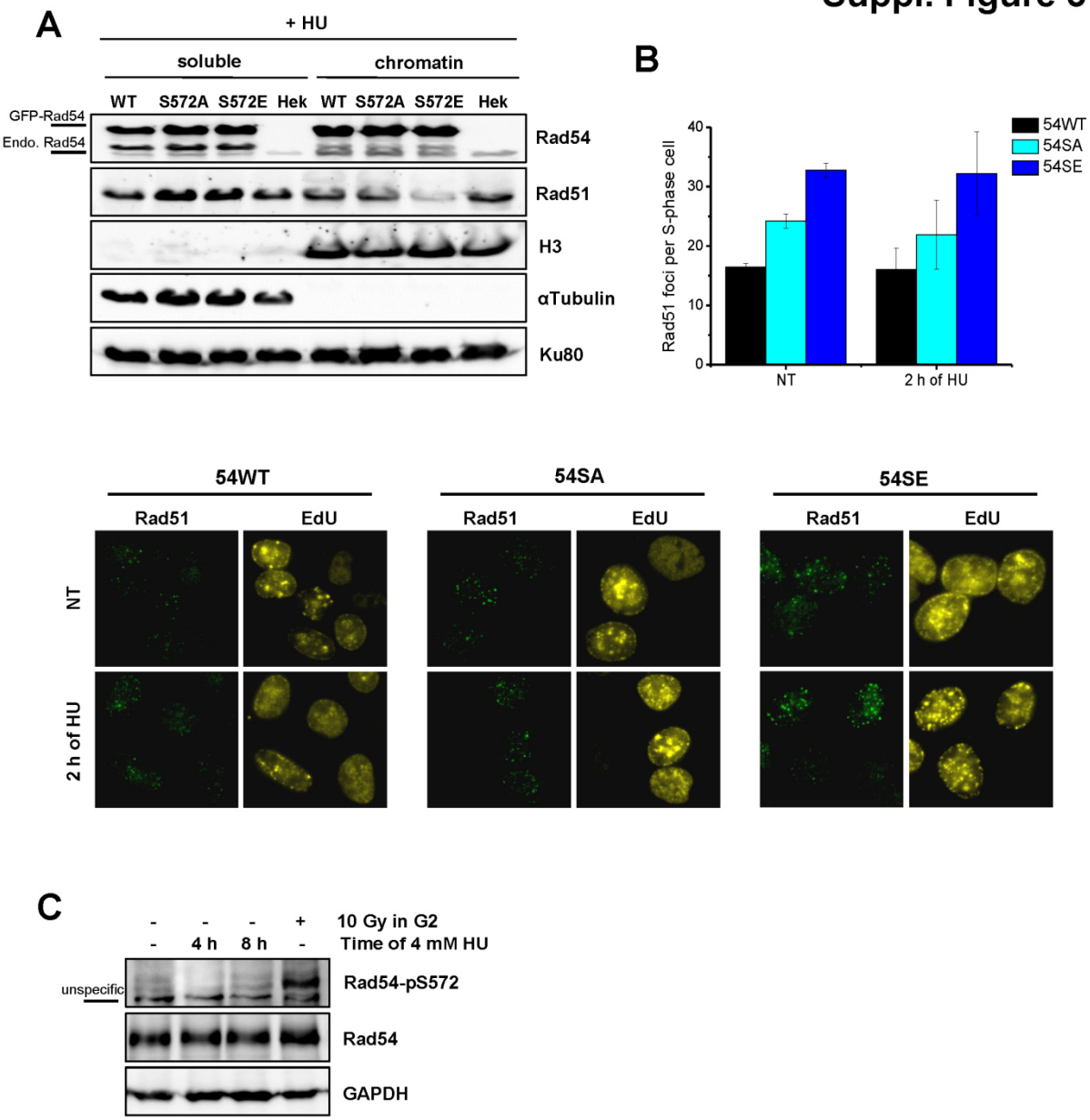

Suppl. Figure 6

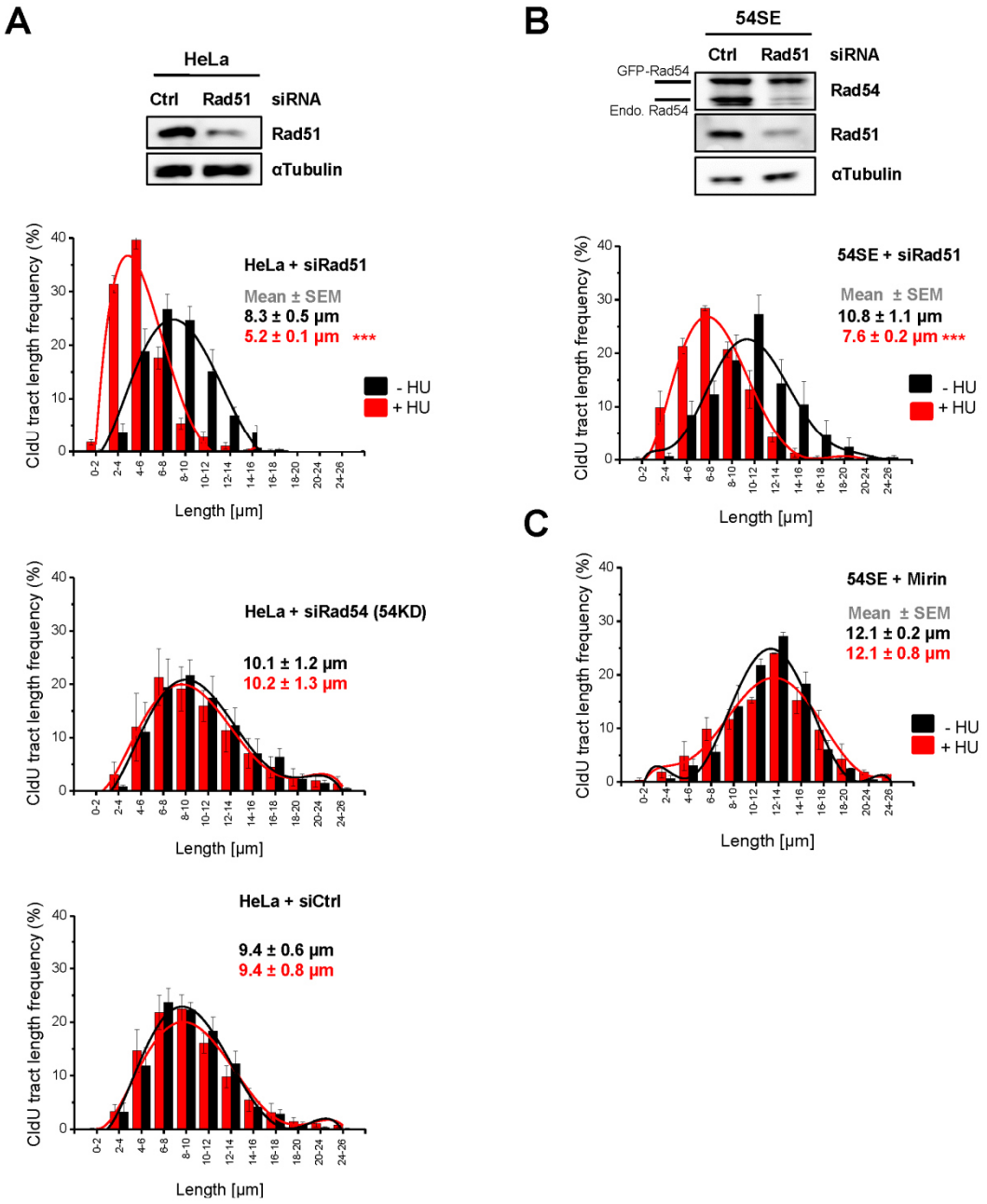

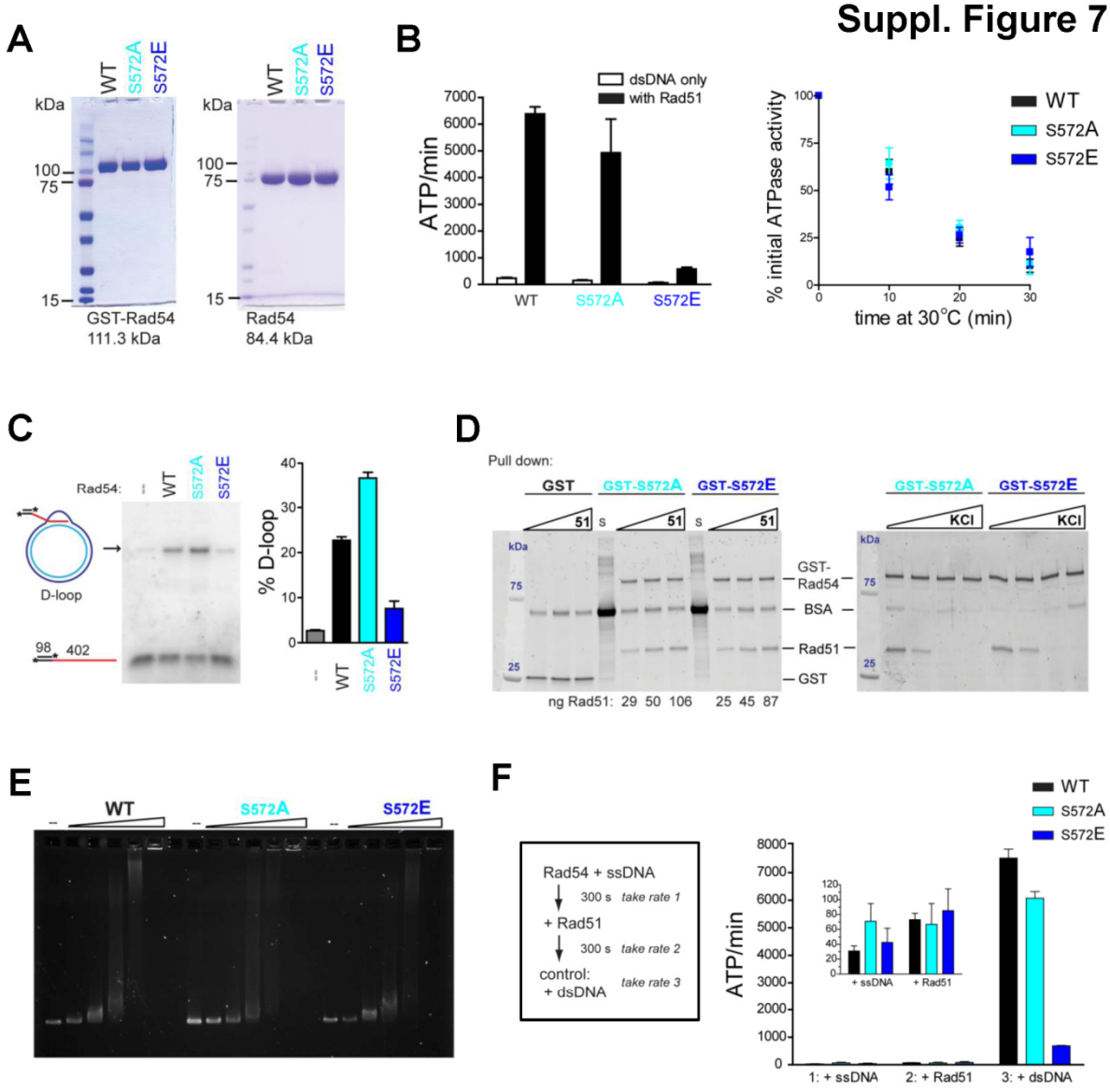
A
WT
S572A
S572E
kDa
100
75
15
GST-Rad54
111.3 kDa
Rad54
84.4 kDa
B
dsDNA only
with Rad51
ATP/min
WT
S572A
S572E
% initial ATPase activity
time at 30°C (min)
C
Rad54:
D-loop
98
402
% D-loop
D
Pull down:
GST
GST-S572A
GST-S572E
KCl
GST-Rad54
BSA
Rad51
GST
ng Rad51: 29 50 106 25 45 87
E
F
Rad54 + ssDNA
300 s take rate 1
+ Rad51
300 s take rate 2
control:
+ dsDNA
take rate 3
+ ssDNA
+ Rad51
1: + ssDNA
2: + Rad51
3: + dsDNA

4.10 Declaration of own achievements

Within the publication "*Nek1 Regulates Rad54 to Orchestrate Homologous Recombination and Replication Fork Stability*", some data were already published in the PhD thesis of Julian Spies and the Master thesis of Michael Sürder. The Nek1 project was initiated in 2010 by Julian Spies and Markus Löbrich four years before I joined. For the last 2 years of my PhD I supported this project by establishing new techniques and performing experiments to proof already existing ideas and models. Julian Spies and Markus Löbrich designed the study and wrote the original manuscript. I was involved in analyzing and interpreting my data. Additionally, during the revision I was involved in rewriting, restructuring and proofreading the paper. I also illustrated the graphical abstract and model, which was designed by Markus Löbrich, Julian Spies, Wolf-Dietrich Heyer, William D. Wright and input from myself. The following experiments were performed and analyzed by myself or, if indicated, in collaboration with my supervisor Julian Spies or my colleague Michael Sürder, who was a master student in the lab.

Figure 1B→ The generation of stable shNek1 cell lines was performed in collaboration with Julian Spies. The clonogenic survival assay after Olaparib treatment was carried out by myself.

Figure 1C→ The generation of an shRNA-resistant GFP-Nek1 plasmid for the complementation study was performed by myself. I quantified theγH2AX and Rad51 foci numbers in shNek1 cells complemented with the generated shRNA-resistant GFP-Nek1 wt plasmid and provided the Western Blot.

Figure 4A→ The generation of stable Rad54 mutant cell lines was performed in collaboration with Julian Spies. I generated the Rad54 S572A cell line and a backup clone for Rad54 WT. I provided the representative immunofluorescence pictures.

Figure 4D

Figure 5A→ I performed pilot experiments of chromatin fractionation and first observed the key finding. The presented Western Blot was performed in collaboration with Julian Spies.

Figure 5B

Figure 6C→ The fibre data were generated in collaboration with Michael Sürder. I provided the Western Blot demonstrating the siRNA downregulation.

Figure 6D

Figure 7C

Figure 7D→ I graphically illustrated the displayed model.

Figure S4B

Figure S4E

Figure S5B

Figure S6A→ The first experiments were performed and key findings were initially observed by Michael Sürder. I repeated the data for siRad54 and siCtrl treated cells. Additionally I performed the demonstrated Western Blot.

Figure S6B→ The fibre data were generated in collaboration with Michael Sürder. I provided the Western Blot demonstrating the siRNA downregulation.

5 Manuscript: Involvement of ATRX in Homologous Recombination Repair

5.1 Summary

The chromatin remodeler ATRX (alpha-thalassemia/mental retardation X-linked) has crucial roles in preventing replication fork stalling, deposition of histones and gene regulation. The ATRX protein structure harbors a PHD-like domain and an ATPase domain and mutations within these two domains cause severe phenotypes in humans and mice. Here we showed that ATRX localizes to DNA damage sites and discovered a specific defect for ATRX-depleted human cells in repairing radiation-induced double strand breaks (DSBs) specifically in G2 phase. A reporter assay specific for homologous recombination (HR) suggested the involvement of ATRX in HR, which was confirmed by a decrease in radiation-induced sister chromatid exchanges (SCEs). We found epistasis with the HR factor Rad54 and could further establish that ATRX functions downstream of Rad51 removal. As the subsequent step during HR is recombination-associated DNA synthesis, we hypothesized that ATRX is involved during this late process of HR repair. Interestingly, depletion of the DNA clamp protein PCNA (proliferating cell nuclear antigen) displayed a very similar defect in repairing radiation-induced DSBs and we could moreover show that PCNA physically interacts with ATRX. Together these data suggest a novel role for ATRX in the repair of DSBs, cooperating with PCNA at late stages during HR to maintain genomic integrity.

5.2 Introduction

DSBs represent the most harmful type of DNA lesions which can arise from various exogenous sources or endogenously during replication (Ensminger et al., 2014; van Gent et al., 2001; Jackson and Bartek, 2009). For the repair of DSBs two main pathways exist in mammalian cells, non-homologous end-joining (NHEJ) and homologous recombination (HR). NHEJ functions throughout the whole cell cycle, whereas HR can only operate during S and G2 phase, when the sister chromatid is available as a template for repair (Chapman et al., 2012; Lukas and Lukas, 2013). If DSBs are not repaired appropriately, chromosomal translocations can occur, which in turn promote carcinogenesis (Bunting and Nussenzweig, 2013; Ghezraoui et al., 2014). Therefore, HR with its high-fidelity repair is essential to maintain genomic integrity. For the initiation of HR, the 5'-end of the single-stranded DNA (ssDNA) needs to be resected and Rad51 is loaded by BRCA2 to form a nucleoprotein filament. The next steps involve homology search, strand invasion into the sister chromatid and D-loop formation (van Gent et al., 2001; Lukas and Lukas, 2013). When homology search is completed,

Rad54 actively removes Rad51 from the DNA. HR is then finalized by DNA repair synthesis, which copies the missing sequence at the DSB site, and dissolution or resolution of formed Holliday junctions can proceed (Matos and West, 2014; Renkawitz et al., 2014). It has not yet been elucidated, by which mechanisms DNA synthesis is initiated and executed during the HR repair pathway, however an involvement of the clamp protein PCNA and DNA polymerase delta (Pol δ) was proposed (Li et al., 2013; Sneeden et al., 2013; Wang et al., 2004). During the process of replication, PCNA is loaded onto the DNA by the replication factor C and mediates subsequent binding of polymerases to the DNA (Bloom, 2009; Podust et al., 1998; Tsurimoto and Stillman, 1991). Taken together, PCNA is an essential protein for replication and is additionally involved in HR. Vice versa it is known that many factors which are involved in HR have additional roles during replication or replication stress response, *e.g.* BRCA2, Rad54 and Rad51 have been implicated in stabilizing and processing replication forks during replication stress conditions (Bugreev et al., 2011; Schlacher et al., 2011).

The ATRX gene encodes a protein that belongs to the SWI2/SNF2 (switching defective/sucrose non-fermenting) family of chromatin remodelers and contains two main functional domains: An N-terminal ADD (ATRX-DNMT3-DNMT3L) domain including a PHD-like zinc finger, and a C-terminal ATPase/helicase domain which shows high similarity to that of Rad54. The ATPase domain allows ATP-dependent translocation along DNA and chromatin remodeling. The ADD domain serves as a dual histone modification recognition module ($H3K9me^3/H3K4me^0$) and ATRX can thereby localize to heterochromatin (Eisen et al., 1995; Picketts et al., 1996; Xie et al., 1999). Further it is reported that ATRX functions in concert with DAXX (death associated protein 6) as a histone chaperone complex which incorporates the histone variant H3.3 for heterochromatin maintenance (Tang et al., 2004; Voon and Wong, 2016). On an organismic level, mutations within ATRX mainly occur in the ADD or ATPase domain and lead to an X-linked mental retardation syndrome in humans, mostly accompanied by α–thalassemia (Watson et al., 2013). The cellular localization of ATRX is regulated through cell cycle-specific phosphorylation, which mediates its recruitment to the nuclear matrix during interphase or to condensed chromatin at the onset of mitosis (Bérubé et al., 2000; Ishov et al., 2004). Therefore, ATRX depletion resulted in mitotic and meiotic defects such as chromosomal alignment and segregation impairment, failure in chromosome condensation and increased formation of micronuclei (Leung et al., 2013; Lovejoy et al., 2012; Ritchie et al., 2008). ATRX also functions during replication and consequently, ATRX knockdown cells showed several defects during replication processes, such as hypersensitivity towards replication stress, perturbed S-phase progression, an increase in stalled replication forks, less new origin firing and Mre11-dependent fork degradation (Huh et al., 2012, 2016; Leung et al., 2013). Taken together, this indicates several distinct roles for ATRX to maintain genomic stability. It is known that ATRX shows high similarity with the conserved ATPase domain of Rad54 (Mitson et al., 2011; Watson et al., 2013). Since Rad54 is involved in HR and has additional roles at stalled replication forks we speculated that ATRX might

also be involved HR, as it has crucial functions at stalled forks. Multiple proteins which maintain replication fork stability have distinct roles during HR, however not much is known about the role of ATRX during DNA repair.

In this study, we established that ATRX is involved in the repair of DSBs via HR and functions during late stages of this repair pathway. ATRX is involved in a step downstream of Rad51 removal and interacts with PCNA, suggesting that both proteins cooperate to allow DNA repair synthesis and thereby finalize HR.

5.3 Results

ATRX has a role in DSB repair via HR

ATRX has established functions during replication processes and as several HR-proteins are involved in replication fork stability, we aimed to uncover the vice versa possibility that ATRX might also function during HR. For many HR-proteins it was already shown that they localize to DSBs after damage induction. We could confirm, that ATRX is also present at DNA damage sites at late times after laser micro-irradiation, supporting a direct involvement of ATRX in the repair of DSBs (Figure S1A) (Leung at al., 2013).

To investigate in which DSB repair pathway ATRX is involved, we performed GFP-based reporter assays specific for HR and NHEJ, using HeLa pGC cells for the HR- and HeLa pEJ cells for the NHEJ-reporter assay, respectively. Both cell lines contain single stably integrated copies of either reporter construct (Mansour et al., 2008). Repair of the endonuclease I-*Sce*I-induced DSB by HR or NHEJ restores GFP expression, which can then be quantified. HR frequencies measured by the fraction of GFP-positive cells were decreased in ATRX-depleted cells compared to control cells and showed a similar reduction as core HR factors like Rad54 or BRCA2 (Figure 1A and S1B). Depletion of Ku80, a known NHEJ factor however did not influence GFP expression. The NHEJ reporter assay revealed no impact of depleting ATRX or Rad54 on this repair pathway, suggesting that ATRX is involved exclusively in HR and not in NHEJ (Figure 1A and S1B). As many HR proteins functions during replication in S phase and during DSB repair in G2 phase and these reporter assays do not allow separation of cell cycle-specific effects, we next analyzed the DSB repair kinetics in ATRX-depleted cells excluding the S-phase population. Cells were therefore labeled with EdU prior to irradiation with 2 Gy and γH2AX foci, as a marker for DSBs, were quantified in EdU-negative G1 and G2 cells as previously described (Löbrich et al., 2010) (Figure S1C). In G1 radiation-induced DSBs can only be repaired by NHEJ, because the second DSB repair pathway HR needs a sister chromatid as a template for repair and can therefore only function during S and G2 phase. In G1 phase cells, we observed similar γH2AX foci levels in ATRX-depleted cells compared to control cells or Rad54-/BRCA2-depleted cells at all time points (Figure 1B). In G2 phase, γH2AX foci levels were again

similar up to 4 h after irradiation in ATRX-depleted cells compared to control cells or Rad54-/BRCA2-depleted cells. Only at 8 h post IR, ATRX-, Rad54- and BRCA2-depleted cells showed increased γH2AX foci levels, indicating a DSB repair defect which is typical for impaired HR, the slow component of DSB repair in G2 (Beucher et al., 2009). A complementation of ATRX-depleted cells with an siRNA-resistant ATRX-WT plasmid resulted in normal γH2AX levels (Figure S1D). To consolidate the involvement of ATRX during HR in G2, we measured the formation of IR-induced SCEs in EdU-negative G2 cells, which arise between the two sister chromatids during HR repair. SCEs are known to increase after irradiation and depletion of HR factors prevents this additional formation (Conrad et al., 2011). Cells lacking ATRX, Rad54 or BRCA2 showed no radiation-induced increase of SCEs compared to HR-proficient control cells (Figure 1C). Together, these data established that ATRX is involved in HR, the slow DSB repair pathway in G2-phase cells.

ATRX is involved in late steps of homologous recombination

We next aimed to uncover at which step of HR ATRX is involved. Therefore, we quantified Rad51 foci as a specific marker for HR in G2 phase at different times post IR in ATRX-, Rad54- and BRCA2-depleted cells. At early times post IR, the formation of Rad51 foci was normal in ATRX- and Rad54-depleted cells, compared to control cells (Figure 2A). Only in BRCA2-depleted cells very few Rad51 foci formed at all times, as BRCA2 is normally responsible for Rad51 loading onto the single-stranded DNA (ssDNA) prior to strand invasion. At later times (8 h), Rad51 foci decreased in control cells, but the removal in Rad54-depleted cells was strongly impaired, as the function of Rad54 during a regular HR process is to remove Rad51 after strand invasion. In ATRX depleted cells at 8 h post IR, the majority of Rad51 molecules was removed, however, some Rad51 foci persisted (Figure 2A). Intriguingly, Rad51 removal in ATRX deficient cells was almost normal, but a high number of unrepaired DSBs was observed (Figure 1B), indicating a function for ATRX downstream of Rad54. We next analyzed chromatid breaks as a readout for unrepaired DSBs in ATRX-depleted G2-phase cells and found that the absence of ATRX resulted in slightly increased chromatid breaks after irradiation compared to control cells (Figure 2B). However, the effect of ATRX depletion was less pronounced than that of Rad54, and BRCA2 depletion clearly revealed the highest number of chromatid breaks. This indicates that early HR intermediates, where a D-loop has not yet been formed are very unstable and much more likely to result in a visible chromatid break than more advanced structures, when strand invasion has already occurred. In line with this finding are previous observations that only a small fraction of unrepaired DSBs, mirrored by γH2AX foci, result in visible chromatid breaks (Beucher et al., 2009). Hence, the three factors can most likely be placed in the following order, with BRCA2 being involved in early HR steps, followed by Rad54 during and ATRX during or after Rad51 removal. To validate the observed effects of ATRX depletion, two independent HeLa shATRX cell lines with a doxycycline-inducible (+Dox) knockdown of the protein and

additionally a CRISPR-Cas9 based knockout (KO) cell line were generated and the DSB repair kinetics were analyzed (Figure S2A, S2C and 2C). All cell lines confirmed the already described HR-specific repair defect on γH2AX and Rad51 foci levels. ATRX knockdown cell lines were furthermore used to analyze the impact on overall cell survival after treatment with MMS or MMC. Both agents are known to induce damage in S-phase and the resulting DSBs are predominantly repaired via HR. Additionally, we analyzed cell survival after IR but as IR-induced DSBs and other DNA damages are not predominantly repaired via HR, the effects of ATRX depletion were less pronounced (data not shown). The plating efficiency in ATRX knockdown cell lines compared to control cells was more than 50% reduced and the clonogenic survival was strongly impaired in both ATRX-deficient cell lines (Figure S2B). Epistasis analysis with Rad54 in the ATRX KO cell line showed no additional effect of Rad54 depletion compared to siRad54-treated HeLa cells, which approves that ATRX functions in the same pathway as Rad54 (Figure 2C). In summary, it is likely that ATRX functions downstream of Rad54, after the process of Rad51 removal. As the subsequent step during HR is recombination-associated DNA synthesis, where the undamaged sister chromatid is used as a template for repair, we speculated that ATRX might be involved just before or during this step.

Interaction between ATRX and PCNA

As PCNA was already postulated to play a role in DNA repair synthesis at late stages of HR in yeast and humans (Burgess et al., 2013; Li et al., 2013; Sebesta et al., 2013; Sneeden et al., 2013), we first aimed to confirm this observation with various assays in human cells. Therefore we analyzed γH2AX and Rad51 foci levels at 2 and 8 h post 2 Gy irradiation and found a DSB repair defect in PCNA-depleted G2-phase cells, which was very similar to that of ATRX depletion (Figure 3A). We then applied the I-*Sce*I-based HR-reporter assay and could also detect reduced GFP-expression in cells deficient of PCNA, indicating a direct role for PCNA during HR (Figure 3B). As we found that PCNA and ATRX protein depletion resulted in a comparable, HR-specific repair defect, we next investigated via co-IP experiments if both proteins physically interact. Indeed, we observed an interaction between ATRX and PCNA in unsynchronized nuclear cell extracts, which was slightly more pronounced after DNA damage induction (Figure 3C). Additionally, we analyzed other potential interaction partners of ATRX in unsynchronized cell extracts and found an interaction with Rad54 and could moreover confirm the already described interaction between ATRX and the histone chaperone DAXX (Voon and Wong, 2016; Xue et al., 2003) (Figure 3C). Interestingly, no interaction between ATRX and Rad51 was observed, which is in line with the suggested role for ATRX during late HR steps, when Rad51 is already removed from the DNA, and not during early steps which involve Rad51 formation.

Next, we wanted to focus on the interaction between ATRX and PCNA to understand the relevance of this interplay for HR. As it is known that several proteins interact with PCNA via their PIP box, we screened for potential PIP box consensus sequences Qxx(M/L/I)xx(F/Y)(F/Y) within the ATRX amino

acid sequence. Strikingly, we found such a PIP box within the C-terminal part of ATRX (QCKLYQYY), suggesting that the interaction between ATRX and PCNA is mediated by this interaction motif (Figure 3D).

Taken together, we could establish the chromatin remodeler ATRX as a new factor involved in HR and propose the following model. ATRX functions after the step of Rad54-dependent Rad51 removal and interacts with PCNA to allow subsequent recombination-associated repair synthesis (Figure 3E).

5.4 Discussion

In this study we discovered that ATRX plays an important role to maintain genomic integrity by functioning during HR repair. We established this additional function for ATRX besides its described roles during replication by using various HR-specific assays. γH2AX foci levels were increased specifically in G2 at late times after IR, HR-dependent GFP expression was decreased and the formation of radiation-induced SCEs was inhibited after depletion of ATRX (Figure 1). By analyzing the formation and removal of Rad51 foci we gained insight into the step of ATRX involvement during HR. In the absence of ATRX, Rad51 formation was not affected and at late stages of HR Rad51 foci removal was almost comparable to control cells, indicating an involvement after Rad54-dependent Rad51 removal (Figure 2A). Hence, we speculate about a function for ATRX at the subsequent step of HR, which is recombination-associated DNA synthesis. The DNA clamp protein PCNA was already described to be involved in HR in yeast and humans (Burgess et al., 2013; Li et al., 2013; Sebesta et al., 2013; Sneeden et al., 2013), where it allows the DNA polymerase to perform repair synthesis, and we could confirm such an involvement of PCNA in HR with several assays (Figure 3A and 3B). Moreover, we found a physical interaction between ATRX and PCNA at late times after DNA damage induction, suggesting that both proteins cooperate during HR. As PCNA is a key factor of replication and ATRX was also described to function during replication processes, we can speculate whether the interaction between ATRX and PCNA during HR in G2 also holds true for replication in S phase. It is known that ATRX is involved in processing G4 structures (Clynes et al., 2015), which might represent a barrier to replication, however if a direct interaction between ATRX and PCNA promotes replication remains elusive. Nevertheless, another distinct function for ATRX in replication was recently elucidated, as it is involved in the protection of stalled replication forks by inhibiting Mre11-dependent degradation (Huh et al., 2016).

Chromatin remodelers like ATRX gain more and more attention as accumulated evidence has suggested an important role during DNA damage response and an involvement at several steps during HR is known (Lans et al., 2012; Liu et al., 2012; Price and Andrea, 2014). Rad54 belongs to the same family of chromatin remodelers as ATRX and fulfills multiple roles during HR, with ATPase-dependent and –independent functions (Wolner and Peterson, 2005). With regards to chromatin

remodeling, it was shown that Rad54 interacts with the histone chaperone Nap1 during HR, which stimulates Rad54's nucleosome remodeling activity and mediates the ejection of histone H1, which in turn abrogates the suppression of HR by H1 (Machida et al., 2014). ATRX also interacts with a histone chaperone (DAXX) during incorporation of the histone variant H3.3 into heterochromatin, which might also be relevant for HR repair in heterochromatic regions (Clynes et al., 2013; Voon and Wong, 2016). Furthermore, it was shown that Rad54 also interacts with PCNA, however not through its PIP box (Burgess et al., 2013; Zhang et al., 2013). Since PCNA is a homotrimeric protein with an interdomain connecting loop for protein binding at each subunit, it was suggested that PCNA can interact with multiple binding partners simultaneously (Burgess et al., 2013; Freudenthal et al., 2010). As we found and interaction between ATRX and PCNA, as well as ATRX and Rad54 in co-IP experiments, it might be possible that these three proteins form a functional complex at late stages of HR. Maybe, by interacting with both proteins, ATRX links the process of Rad51 removal by Rad54 with the subsequent step of PCNA-mediated DNA repair synthesis. This could explain the small amount of persisting Rad51foci, as the removal step might be slowed down if the mediator protein for the subsequent step is not present. Another possibility would be, that ATRX aids in maintaining the D-loop during Rad51 removal, which is consequently impaired if this chromatin remodeler is absent. Whether the main function of ATRX during HR is chromatin remodeling-dependent or independent remains elusive, however it was shown that its ATPase activity is stimulated much more by DNA than by the presence of nucleosomes (Mitson et al., 2011). Interestingly, for PCNA it was proposed that the essential role during HR is stimulating Pol δ to displace a DNA strand during D-loop extension (Li et al., 2013), which might be facilitated by the chromatin remodeling function of ATRX.

Taken together, ATRX was characterized as a novel HR factor, with Rad54 and PCNA as interaction partners during late steps of DSB repair. We propose a model for ATRX involvement during the final steps of HR when repair synthesis takes place, allowing access for PCNA and the DNA-polymerase (Fig 3E). Future studies will clarify if the interaction between ATRX and PCNA is mediated by the discovered PIP box motif of ATRX and investigate potential effects of a PIP box mutation to further elucidate the interacting with PCNA during repair synthesis. Further on, biochemical experiments will gain mechanistic insight in the precise function of ATRX during HR, answering the question if the chromatin remodeling activity of ATRX is additionally relevant for this repair process.

5.5 Experimental Procedures

Cell lines and cell culture

Immortalized and transformed cell lines used were HeLa-S3, HeLa-pGC, HeLa-pEJ, HeLa-shATRX, and HeLa ATRX KO cells. All cell lines were cultured in DMEM supplemented with 10% FCS and 1% NEAA and were maintained at 37°C in a 5% CO2 incubator.

Generation of stable cell lines

To generate HeLa-shATRX expressing knockdown cell lines, lentiviral transduction of a pTRIPZ vector was performed according to the manufacturer's protocol (ThermoFisher Scientific). Two different shRNA sequences against ATRX and a non-silencing control sequence were used: (shATRX-1:TAAATCTATTCCTGAACTC; shATRX-2:ATCCTCAAGAGGTTGAATC; shNS: CTTACTCTCGCCCAAGCGAGAG). Depletion of the protein was achieved by doxycycline addition to the media (2µg/ml) every 48 h for 5 days. Knockdown cell lines were identified by immunoblotting. To generate HeLa ATRX KO cell lines, a CRISPR Nickase Ninja plasmid including two different gRNAs for ATRX (gRNA1: TCTACGCAACCTTGGTCGAA; gRNA2: ATTTCTTGCAGAAAGCATTA) was used according to the manufacturer's protocol (DNA2.0). The knockout cell line was confirmed by immunoblotting, immunostaining and sequencing.

RNA interference and plasmid transfection

Transfection of HeLa cells with specific siRNAs was carried out using HiPerFect Transfection Reagent according to the manufacturer's instructions (Qiagen). Cells were transfected directly after cell seeding and all siRNAs were used at a final concentration of 25nM. A second transfection was performed 24h later. siRNA sequences were as follows: siATRX (GAG GAA ACC TTC AAT TGT ATT), siBRCA2 (TTG GAG GAA TAT CGT AGG TAA), siCtrl (AAT TCT CCG AAC GTG TCA CGT), siKu80 (AAG ACA GAC ACC CTT GAA GAC), siPCNA (CGGTGACACTCAGTATGTC), siRad54 (GAA CTC CCA TCC AGA ATG ATT). Lipofectamine® LTX (Thermo Fisher) and Effectene® (Qiagen) were used for plasmid transfection, all according to the manufacturer's instructions.

DNA damage induction

X-irradiation was performed at 90 kV and 19 mA (37 mA for 10 Gy) with an aluminium filter at a dose rate of 2 Gy/min. For laser micro-irradiation, cells were grown on petri dishes and treated with 50 µM BrdU for at least 24 h. Cells were transferred into a µ-slide VI (Ibidi) and incubated for 24 h. The µ-slide VI was placed in an incubated chamber of an Axio Observer D microscope (Zeiss). A diode laser (LuxX 375-20, Omicron) was used for micro-irradiation (375 nm) coupled to the

epifluorescence path of the microscope and focused through a Ph 3 objective. The laser output was set to 80% (16 mW) controlled by Omicron PhoxX Controller v.1.2.6 software. The stage speed (0.201 mm per second) was controlled by µManager software.

Antibodies and Plasmids

Antibodies used for immunofluorescence staining were rabbit anti-**Rad51** (Abcam, ab63801), mouse anti-**GFP** (Roche, 11814460001), mouse anti-**γH2AX** (Millipore, 05-636), rabbit anti-**ATRX** (Santa Cruz, sc-15408); Goat anti-mouse AlexaFluor 488 or 594 (Molecular Probes), Goat anti-rabbit AlexaFluor 488 or 594 (Molecular Probes).

Antibodies used for immunoblotting were rabbit anti-**Rad51** (Abcam, ab63801), rabbit anti-**Ku80** (Cell Signaling Technology, 2180S), mouse anti-**Rad54** (Santa Cruz, sc-163370), mouse anti-**αTubulin** (Santa Cruz, sc-8035), mouse anti-**ATRX** (Santa Cruz, sc-55584), rabbit anit-**BRCA2** (Cell Signaling Technology, 9012), mouse anti-**PCNA** (Santa Cruz, sc-56), rabbit anti-**DAXX** (Santa Cruz, sc-7152); Goat anti-mouse IgG-HRP or Goat anit-rabbit IgG-HRP (Santa Cruz).

For the generation of an siRNA-resistant ATRX plasmid, a GFP-ATRX plasmid containing Isoform2 (missing aa 1-117) was purchased (addgene: #45444).

Immunofluorescence

For immunofluorescence staining cells were seeded on glass coverslips and fixed with 2.5% formaldehyde (in PBS) for 15 min at RT. Cells were then washed three times with PBS before permeabilization for 10 min at 4°C with 0.5% Triton-X-100 (in PBS/1% FCS). Subsequently, cells were washed and blocked for 30 min at RT with 5% BSA (in PBS/1% FCS). Incubation with primary antibodies was carried out over night at 4°C. Cells were then washed and incubated with secondary antibodies for 1 h at RT. For EdU staining, allowing cell cycle-specific analysis, the Click-iT® EdU Imaging Kit (Invitrogen) was used according to the manufacturer's protocol. DAPI staining was performed for 5 min at RT before embedding the cells with Vectashield mounting medium (Vector Laboratories). For PCNA staining, cells were preincubated with 10 mM Tris-HCl, 2.5 mM $MgCl_2$, 0.5% NP-40, 1 mM PMSF on ice for 8 min and then fixed with MeOH on ice for 15 min. At least 40 nuclei per experiment were examined using a Zeiss microscope and MetaCyte software (Metasystems).

Reporter assays (HR, NHEJ)

HeLa pGC (HR) or HeLa pEJ (NHEJ) cells were seeded and treated with siRNA. Transfection with a *I*-Sce*I* plasmid was carried out 24 h later and cells were then incubated for another 48 h at 37°C and

5% CO_2. Fixation and staining with GFP and DAPI or GFP, RFP and DAPI was performed as described. At least 10000 cells were analyzed using a Zeiss microscope and MetaCyte software. GFP-positive cells (or GFP and RFP-positive cells) were enumerated and set in ratio to the total cell number. Both cell lines were a kind gift of Jochen Dahm-Daphi and were used as described (Mansour et al., 2008).

Cell cycle-specific DNA repair

For cell cycle-specific analysis of immunofluorescence staining, EdU (10 µM) was added to the cells 30 min prior to irradiation to allow labeling of S phase. Nocodazole (100 ng/ml) was added additionally to prevent the progression of G2 cells into G1 phase during repair times. After fixation and staining of the cells, Metafer software at a Zeiss microscope was used to measure DAPI and EdU-intensities of the nuclei. Accordingly cell populations were blotted in a diagram allowing the discrimination between G1, G2 and S phase. The respective population was gated and single cells were relocated for foci evaluation (Beucher et al., 2009), with at least 40 cells per experiment.

Clonogenic survival

For clonogenic survival studies in ATRX-knockdown cell lines defined numbers of HeLa-shNS or doxycycline-treated HeLa-shATRX were seeded. 24 h post cell seeding DNA damage was induced by X-rays (2 Gy, 5 Gy, 7Gy), MMS (0.5, 1, 1.5 mM) or MMC (0.5, 1, 1.5 µg/ml) treatment and cells were then incubated for 10 days at 37°C and 5% CO_2. Colonies were stained with crystal violet for enumeration.

Chromosomal studies

To analyze sister chromatid exchanges (SCEs) and chromosomal breaks HeLa cells were seeded, treated with siRNA and incubated with BrdU for 48 h. Cells were then irradiated with 2 Gy and supplemented with EdU, 5 h later Coffein and Colcemid was added. 8 h after irradiation cells were harvested. For preparation of chromosome spreads, cells were pelleted and resuspended in 75 mM KCl. After 20 min incubation at 37°C cells were centrifuged at 200 x g and 4°C for 10 min and fixed (acetic acid:methanol = 1:3) dropwise. Fixation was repeated 3 times and cells were stored at -20°C over night. For EdU staining and specific evaluation of EdU-negative cells irradiated in G2 phase chromosomes were spread onto cover slips. Spreads were air-dried and staining was performed using the Click-iT® EdU Imaging Kit (Invitrogen) according to the manufacturer's instructions. For each experiment 40 chromosome spreads were captured and analyzed using an Axioplan2 microscope (Zeiss) with Metafer software (MetaSystems). Only EdU-negative spreads were evaluated.

Protein extracts and co-immunoprecipitation

For nuclear cell extracts (NCEs) cell pellets were resuspended in Chelsky buffer (10 mM Tris-HCl, 10 mM NaCl, 3 mM $MgCl_2$, 30 mM sucrose, pH 6.8) supplemented with 0.5% NP-40 and incubated for 10 min on ice. Cells were then centrifuged and pellets were resuspended in Lysis buffer (20 mM Tris-HCl, 150 mM NaCl, 1% Triton X-100, pH 8.2) before sonication (Bandelin Sonorex) three times for 1 min. Afterwards cells were incubated rotating at 4°C for 30 min, followed by centrifugation at max speed for 30 min at 4°C. For Co-immunoprecipitation analysis antibodies (4 µg) were coupled to Dynabeads™ Protein G (Invitrogen) by overnight incubation at 4°C. Beads were washed in PBS and NCEs were used for overnight incubation at 4°C. Immune complexes were then washed three times in Lysis buffer, mixed with Laemmli buffer and analyzed via immunoblotting.

Immunoblotting

Protein extracts were generated as described. Samples were mixed with Laemmli buffer for SDS-PAGE analysis and afterwards transferred onto PVDF or nitrocellulose membranes for 2.5 h or overnight. Blocking of membranes was performed for 1 h at RT in 5% milk (in TBST) before incubation with primary antibodies overnight at 4°C. Membranes were then washed and incubated with HRP-conjugated secondary antibodies for 1 h at RT, again washed and chemiluminescence signals were detected using ECL substrate solution (Biozym) and a Chemi-Smart system (Vilber Lourmat).

Statistical analysis was performed by student's t-test: *, $p < 0.05$; **, $p < 0.01$; ***, $p < 0.001$.

5.6 References

Acharya, N., Klassen, R., Johnson, R.E., Prakash, L., and Prakash, S. (2011). PCNA binding domains in all three subunits of yeast DNA polymerase modulate its function in DNA replication. Proc. Natl. Acad. Sci. *108*, 17927–17932.

Argentaro, A., Yang, J.-C., Chapman, L., Kowalczyk, M.S., Gibbons, R.J., Higgs, D.R., Neuhaus, D., and Rhodes, D. (2007). Structural consequences of disease-causing mutations in the ATRX-DNMT3-DNMT3L (ADD) domain of the chromatin-associated protein ATRX. Proc. Natl. Acad. Sci. U. S. A. *104*, 11939–11944.

Bérubé, N.G., Smeenk, C. a, and Picketts, D.J. (2000). Cell cycle-dependent phosphorylation of the ATRX protein correlates with changes in nuclear matrix and chromatin association. Hum. Mol. Genet. *9*, 539–547.

Beucher, A., Birraux, J., Tchouandong, L., Barton, O., Shibata, A., Conrad, S., Goodarzi, A.A., Krempler, A., Jeggo, P.A., and Löbrich, M. (2009). ATM and Artemis promote homologous recombination of radiation-induced DNA double-strand breaks in G2. EMBO J. *28*, 3413–3427.

Bloom, L.B. (2009). Loading Clamps for DNA Replication and Repair. DNA Repair (Amst). *8*, 570–578.

Bugreev, D. V., Rossi, M.J., and Mazin, A. V. (2011). Cooperation of RAD51 and RAD54 in regression of a model replication fork. Nucleic Acids Res. *39*, 2153–2164.

Bunting, S.F., and Nussenzweig, A. (2013). End-joining, translocations and cancer. Nat Rev Cancer *13*, 443–454.

Burgess, R.C., Sebesta, M., Sisakova, A., Marini, V.P., Lisby, M., Damborsky, J., Klein, H., Rothstein, R., and Krejci, L. (2013). The PCNA interaction protein box sequence in Rad54 is an integral part of its ATPase domain and is required for efficient DNA repair and recombination. PLoS One *8*.

Chapman, J.R., Taylor, M.R.G., and Boulton, S.J. (2012). Playing the End Game: DNA Double-Strand Break Repair Pathway Choice. Mol. Cell *47*, 497–510.

Clynes, D., Higgs, D.R., and Gibbons, R.J. (2013). The chromatin remodeller ATRX: A repeat offender in human disease. Trends Biochem. Sci. *38*, 461–466.

Clynes, D., Jelinska, C., Xella, B., Ayyub, H., Scott, C., Mitson, M., Taylor, S., Higgs, D.R., and Gibbons, R.J. (2015). Suppression of the alternative lengthening of telomere pathway by the chromatin remodelling factor ATRX. Nat. Commun. *6*, 7538.

Conrad, S., Künzel, J., and Löbrich, M. (2011). Sister chromatid exchanges occur in G2-irradiated cells. Cell Cycle *10*, 222–228.

Das-Bradoo, S., Ricke, R.M., and Bielinsky, A.-K. (2006). Interaction between PCNA and diubiquitinated Mcm10 is essential for cell growth in budding yeast. Mol. Cell. Biol. *26*, 4806–4817.

Eisen, J.A., Sweder, K.S., and Hanawalt, P.C. (1995). Evolution of the SNF2 family of proteins: subfamilies with distinct sequences and functions. Nucleic Acids Res. *23*, 2715–2723.

Ensminger, M., Iloff, L., Ebel, C., Nikolova, T., Kaina, B., and Löbrich, M. (2014). DNA breaks and chromosomal aberrations arise when replication meets base excision repair. J. Cell Biol. *206*, 29–43.

Essers, J., Theil, A.F., Baldeyron, C., van Cappellen, W.A., Houtsmuller, A.B., Kanaar, R., and Vermeulen, W. (2005). Nuclear Dynamics of PCNA in DNA Replication and Repair. Mol. Cell. Biol. *25* , 9350–9359.

Eustermann, S., Yang, J.-C., Law, M.J., Amos, R., Chapman, L.M., Jelinska, C., Garrick, D., Clynes, D., Gibbons, R.J., Rhodes, D., et al. (2011). Combinatorial readout of histone H3 modifications specifies localization of ATRX to heterochromatin. Nat. Struct. Mol. Biol. *18*, 777–782.

Freudenthal, B.D., Gakhar, L., Ramaswamy, S., and Washington, M.T. (2010). Structure of monoubiquitinated PCNA and implications for translesion synthesis and DNA polymerase exchange. Nat Struct Mol Biol *17*, 479–484.

Gary, R., Kim, K., Cornelius, H.L., Park, M.S., and Matsumoto, Y. (1999). Proliferating Cell Nuclear Antigen Facilitates Excision in Long-patch Base Excision Repair. J. Biol. Chem. *274* , 4354–4363.

van Gent, D.C., Hoeijmakers, J.H.J., and Kanaar, R. (2001). Chromosomal stability and the DNA double-stranded break connection. Nat Rev Genet *2*, 196–206.

Ghezraoui, H., Piganeau, M., Renouf, B., Renaud, J.-B., Sallmyr, A., Ruis, B., Oh, S., Tomkinson, A., Hendrickson, E.A., Giovannangeli, C., et al. (2014). Chromosomal translocations in human cells are generated by canonical nonhomologous end-joining. Mol. Cell *55*, 829–842.

Huh, M.S., O'Dea, T.P., Ouazia, D., McKay, B.C., Parise, G., Parks, R.J., Rudnicki, M.A., and Picketts, D.J. (2012). Compromised genomic integrity impedes muscle growth after Atrx inactivation. J. Clin. Invest. *122*, 4412–4423.

Huh, M.S., Ivanochko, D., Hashem, L.E., Curtin, M., Delorme, M., Goodall, E., Yan, K., and Picketts, D.J. (2016). Stalled replication forks within heterochromatin require ATRX for protection. Cell Death Dis. *7*, e2220.

Ishov, A.M., Vladimirova, O. V, and Maul, G.G. (2004). Heterochromatin and ND10 are cell-cycle regulated and phosphorylation-dependent alternate nuclear sites of the transcription repressor Daxx and SWI/SNF protein ATRX. J. Cell Sci. *117*, 3807–3820.

Iwase, S., Xiang, B., Ghosh, S., Ren, T., Lewis, P.W., Cochrane, J.C., Allis, C.D., Picketts, D.J., Patel, D.J., Li, H., et al. (2011). ATRX ADD domain links an atypical histone methylation recognition mechanism to human mental-retardation syndrome. Nat. Struct. Mol. Biol. *18*, 769–776.

Jackson, S.P., and Bartek, J. (2009). The DNA-damage response in human biology and disease. Nature *461*, 1071–1078.

Lans, H., Marteijn, J.A., and Vermeulen, W. (2012). ATP-dependent chromatin remodeling in the DNA-damage response. Epigenetics Chromatin *5*, 4.

Leung, J.W.C., Ghosal, G., Wang, W., Shen, X., Wang, J., Li, L., and Chen, J. (2013). Alpha thalassemia/mental retardation syndrome X-linked gene product ATRX is required for proper replication restart and cellular resistance to replication stress. J. Biol. Chem. *288*, 6342–6350.

Li, J., Holzschu, D.L., and Sugiyama, T. (2013). PCNA is efficiently loaded on the DNA recombination intermediate to modulate polymerase δ, η, and ζ activities. Proc. Natl. Acad. Sci. U. S. A. *110*, 7672–7677.

Liu, B., Yip, R.K., and Zhou, Z. (2012). Chromatin remodeling, DNA damage repair and aging. Curr. Genomics *13*, 533–547.

Löbrich, M., Shibata, A., Beucher, A., Fisher, A., Ensminger, M., Goodarzi, A.A., Barton, O., and Jeggo, P.A. (2010). γH2AX foci analysis for monitoring DNA double-strand break repair: Strengths, limitations and optimization. Cc *9*, 662–669.

Lovejoy, C.A., Li, W., Reisenweber, S., Thongthip, S., Bruno, J., de Lange, T., De, S., Petrini, J.H.J., Sung, P.A., Jasin, M., et al. (2012). Loss of ATRX, genome instability, and an altered DNA damage response are hallmarks of the alternative lengthening of Telomeres pathway. PLoS Genet. *8*, 12–15.

Lukas, J., and Lukas, C. (2013). Shielding Broken DNA for a Quick Fix. Science (80-.). *339*, 652–653.

Machida, S., Takaku, M., Ikura, M., Sun, J., Suzuki, H., Kobayashi, W., Kinomura, A., Osakabe, A., Tachiwana, H., Horikoshi, Y., et al. (2014). Nap1 stimulates homologous recombination by RAD51 and RAD54 in higher-ordered chromatin containing histone H1. Sci. Rep. *4*, 4863.

Mansour, W.Y., Schumacher, S., Rosskopf, R., Rhein, T., Schmidt-Petersen, F., Gatzemeier, F., Haag, F., Borgmann, K., Willers, H., and Dahm-Daphi, J. (2008). Hierarchy of nonhomologous end-joining, single-strand annealing and gene conversion at site-directed DNA double-strand breaks. Nucleic Acids Res. *36*, 4088–4098.

Matos, J., and West, S.C. (2014). Holliday junction resolution: Regulation in space and time. DNA Repair (Amst). *19*, 176–181.

Mitson, M., Kelley, L.A., Sternberg, M.J.E., Higgs, D.R., and Gibbons, R.J. (2011). Functional significance of mutations in the Snf2 domain of ATRX. Hum. Mol. Genet. *20*, 2603–2610.

Mortusewicz, O., and Leonhardt, H. (2007). XRCC1 and PCNA are loading platforms with distinct kinetic properties and different capacities to respond to multiple DNA lesions. BMC Mol. Biol. *8*, 1–8.

Nichols, A.F., and Sancar, A. (1992). Purification of PCNA as a nucleotide excision repair protein. Nucleic Acids Res. *20*, 2441–2446.

Picketts, D.J., Higgs, D.R., Bachoo, S., Blake, D.J., Quarrell, O.W., and Gibbons, R.J. (1996). ATRX encodes a novel member of the SNF2 family of proteins: mutations point to a common mechanism underlying the ATR-X syndrome. Hum. Mol. Genet. *5*, 1899–1907.

Podust, V.N., Tiwari, N., Stephan, S., and Fanning, E. (1998). Replication Factor C Disengages from Proliferating Cell Nuclear Antigen (PCNA) upon Sliding Clamp Formation, and PCNA Itself Tethers DNA Polymerase δ to DNA. J. Biol. Chem. *273* , 31992–31999.

Price, B.D., and Andrea, A.D.D. (2014). NIH Public Access. *152*, 1344–1354.

Renkawitz, J., Lademann, C.A., and Jentsch, S. (2014). Mechanisms and principles of homology search during recombination. Nat Rev Mol Cell Biol *15*, 369–383.

Ritchie, K., Seah, C., Moulin, J., Isaac, C., Dick, F., and Bérubé, N.G. (2008). Loss of ATRX leads to chromosome cohesion and congression defects. J. Cell Biol. *180*, 315–324.

Schlacher, K., Christ, N., Siaud, N., Egashira, A., Wu, H., and Jasin, M. (2011). Double-Strand Break Repair-Independent Role for BRCA2 in Blocking Stalled Replication Fork Degradation by MRE11. Cell *145*, 529–542.

Sebesta, M., Burkovics, P., Juhasz, S., Zhang, S., Szabo, J.E., Lee, M.Y.W.T., Haracska, L., and Krejci, L. (2013). Role of PCNA and TLS polymerases in D-loop extension during homologous recombination in humans. DNA Repair (Amst). *12*, 691–698.

Sneeden, J.L., Grossi, S.M., Tappin, I., Hurwitz, J., and Heyer, W.-D. (2013). Reconstitution of recombination-associated DNA synthesis with human proteins. Nucleic Acids Res. *41*, 4913–4925.

Tang, J., Wu, S., Liu, H., Stratt, R., Barak, O.G., Shiekhattar, R., Picketts, D.J., and Yang, X. (2004). A Novel Transcription Regulatory Complex Containing Death Domain-associated Protein and the ATR-X Syndrome Protein. J. Biol. Chem. *279*, 20369–20377.

Tsurimoto, T., and Stillman, B. (1991). Replication factors required for SV40 DNA replication in vitro. II. Switching of DNA polymerase alpha and delta during initiation of leading and lagging strand synthesis. J. Biol. Chem. *266* , 1961–1968.

Valle-García, D., Griffiths, L.M., Dyer, M. a, Bernstein, E., and Recillas-Targa, F. (2014). The ATRX cDNA is prone to bacterial IS10 element insertions that alter its structure. Springerplus *3*, 222.

Voon, H.P.J., and Wong, L.H. (2016). New players in heterochromatin silencing: histone variant H3.3 and the ATRX/DAXX chaperone. Nucleic Acids Res. *44*, 1496–1501.

Wang, X., Ira, G., Tercero, J.A., Holmes, A.M., Diffley, J.F.X., and Haber, J.E. (2004). Role of DNA Replication Proteins in Double-Strand Break-Induced Recombination in Saccharomyces cerevisiae. Mol. Cell. Biol. *24*, 6891–6899.

Watson, L.A., Solomon, L.A., Li, J.R., Jiang, Y., Edwards, M., Shin-ya, K., Beier, F., and Bérubé, N.G. (2013). Atrx deficiency induces telomere dysfunction, endocrine defects, and reduced life span . J. Clin. Invest. *123*, 2049–2063.

Wolner, B., and Peterson, C.L. (2005). ATP-dependent and ATP-independent Roles for the Rad54 Chromatin Remodeling Enzyme during Recombinational Repair of a DNA Double Strand Break. J. Biol. Chem. *280* , 10855–10860.

Xie, S., Wang, Z., Okano, M., Nogami, M., Li, Y., He, W.-W., Okumura, K., and Li, E. (1999). Cloning, expression and chromosome locations of the human DNMT3 gene family. Gene *236*, 87–95.

Xue, Y., Gibbons, R., Yan, Z., Yang, D., McDowell, T.L., Sechi, S., Qin, J., Zhou, S., Higgs, D., and Wang, W. (2003). The ATRX syndrome protein forms a chromatin-remodeling complex with Daxx and localizes in promyelocytic leukemia nuclear bodies. Proc. Natl. Acad. Sci. U. S. A. *100*, 10635–10640.

Zhang, X.-P., Janke, R., Kingsley, J., Luo, J., Fasching, C., Ehmsen, K.T., and Heyer, W.-D. (2013). A Conserved Sequence Extending Motif III of the Motor Domain in the Snf2-Family DNA Translocase Rad54 Is Critical for ATPase Activity. PLoS One *8*, e82184.

5.7 Figure legends

Figure 1: ATRX has a role in DSB repair via HR

(A) GFP-based reporter assays with ATRX-, Rad54-, BRCA2- or Ku80-depleted cells. HeLa pGC cells (for HR reporter assay) or HeLa pEJ cells (for NHEJ reporter assay) were treated with siRNAs after cell seeding and transfected with a I-*Sce*I plasmid 24 h later. The number of GFP-positive cells was analyzed 48 h post plasmid transfection by scanning DAPI and GFP signals using IF microscopy. The number of GFP-positive cells after siRNA depletion is shown relatively to siCtrl cells. Immunoblots demonstrating the siRNA efficiencies are shown in Figure S1A. Mean ± SEM (n=3). P values were obtained by student's t-test and represent a comparison of the indicated siRNA condition with siCtrl-treated cells. *, $p < 0.05$; **, $p < 0.01$; ***, $p < 0.001$.

(B) Quantification of γH2AX foci in ATRX-, Rad54- or BRCA2-depleted cells. HeLa cells were treated with siRNAs for 48 h and labeled with EdU 10 min prior to X-irradiation with 2 Gy. γH2AX foci were analyzed in EdU-negative G1- or G2-phase cells at different times post irradiation. Spontaneous foci numbers were subtracted. Representative immunofluorescence images show γH2AX foci at 8 h post 2 Gy. Immunoblots demonstrate the siRNA efficiencies. Mean ± SEM (n=3). P values were obtained by student's t-test and represent a comparison of the indicated siRNA condition with siCtrl-treated cells. *, $p < 0.05$; **, $p < 0.01$; ***, $p < 0.001$.

(C) Sister chromatid exchanges (SCEs) in ATRX-, Rad54 or BRCA2-depleted cells. HeLa cells were treated with siRNAs for 48 h, labeled with EdU, and X-irradiated with 2 Gy. SCEs were analyzed in EdU-negative mitotic spreads from G2-irradiated or untreated cells and normalized to 70 chromosomes per spread. Mean ± SEM (n=3). P values were obtained by student's t-test and represent a comparison of the indicated siRNA condition with siCtrl-treated cells. *, $p < 0.05$; **, $p < 0.01$; ***, $p < 0.001$.

Figure 2: ATRX functions during late steps of homologous recombination

(A) Quantification of Rad51 foci in ATRX-, Rad54- or BRCA2-depleted cells. HeLa cells were treated with siRNAs for 48 h and labeled with EdU 10 min prior to X-irradiation with 2 Gy. Rad51 foci were analyzed in EdU-negative G2-phase cells at different times post irradiation. Spontaneous foci numbers were subtracted. Representative immunofluorescence images show Rad51 foci at 8 h post 2 Gy. Mean ± SEM (n=3). P values were obtained by student's t-test and represent a comparison of the indicated siRNA condition with siCtrl-treated cells. *, $p < 0.05$; **, $p < 0.01$; ***, $p < 0.001$.

(B) Chromatid breaks in ATRX-, Rad54 or BRCA2-depleted cells. HeLa cells were treated with siRNAs for 48 h, labeled with EdU, and X-irradiated with 2 Gy. Chromatid breaks were analyzed in EdU-negative mitotic spreads from G2-irradiated or untreated cells, and normalized to 70 chromosomes per spread. Mean ± SEM (n=3). P values were obtained by student's t-test and

represent a comparison of the indicated siRNA condition with siCtrl-treated cells. *, $p < 0.05$; **,$p < 0.01$; ***, $p < 0.001$.

(C) Quantification of γH2AX and Rad51 foci in HeLa ATRX knockout (KO) cells or ATRX KO cells with additional Rad54 depletion. HeLa cells were treated with Rad54 siRNA for 48 h, if indicated, and cells were labeled with EdU 10 min prior to X-irradiation with 2 Gy. γH2AX and Rad51 foci were analyzed in EdU-negative G2-phase cells at 2 and 8 h post irradiation. HeLa cells treated with siCtrl and siRad54 are shown for comparison. Spontaneous foci numbers were subtracted. Mean ± SEM (n=3). P values were obtained by student's t-test and represent a comparison of the indicated siRNA condition with siCtrl-treated cells. *, $p < 0.05$; **, $p < 0.01$; ***, $p < 0.001$.

Figure 3: Interaction between ATRX and PCNA

(A) Quantification of γH2AX, Rad51 foci and HR frequency in PCNA-depleted cells. For foci analysis HeLa cells were treated with siRNAs for 48 h and labeled with EdU 10 min prior to X-irradiation. γH2AX and Rad51 foci were analyzed in EdU-negative G2-phase cells at 2 and 8 h post irradiation. Spontaneous foci numbers were subtracted.

(B) GFP-based HR reporter assay with PCNA- or ATRX-depleted cells. HeLa pGC cells were treated with siRNAs and transfected with a I-*Sce*I plasmid 24 h later. The number of GFP-positive cells was analyzed 48 h post plasmid transfection by IF microscopy. The number of GFP-positive cells after siRNA depletion is shown relatively to siCtrl cells. The immunoblot demonstrates the siRNA efficiency. Mean ± SEM (n=3). P values were obtained by student's t-test and represent a comparison of the indicated siRNA condition with siCtrl-treated cells. *, $p < 0.05$; **, $p < 0.01$; ***, $p < 0.001$.

(C) Analysis of potential interaction partners of ATRX in unsynchronized HeLa cells. ATRX was immunoprecipitated from untreated (NT) nuclear cell extracts or at 8 h post irradiation. An interaction between ATRX and Rad54, PCNA, Rad51 or DAXX was analyzed by immunoblotting.

(D) Schematic structure of ATRX with functional domains. At the N-terminal part the ADD domain of ATRX is located and includes a PHD-like domain. The ATPase/helicase domain of ATRX is depicted at the C-terminal part of the protein structure, harboring highly conserved SNF2-specific sequences. The discovered PIP box of ATRX is located within the ATPase domain, however not directly within one of the conserved SNF2 motifs.

(E) Model for ATRX involvement in HR. During HR, the Rad51-covered nucleoprotein filament performs strand invasion into the sister chromatid and a D-loop is formed. When homologous sequences have been found, Rad51 removal is promoted by Rad54, allowing the subsequent steps to proceed. ATRX associates to the D-loop and exerts chromatin remodeling to allow PCNA binding. ATRX and PCNA interact to promote recombination-associated DNA synthesis and finalization of HR.

5.8 Supplemental information

Supplemental Figure 1 (related to Figure 1):

(A) Localization of ATRX to laser-induced DNA damage sites. The presence of ATRX at laser tracks marked by γH2AX was analyzed 8 h post damage induction, representative immunofluorescence images are shown.

(B) Immunoblots for GFP-based reporter assays corresponding to Figure 1A. For the HR reporter assay, HeLa pGC cells were treated with siRNAs (siKu80, siRad54, siBRCA2, siATRX, siATRX+siRad54). For the NHEJ reporter assay, HeLa pEJ cells were treated with siRNAs (siKu80, siRad54, siATRX). Immunoblots show siRNA efficiencies.

(C) Exemplary cell cycle distribution profile for cell cycle phase-specific foci analysis. Cells were stained with DAPI and EdU, scanned at a microscope and plotted with regards to their DAPI and EdU intensity. Each black dot represents one cell, G1, G2 and S-phase are highlighted in red ovals.

(D) Quantification of γH2AX foci in ATRX-depleted cells complemented with an ATRX-WT plasmid. HeLa cells were treated with ATRX siRNA for 72 h and transfected with an siRNA-resistent ATRX-WT plasmid 24 h later. Cells were labeled with EdU 10 min prior to X-irradiation with 2 Gy, γH2AX foci were analyzed in EdU-negative G2-phase cells at different times post irradiation. Spontaneous foci numbers were subtracted. Mean ± SEM (n=3). P values were obtained by student's t-test and represent a comparison of the indicated siRNA condition with siCtrl-treated cells. *, $p < 0.05$; **, $p < 0.01$; ***, $p < 0.001$.

Supplemental Figure 2 (related to Figure 2):

(A) Quantification of γH2AX and Rad51 foci in HeLa shATRX and HeLa shNS control cells. Two independently generated HeLa shATRX cell lines (shATRX1, shATRX2) were treated with doxycycline for 5 days, to induce the knockdown of ATRX, and labeled with EdU 10 min prior to X-irradiation with 2 Gy. A non-silencing shRNA (shNS) was used as a control. γH2AX and Rad51 foci were analyzed in EdU-negative G2-phase cells at 2 and 8 h post irradiation. Spontaneous foci numbers were subtracted. The immunoblot shows shRNA efficiencies. Mean ± SEM (n=3). P values were obtained by student's t-test and represent a comparison of the indicated shRNA condition with shNS-treated cells. *, $p < 0.05$; **, $p < 0.01$; ***, $p < 0.001$.

(B) Clonogenic survival of ATRX-deficient cells. HeLa shATRX cell lines (shATRX1, shATRX2) were treated with doxycycline for 5 days prior to DNA damage induction. A non-silencing shRNA (shNS) was used as a control. DNA damage was induced by a 1 h pulse-treatment with different concentrations of MMS or MMC. Colony numbers are shown relative to untreated samples and plating efficiencies illustrate reduced colony formation in ATRX depleted cells without damage induction.

Mean ± SEM (n=3). P values were obtained by student's t-test and represent a comparison of the indicated shRNA condition with shNS-treated HeLa cells. *, $p < 0.05$; **, $p < 0.01$; ***, $p < 0.001$.
(C) Validation of the ATX KO cell line via immunofluorescence staining, immunoblotting and sequence analysis. A detailed section of the sequencing data is shown to demonstrate that the ATRX WT sequence could not be found within the analyzed sequence, although two or three sequence possibilities are visible. The appearance of several nucleobase signals for the sequence after the gRNA and Cas9 binding site is most likely due to the polyploidy of the HeLa cell line.

5.9 Figures

Figure 1

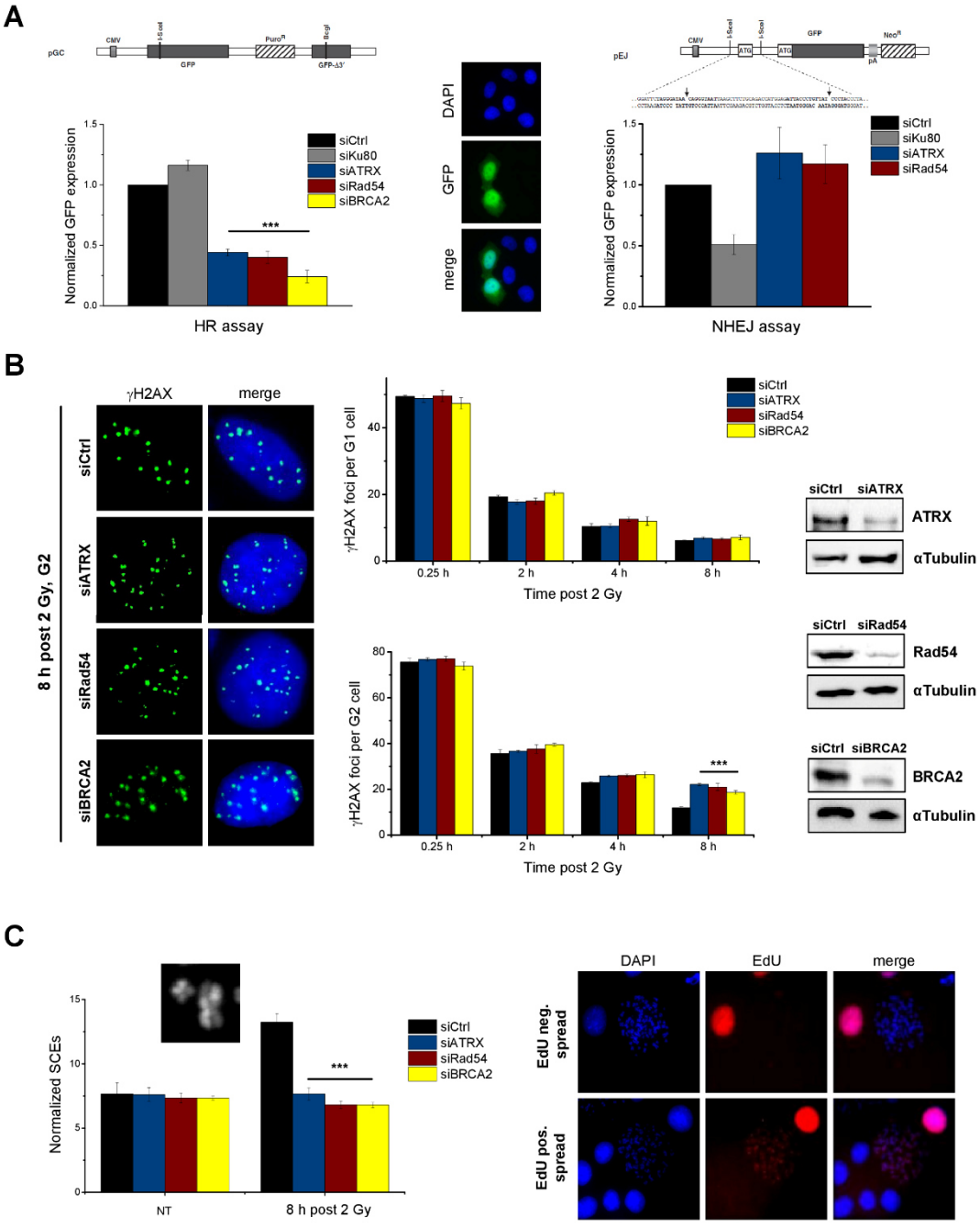

Figure 2

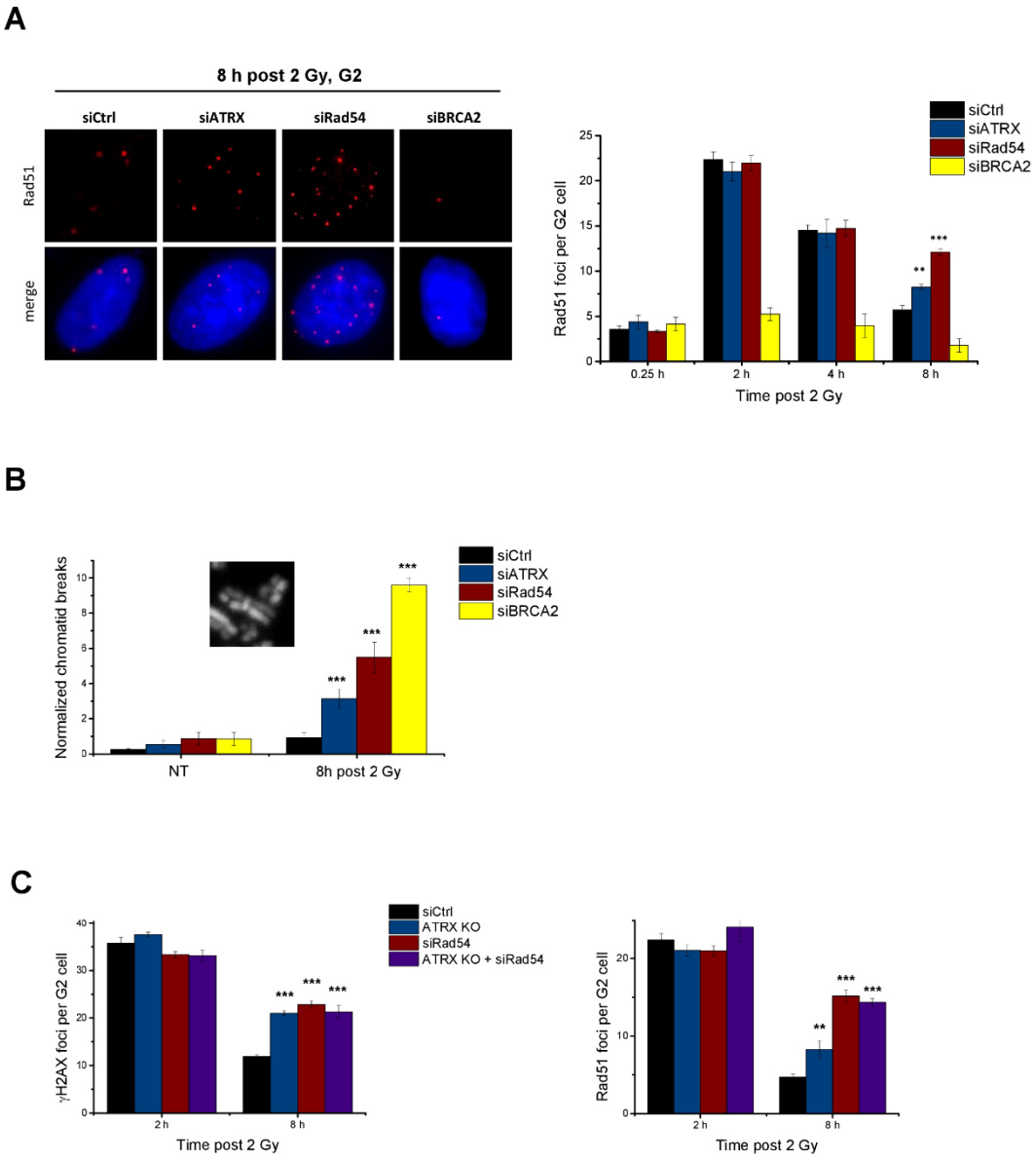
A
8 h post 2 Gy, G2
siCtrl
siATRX
siRad54
siBRCA2
Rad51
merge
Rad51 foci per G2 cell
Time post 2 Gy
0.25 h
2 h
4 h
8 h
B
Normalized chromatid breaks
NT
8h post 2 Gy
C
γH2AX foci per G2 cell
siCtrl
ATRX KO
siRad54
ATRX KO + siRad54
Time post 2 Gy
Rad51 foci per G2 cell

Figure 3

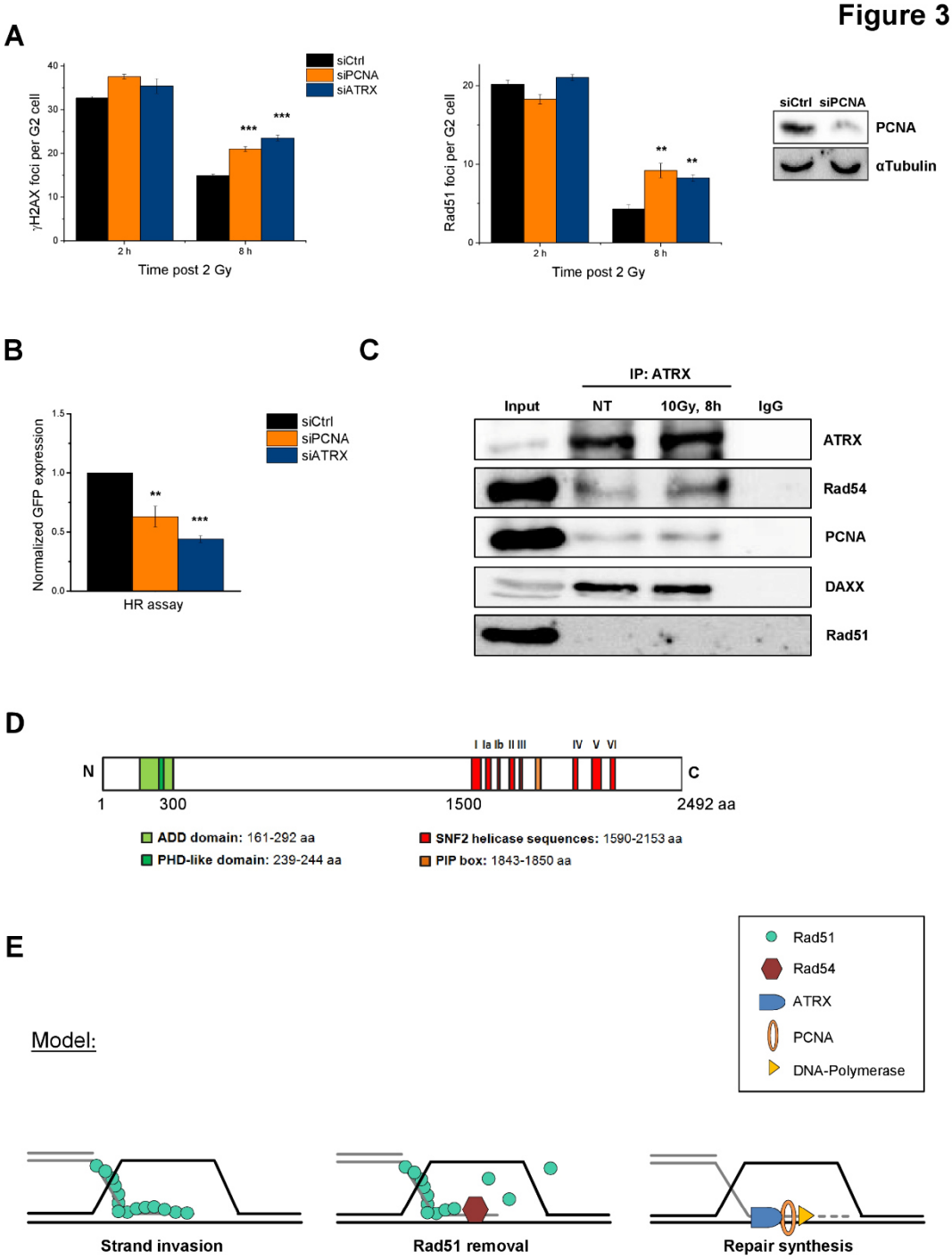
A
siCtrl
siPCNA
siATRX
γH2AX foci per G2 cell
Time post 2 Gy
Rad51 foci per G2 cell
Time post 2 Gy
siCtrl siPCNA
PCNA
αTubulin
B
Normalized GFP expression
HR assay
C
IP: ATRX
Input
NT
10Gy, 8h
IgG
ATRX
Rad54
PCNA
DAXX
Rad51
D
N
C
1
300
1500
2492 aa
ADD domain: 161-292 aa
PHD-like domain: 239-244 aa
SNF2 helicase sequences: 1590-2153 aa
PIP box: 1843-1850 aa
E
Model:
Rad51
Rad54
ATRX
PCNA
DNA-Polymerase
Strand invasion
Rad51 removal
Repair synthesis

Suppl. Figure 1

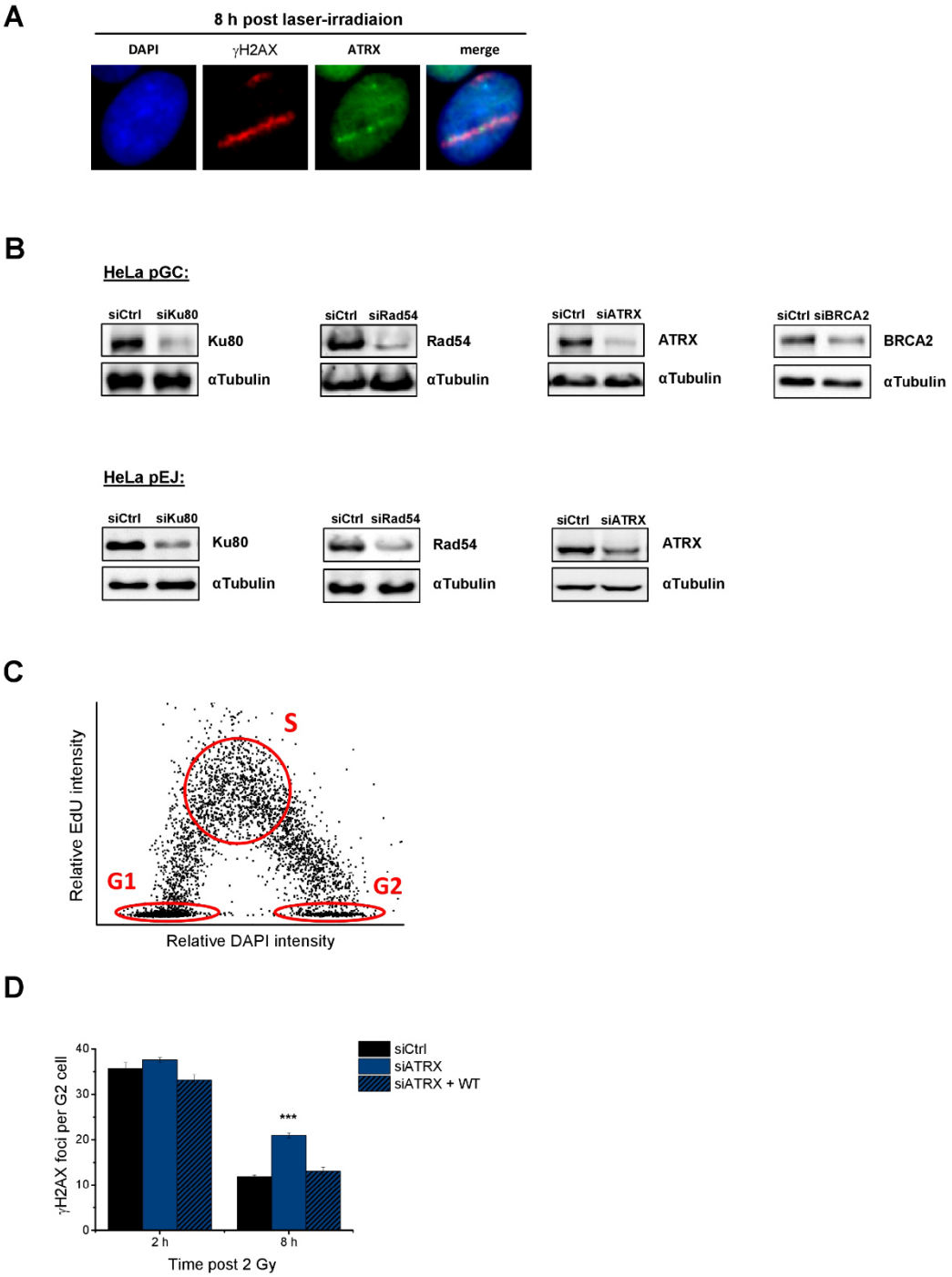

Suppl. Figure 2

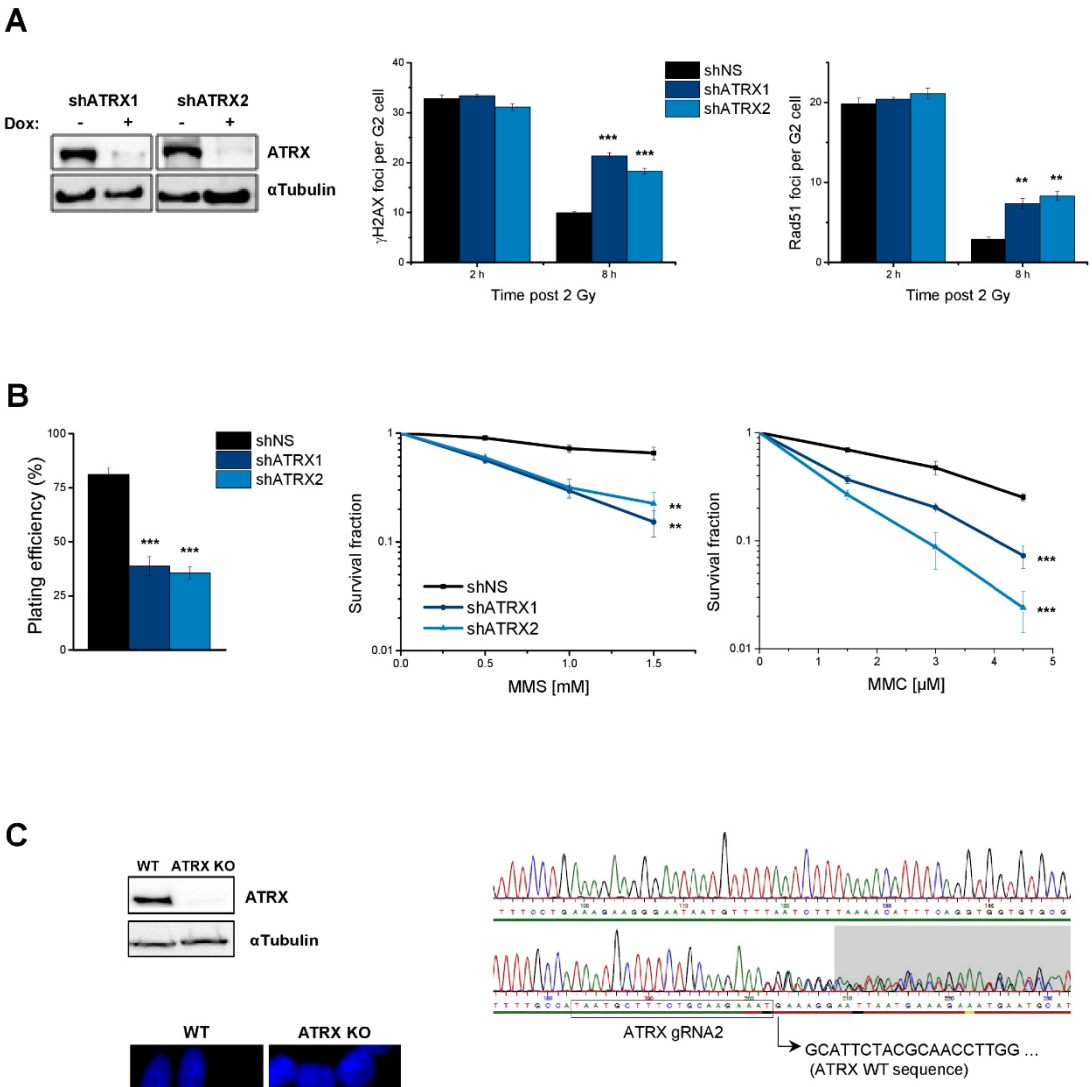

5.10 Declaration of own achievements

The ATRX project was initiated in 2011 by my supervisor Julian Spies. This was my main project for the first two years of my PhD and during the last two years I supported this study part-time. In July 2015 my colleague Szilvia Juhász has joined this project and will furthermore continue to finalize the study. I generated the two inducible shATRX knockdown cell lines and the CRISPR-Cas9 ATRX knockout cell line, which were used in many assays of this study. I designed and illustrated the model and wrote the manuscript independently with input from Markus Löbrich and Julian Spies. All shown experiments were performed and analyzed by myself.

6 Discussion

HR represents an important mechanism for the repair of DSBs as well as the recovery of stalled or broken replication forks. Being involved in the restoration of chromosome damage, HR is indispensable for maintaining genome integrity. HR dysfunction caused by depletion or mutation of key factors of this repair pathway inevitably leads to error-prone repair, which can give rise to translocations and mutations resulting in cancer (Nussenzweig and Nussenzweig, 2010).
Hence, understanding precisely each step during HR, allows modulation of this important DSB repair pathway with regards to cancer therapy. Until now not all single steps are perfectly understood, especially post-synaptic processes await further investigation, as well as the regulation of HR with other cellular processes. This dissertation contributes to a better understanding of late steps of HR, and also investigated the regulation of this pathway, since two new factors involved in theses late steps were identified.

6.1 Conclusions of both manuscripts

6.1.1 Role of Nek1 and Rad54 during HR

Nek1 was already described to be involved in meiotic recombination and at multiple steps during the DNA damage response. In this study, we identified Nek1 as a novel HR protein, namely the kinase responsible for Rad54 phosphorylation at late stages of HR. To investigate the effect of this phosphorylation, a non-phosphorylatable version (Rad54-S572A) and a phospho-mimic version (Rad54-S572E) of Rad54 were generated. The Rad54-S572A mutant as well as Nek1-depleted cells displayed a G2-specific defect in repairing IR-induced DSBs. We found, that this HR defect was due to the inability to remove Rad51 from the heteroduplex DNA in G2, which is essential to allow subsequent steps of HR. The Rad54-S572E mutant on the other hand did not exhibit a defect in repairing DSBs via HR, Rad51 was efficiently removed from the DNA, indicating that phosphorylated Rad54 is necessary to allow Rad51 removal. By analyzing the Nek1-dependent phosphorylation kinetic of Rad54 we surprisingly found that this phosphorylation is restricted to G2 phase and does not occur in S phase. To uncover the physiological relevance of this observation we analyzed replication processes in S phase using both mutants. Here, we could not detect any negative consequence of the Rad54-S572A mutation, but severe effects on the replication fork stability in the Rad54-S572E mutant, as Rad51 was removed from replication forks leading to fork degradation by Mre11. The overall cell survival was strongly impaired in both mutants, indicating that phosphorylation of Rad54 needs to be finely tuned throughout the cell cycle. Phosphorylation of Rad54 is mandatory during HR

in G2, but undesired in S phase where Rad51 has additional functions at replication forks and untimely Rad51 removal results in replication fork instability.

6.1.2 Role of ATRX during HR

ATRX was identified as another new factor of HR, as ATRX depletion resulted in G2-specific DSB repair defects in various assays. A high number of unrepaired DSBs persisted and the frequency of HR was strongly decreased. Interestingly, Rad51 formation was identical to control cells and also Rad51 removal after strand invasion was almost normal, indicating a function for ATRX downstream of Rad54. ATRX is a chromatin remodeler with a Rad54-like ATPase domain and interestingly a PIP box was found, which is a known motif for PCNA interaction. Via co-IP experiments, a physical interaction between ATRX and PCNA was detected, and similar effects were observed after siRNA depletion of both proteins respectively with regards to DBS repair. ATRX was already known to execute important functions during replication, where it is *e.g.* involved in the initiation of new origin firing to start DNA synthesis. In line with this, it is possible that during HR ATRX also mediates the process of DNA repair synthesis, by cooperating with the DNA clamp protein PCNA. A potential model could be, that ATRX functions during late steps of HR by interacting with PCNA to allow repair synthesis and finalize HR. The role of ATRX during this process might include both, the interaction with other HR repair proteins, and its chromatin remodeling function.

6.2 Regulation of HR

Chromosome segregation in meiosis, ICL and DSB repair, as well as the recovery of stalled or broken replication forks rely on faithful HR (Li and Heyer, 2008). However, besides these beneficial aspects, unrestrained HR can lead to chromosomal rearrangements such as translocations, deletions or inversions and toxic recombination intermediates like unproductive Rad51 filaments (Esta et al., 2013; Heyer et al., 2010; Veaute et al., 2003). Therefore, HR needs to be finely regulated to match the specific cellular needs at the right place and time. HR is generally restricted to S and G2 phase of the cell cycle as a sister chromatid is needed to copy the information (Shahar et al., 2012). In G2 phase, where NHEJ and HR can occur, resection of the DSB ends displays a commitment for the cell to utilized HR repair (Huertas and Jackson, 2009). If HR is initiated, three main sub-pathways exist (DHJ, SDSA, BIR) and depending on the conditions or requirements the appropriate pathway is used (Heyer et al., 2010). At several steps during HR (pre-synapsis, synapsis, post-synapsis) modulations can occur. Post-translational modifications like phosphorylation, ubiquitination or sumoylation on HR proteins can influence protein interactions and thereby regulate the process of HR (Branzei and Foiani,

2008). Cyclin-dependent kinases (CDKs) are expressed in a cell cycle-dependent manner and phosphorylate HR proteins for positive or negative regulation. A CDK-dependent phosphorylation of *e.g.* CtIP in S/G2 initiates resection of DSB ends, CDK-dependent phosphorylation of BRCA2 in mitosis however prevents the interaction with Rad51 which is needed for Rad51 loading only in S/G2 (Esashi et al., 2005; Yun and Hiom, 2009). Rad51 is one of the central regulatory HR proteins, as it is involved in early stages of HR and its formation, maintenance and disassembly depends on several other proteins. Many kinases have been reported to phosphorylate Rad51, which affects its recruitment, DNA binding ability and ATP-dependent strand exchange reaction (Flott et al., 2011; Krejci et al., 2012; Sørensen et al., 2005; Yata et al., 2012). Even before Rad51 association, RPA binds to ssDNA, which has a protective function. However it must be replaced with Rad51 to allow homology search and strand invasion into donor sequences. RPA has a higher affinity for ssDNA than Rad51 and the presence of RPA prevents Rad51 association (Krejci et al., 2012). The interplay between Rad51 and RPA is crucial for the initiation of HR. Phosphorylation of RPA by checkpoint kinases and CDKs has been shown to contribute to the recruitment of Rad51 to DSB sites (Zou and Elledge, 2003). Taken together, many proteins involved in HR like CtIP, RPA, BRCA2 and Rad51 are regulated via post-translational modifications.

Rad54 however, another important protein of the HR pathway, was not yet described to be modified during HR in humans. We could show for the first time that Rad54 is phosphorylated at serine 572 during HR, and that this phosphorylation is essential for the removal of Rad51 and progression of HR. We identified Nek1 as the kinase responsible for Rad54 phosphorylation, which only occurs in late G2, irrespective of the cell cycle position during damage induction. Restricting the presence of phosphorylated Rad54 to G2 phase ensures removal of Rad51 only in G2, prior to the onset of mitosis, and not in S phase where Rad51 is needed to stabilize and protect stalled replication forks. Indeed, we could show that the presence of phosphorylated Rad54 in S phase allows Rad51 removal from forks, which resulted in nucleolytic degradation of newly synthesized DNA. Therefore, Nek1 dependent phosphorylation and regulation of Rad54 orchestrates Rad51 removal in G2 phase for proficient HR and protection of forks in S phase to maintain replication fork stability. However, the finding that Rad51 removal predominantly occurs prior to mitosis raises the question how subsequent HR steps can proceed if cells already enter mitosis. It was recently shown that after replication stress conditions, DNA repair synthesis at common fragile sites can occur in mitosis, involving Mus81 and Pol δ (Minocherhomji et al., 2015). Additionally, other publications demonstrated that nucleases like Mus81-Eme1 and Gen1 are most active in mitosis and can therefore resolve late HR structures outside of G2 phase (Matos and West, 2014; Ying et al., 2013). These findings reveal that HR occurs in a highly organized manner at distinct stages of the cell cycle and it might even be possible, that a synchronization of HR with other cellular processes is implemented to allow HR processes only when they are beneficial. In line with this idea, it was proposed that replicative DNA damage due to

replication stress can be processed and repaired during G2 phase and regulation of this repair is mediated by cell-cycle specific kinases (González-Prieto et al., 2013; Karras and Jentsch, 2010). Therefore, damage processing could already start in S phase, is mostly accomplished in G2 and possibly finalized in mitosis. The idea of HR repair synchronization is further substantiated by the observation that HR during meiosis occurs also at very defined stages of the meiotic cycle (Baudat et al., 2013). Our data concerning Rad51 removal in G2, together with published findings suggest a model in which HR is synchronized with the cell cycle, and Nek1 acts as a key factor to regulate Rad51 removal through phosphorylation of Rad54.

6.3 Connection between ATRX and Rad54

Based on sequence homology, ATRX and Rad54 belong to the same family of ATP-dependent chromatin-remodeling factors and share many features. Both proteins possess highly conserved SNF2-specific ATPase/helicase motifs, however no helicase activity was observed in biochemical assays with purified proteins (Dürr et al., 2006; Thomä et al., 2005). Nevertheless, ATRX and Rad54 show dsDNA-dependent ATPase activity, which allows strand displacement of one strand within a triple helix structure (Jaskelioff et al., 2003; Xue et al., 2003). Besides this strand displacement function, biochemical studies in yeast and humans indicated that SWI/SNF complexes play a role in chromatin remodeling by using ATP hydrolysis to modulate nucleosome structures. In yeast, Rad54 was shown to mediate bidirectional nucleosome movement during homology search, which was enhanced by the presence of a Rad51-ssDNA nucleoprotein filament (Alexeev et al., 2003). The chromatin remodeling function of ATRX is directly associated with heterochromatin and will be discussed in detail in the next chapter (Huh et al., 2012).

Both proteins are involved in maintaining genome stability due to their diverse functions in DDR. Cells defective of ATRX or Rad54 show increased sensitivity towards genotoxic agents and accumulate DNA damage (Agarwal et al., 2011; De La Fuente et al., 2015). Rad54 is a long established factor involved in the HR-dependent repair of DSBs and our data revealed ATRX as another important factor for this damage repair pathway. Both proteins function during late stages of HR and might even act in concert as our co-IP experiment showed that both proteins form an immunocomplex. One hypothesis could be that ATRX and Rad54 interact during HR at the D-loop during or after the step where Rad54 actively removes Rad51 from the dsDNA. Chromatin remodeling is most likely needed at all steps during D-loop formation and progression and ATRX might facilitate access to the DNA for proteins involved in further steps of HR. Furthermore, ATRX and Rad54 have been shown to interact with PCNA and both proteins possess a PIP box within their protein structure. In yeast the interaction between Rad54 and PCNA occurs independently of the PIP box motif of

Rad54 and the interaction was not shown specifically for HR repair (Burgess et al., 2013). For ATRX it remains elusive whether the interaction is enabled by its PIP box and is specifically needed for HR repair. This question however could be answered by the generation of an ATRX PIP box mutant and subsequent analysis via co-IP experiments. If the interaction between ATRX and PCNA is indeed mediated by the PIP box of ATRX it would additionally be interesting to investigate the consequences of a PIP box mutation with regards to the functionality of ATRX during HR repair.

Besides their role in HR repair in G2, Rad54 and ATRX are also involved in replication processes. Under replication stress conditions, ATRX can stabilize stalled replication forks and also mediate the reactivation after fork recovery (Leung et al., 2013). Furthermore, it was recently shown that ATRX is directly involved in the protection of replication forks, as a depletion of the protein resulted in Mre11-dependent fork degradation (Huh et al., 2016). Rad54 on the other hand has no direct role in protecting replication forks from degradation. However Rad54 has other functions at the replication fork and is thought to catalyze regression and restoration of replication forks by branch migration, which was shown *in vitro* (Bugreev et al., 2011; Schlacher et al., 2011). Since no direct physiological *in vivo* role of Rad54 could be uncovered, it might be possible that the Rad54 paralog Rad54B can compensate for a Rad54 loss *in vivo*. A potential redundancy of Rad54 and Rad54B at the replication fork might be likely, since both proteins exhibit similar biochemical properties (Wesoly et al., 2006).

As mentioned before, the function of Rad54 during HR is regulated by a Nek1-dependent phosphorylation of Rad54. This phosphorylation occurs in late G2 at Ser572, with a phenylalanine at the -3 position relative to the serine phosphorylation site, displaying the consensus Nek1 phosphorylation motif. In a yeast two-hybrid screen ATRX was also found to interact with Nek1 and two possible Nek1 phosphorylation sites were identified (Surpili et al., 2003). In Rad54 and ATRX the Nek1 phosphorylation sites are found within the ATPase domain, however a phosphorylation of ATRX by Nek1 is unlikely in the context of HR repair in G2. Introducing the phospho-mimic Rad54 mutant in a Nek1-deficient background completely rescued the observed HR defect, which would not be the case if Nek1 has other important targets during this repair pathway. However, a phosphorylation of ATRX by Nek1 would be possible during other cell cycle phases or other cellular processes. As it was shown that Nek1 is active in late G2, has additional functions at the centrosome during mitotic division and ATRX also has an essential role during cell division, it might be possible that Nek1 regulates ATRX actively in mitosis. ATRX is phosphorylated at the onset of mitosis and localizes to chromatin, where it is involved in faithful chromosomal segregation (Bérubé et al., 2000). The phosphorylation of ATRX in mitosis is thought to be performed by a roscovitine-sensitive kinase, suggesting the cyclin B/CDK1complex as it is mostly inactivated by roscovitine treatment and potential CDK phosphorylation motifs were found within the ATRX sequence (Ishov et al., 2004). However, it might be possible that the mitotic kinase Nek1 also regulates ATRX at the predicted

phosphorylation sites during mitosis, additionally to CDKs. Further on, ATRX was shown to change its localization due to phosphorylation and thereby exert different tasks. In contrast to its role in mitosis, during interphase ATRX is unphosphorylated and found at the nuclear matrix, where it is possibly involved in gene regulation (Bérubé et al., 2000). In summary, Rad54 and ATRX are very similar proteins with a common phosphorylation motif and might therefore share Nek1 as an important regulator. This remains to be investigated in further studies, including the generation and characterization of ATRX variants with point mutations in the predicted Nek1 phosphorylation sites, to uncover the impact of this phosphorylation for different cellular processes.

6.4 The impact of chromatin remodeling on genomic stability and HR

Genomic DNA is organized in chromatin, with 147 bp of DNA wrapped around a histone octamer, called a nucleosome subunit. This structure is important to maintain chromosomal stability and protects the DNA from harmful incidents (Saito et al., 2015). However, if DNA damage has occurred, the chromatin structure needs to be reorganized to facilitate DDR, including DNA repair. Such reorganization is also important during transcription and replication and is promoted by histone modification and chromatin remodeling factors (Ehrenhofer-Murray, 2004). Furthermore, after accomplishment of processes like replication, transcription and repair the former chromatin organization has to be re-established. This is most likely of particular importance regarding the re-organization of heterochromatin to ensure chromosomal stability (Bi, 2012).

Modification of chromatin can occur by post-translational modifications of histones via histone-modifying enzymes, such as phosphorylation, acetylation or methylation (van Attikum and Gasser, 2005). Additionally, movement or displacement of histones through ATP-dependent chromatin remodelers in cooperation with histone chaperones can occur. ATP hydrolysis provides the energy for chromatin remodelers to restructure, remove or eject histones, allowing access to specific DNA sites. For example, histone variants like H3.3 can be incorporated or histone dimers like H2A-H2B can be exchanged (Bruno et al., 2003; Lorch et al., 1999; Mizuguchi et al., 2004; Whitehouse et al., 1999). Four structurally related families of chromatin remodelers have been identified and mainly studied in yeast: ISWI, SWI/SNF, INO80 and CHD. Besides their common ATPase domain, each family has additional specific domains, which are responsible for their different functions. However, all 4 families are implicated in transcription, DNA replication and DDR by regulating access to the DNA, recruitment of repair factors or signaling of DNA damage (Clapier and Cairns, 2009; Lans et al., 2012). During HR, chromatin remodeling is required at several steps like resection, homology search, D-loop extension and also for restoration of the chromatin organization after repair.

SMARCA5 (or SNF2h), a component of most ISWI complexes, is rapidly recruited to DSBs to regulate HR and NHEJ (Nakamura et al., 2011; Toiber et al., 2013). The recruitment of SMARCA5 depends on PARP (Poly ADP ribose polymerase) and NuMa (nuclear mitotic apparatus protein) and especially the interaction of SMARCA5 and NuMa was shown to promote the repair pathway of HR, as depletion of both proteins resulted in impaired DSB end resection and decreased recruitment of HR factors (Smeenk et al., 2013; Vidi et al., 2014). Additionally, Nbs1 a component of the MRN complex was recently shown to influence SMARCA5-dependent chromatin remodeling during HR by interacting with the E3 ubiquitin ligase RNF20 (Saito et al., 2015). Therefore, SMARCA5 is an established chromatin remodeler which functions in the regulation of DSB end resection, the initial step of HR and promotes this repair pathway by histone modification in cooperation with other factors. The yeast SWI/SNF complex has also been postulated several times to be directly involved in DSB repair and particularly in HR where it facilitates pairing of homologous DNA strands (Lans et al., 2012). This complex is recruited to DSB sites, where it interacts with γH2AX as well as with acetylated H3. Mutations within SWI/SNF increased the sensitivity towards DSB-causing agents and the absence of this complex severely impaired strand invasion during HR, therefore it was suggested that this complex mediates the clearing of nucleosomes to expose the DNA for homology search (Chai et al., 2005; Lee et al., 2010; Martens and Winston, 2003).

In *S. cerevisiae*, at least 7 members of SNF2-related proteins were described to function during DNA repair (Heyer et al., 2006). Rad54, one of the key factors of HR, and also ATRX belong to the SWI2/SNF2 protein family and share a very similar, highly conserved ATPase domain which provides energy for DNA translocation and chromatin remodeling. In yeast, Rad54 was shown to directly interact with histone 3 via its N-terminal domain (Kwon et al., 2007) and chromatin remodeling functions during HR were suggested at several steps by *in vivo* and *in vitro* studies (Alexiadis and Kadonaga, 2002; Wolner and Peterson, 2005). It was proposed that Rad54 might facilitate homology search by providing accessibility to the donor DNA sequence (Renkawitz et al., 2014). Recently, Rad54 was additionally shown to influence chromatin organization during HR by interaction with the human histone chaperone Nap1. Nap1 accumulates at DNA damage sites and the DSB repair is severely impaired after protein depletion. Binding of Rad54 and Nap1 stimulates the nucleosome remodeling activity of Rad54 and allows ejection of the linker histone H1. H1 is in this context suggested to suppress inappropriate HR repair and therefore needs to be removed to allow this pathway (Machida et al., 2014). Furthermore, nucleosomal remodeling for transient access to the DNA was also shown for the Rad51-ssDNA nucleoprotein filaments, suggesting that Rad51 can also perform ATP-dependent nucleosome unwrapping in addition to its recombinase function (Alexiadis and Kadonaga, 2002; North et al., 2013). Our results suggest also an involvement of ATRX chromatin remodeling activities at several steps during HR. As ATRX was shown to interact with Rad54 in co-IP experiments, it would be possible that it is responsible for maintaining the D-loop, during or after

Rad54 actively removes Rad51 from the DNA. This would be in line with the finding, that ATRX depletion results in slightly increased Rad51 foci levels, as the removal might be impaired or slowed down if ATRX is not there to facilitate access to the DNA for proteins like Rad54 or maintain the D-loop structure. Another interaction of ATRX and PCNA was found in co-IP experiments and indicates a chromatin remodeling function before or during repair synthesis. Furthermore, ATRX could be involved in restructuring the chromatin after recombination-associated DNA synthesis has occurred. Similar to the interaction of Rad54 and the histone chaperone Nap1, ATRX and the histone chaperone DAXX work together during incorporation of the histone variant H3.3 at pericentromeric and telomeric heterochromatin (Conte et al., 2012; Huh et al., 2012). Interestingly, the deposition of H3.3 at sites of DNA damage was recently shown in a PARP1-dependent DSB repair process which links ATP-dependent chromatin remodeling and histone variant incorporation to facilitate DSB repair by NHEJ (Luijsterburg et al., 2016). In summary, only limited information is available about the involvement of chromatin remodeling during late stages of HR, whereas early steps like DSB end resection are much better understood (Chen and Symington, 2013; Dong et al., 2014; Saito et al., 2015). Identifying ATRX as a chromatin remodeler involved in these late steps might shed light on the nucleosome activity that takes place during the final steps of this important repair pathway.

6.5 ATRX and heterochromatin association

In the eukaryotic genome, chromatin is mainly organized in two structurally and functionally different forms, euchromatin and heterochromatin. Genes that are actively transcribed and therefore less condensed are referred to as euchromatin. Heterochromatic chromosome regions are highly condensed, associated with structural proteins like the gene silencer HP1α and are thought to be transcriptionally inactive (Dillon, 2004; Grewal and Moazed, 2003). Within heterochromatin, some regions remain condensed throughout the cell cycle, named constitutive heterochromatin, while others are found at developmentally regulated loci and can change their chromatin state in response to cellular signals, known as facultative heterochromatin (Grewal and Jia, 2007). The presence of heterochromatin at specific loci is crucial for the stability of chromosomal structures and epigenetic regulation. Gene expression can be influenced by heterochromatic spreading, restricting access for the transcription machinery and therefore nearby genes are repressed (Grewal and Jia, 2007). Characteristic features of heterochromatin are histone modifications, which can be recognized by specific chromatin remodeling enzymes. One common modification is the methylation of *e.g.* lysine 9 at histone H3, which is then termed H3K9me^2 or H3K9me^3. Another feature of histones in heterochromatin is hypoacetylation, *e.g.* on histone H3 and termed as H3K4me^0 (Bi, 2012; Grewal and Moazed, 2003). To allow the formation of heterochromatic regions throughout the cell cycle, the histone variant H3.3 is incorporated by the histone chaperone DAXX in cooperation with ATRX,

which allows the establishment and maintenance of heterochromatin at distinct genomic loci like telomeres, centromeres, CpG islands and more, in a replication-independent manner (Goldberg et al., 2010; Voon and Wong, 2016). ATRX directly interacts with DAXX and HP1α via interacting regions within the protein structure and can additionally recognize H3K9me^3 and H3K4me^0 by its ADD domain and thereby bind to the N-terminal tail of H3. The ADD domain mediates the targeting of ATRX to pericentromeric and telomeric heterochromatin, which is notably enhanced by the interaction with HP1α (Eustermann et al., 2011). HP1α is therefore referred to as a heterochromatin binding factor, which helps to direct chromatin remodelers to heterochromatic loci. Moreover, it was shown by *in vitro* and *in vivo* studies, that ATRX binds guanine quadruplex (G4) structures, which are frequently present in heterochromatic regions (Gibbons et al., 2003; Hoffmann et al., 2016; Law et al., 2010). It was proposed, that ATRX recruits DAXX and H3.3 to G4 structures *e.g.* at telomeres, where methyltransferases can then methylate lysine 9 to allow localized heterochromatinization (Huh et al., 2016; Voon and Wong, 2016). G4 structures within the DNA represent an obstacle for replication and can cause replication fork stalling, therefore these unusual secondary structures need to be resolved prior to S phase (Mirkin and Mirkin, 2007). During S phase, ATRX was recently shown to protect stalled forks within heterochromatin under replication stress conditions, as the depletion of ATRX lead to an increase in stalled replication forks and subsequent degradation of the newly synthesized DNA by the exonuclease Mre11 (Huh et al., 2016; Leung et al., 2013). It was proposed that ATRX might bind to and thereby inhibit Mre11 during replication to prevent nucleolytic fork degradation, similar to a suggested role for ATRX at telomeres, which will be discussed below. In summary, ATRX seems to play an important role in the maintenance of heterochromatic regions and particularly in stabilizing stalled replication forks within heterochromatin.

Besides its possible interaction with Mre11 at stalled forks, ATRX was shown to interact with all components of the MRN complex by co-IP and mass spectrometry analysis (Clynes et al., 2014; Leung et al., 2013). The MRN complex plays key roles in the restart of stalled replication forks as well as the repair of DSBs and was furthermore shown to be involved in telomere maintenance (Deng et al., 2009; Lamarche et al., 2010). At telomeres, ATRX and Mre11 physically interact which leads to a sequestration of the MRN complex from the telomeric machinery, thereby preventing MRN-mediated telomeric recombination (Clynes et al., 2015). MRN interestingly not only mediates the recombination-based ALT pathway but was moreover suggested to facilitate telomerase activity in telomerase-dependent cancer cells, *e.g.* by recruitment of the enzyme to telomeres (Lamarche et al., 2010). ATRX therefore has a dual function in restricting the telomere length, first by inhibiting the MRN-dependent telomerase activity and second by inhibiting the ALT-pathway. In ALT tumors without the presence of ATRX, increased occurrence of G4 structures was observed, which somehow facilitates the recombination between telomeric sequences to keep a constant telomere length (Clynes and Gibbons, 2013; Clynes et al., 2015; Lovejoy et al., 2012). Paradoxically, during HR in G2 ATRX

is important for the recombination repair process, at telomeres however the absence of ATRX promotes ALT, which is also thought to be a recombination-based process. Although the exact mechanisms behind the ALT pathway are yet unknown, it has to be considered that the regulation of ALT and HR are most likely different due to the presence of G4 structures at telomeres, which themselves can trigger HR (Cesare and Reddel, 2010; Flynn et al., 2015). A more general suggested role for chromatin remodelers during replication of heterochromatin is the decondensation of chromatin, allowing access to the DNA for the replication machinery, or remodeling of chromatin to facilitate histone modifications for the re-establishment of heterochromatin after replication (Bi, 2012).

Several publications demonstrated an increase in spontaneous γH2AX foci after ATRX depletion, which were mainly localized at telomeres, and a further increase after replication stress (Clynes and Gibbons, 2013; Huh et al., 2012; Leung et al., 2013; Watson et al., 2013). This indicates that after ATRX depletion, the formation of spontaneous DSBs occurs specifically in heterochromatic regions and raises the question if the unrepaired DSBs which we found in ATRX-depleted cells in G2 after IR are also localized in heterochromatin. DSBs induced by IR occur much less frequent in heterochromatin (10-25%) than in euchromatic regions, probably due to the compact structure of heterochromatin. Interestingly, heterochromatic DSBs were shown to be repaired with a slow repair kinetic via HR in G2 phase (Beucher et al., 2009; Goodarzi et al., 2008). To allow access for the repair machinery, the condensed heterochromatin has to be relaxed, which occurs in an ATM-dependent manner by phosphorylation and inactivation of Kap1 (Geuting et al., 2013). HP1α and Kap1 co-localize at heterochromatic regions, as well as HP1α and ATRX, linking all three proteins to the HR repair of DSBs within heterochromatin (Baldeyron et al., 2011; Geuting et al., 2013; Ishov et al., 2004; White et al., 2012). Our data, that ATRX functions during HR in G2 after IR is therefore nicely complemented by the earlier findings that ATRX is connected to heterochromatin organization in general and that IR-induced DSBs which are repaired by HR are localized within heterochromatic regions. Taken together, ATRX functions in the assembly or rearrangement of histones during the formation of heterochromatin and stabilizes or maintains its structure. ATRX is specifically involved in the incorporation of H3.3 and ATRX's chromatin remodeling activity might also be essential for the HR-dependent DSB repair in heterochromatic regions. However, this hypothesis awaits further clarification.

6.6 Nek1, Rad54 and ATRX in cancer and cancer therapy

Understanding the exact mechanisms of DNA repair pathways is a valuable tool in cancer therapy, as it allows the dysregulation of these processes by targeting specific factors. If cancer cells have

impaired DNA repair abilities, the induction of DNA damage will have a more severe effect on cell survival. Radiotherapy is therefore very frequently used to induce DSBs by IR and the ability of tumor cells to repair these DSBs determines the effectiveness of the respective therapy (Helleday, 2010; Kelley et al., 2014).

Nek1, Rad54 and ATRX are involved in DSB repair and other important cellular processes and thereby contribute largely to maintain genomic integrity. Depletion or mutation of Nek1, Rad54 or ATRX and was found in many human cancers and correlates with tumorigenesis (Chen et al., 2011a, 2014; Clynes and Gibbons, 2013; Mason et al., 2015; Matsuda et al., 1999; Moniz et al., 2011). As one hallmark of cancer, tumor cells can divide indefinitely by evading the Hayflick limit of progressive telomere shortening that accompanies each cell division. In 90% of all human tumors the enzyme telomerase is re-activated to escape this limitation, however the remaining 10% of cancers employ an alternative pathway called ALT to prevent telomere shortening and thereby become immortal (Henson et al., 2002; Shay and Bacchetti, 1997). The exact mechanism behind the ALT pathway is yet not fully understood, but it is likely dependent on recombination events at the telomeres. Loss of ATRX and its interaction partner DAXX was found in the majority of ALT-dependent cancer cell lines, suggesting an involvement of both proteins to suppress this pathway in normal cells (Clynes and Gibbons, 2013; Lovejoy et al., 2012).

As cancer cells divide rapidly, it is known that they rely much more on HR pathways to deal with DNA damage or replication errors compared to normal cells. Proteins involved in the repair of DSBs via HR are often targets in tumor therapy, as HR is active in S and G2 and dividing cells pass these cell cycle phases with each cell division. Most of the cells in our body on the other hand are non- or slowly proliferating and found in G1/G0 phase of the cell cycle. Thus, they mainly use the NHEJ repair pathway to repair induced DSBs and would be less affected by the inability to use HR (Willers et al., 2002). In conclusion, the development of inhibitors specific for HR factors would be a potent target for combined therapy together with traditional chemotherapeutics or radiotherapy for DNA damage induction. Especially kinases like Nek1 display a promising target to develop inhibitors, since they are already well studied and different domains like the ATP binding pocket can be blocked by small-molecule inhibitors. Besides its role in repairing DSBs, Nek1 also regulates apoptosis by interaction with the mitochondrial outer membrane protein VDAC1, which makes Nek1 again a suitable target for cancer therapy. Depletion of Nek1 leads to a hypersensitivity towards IR or other genotoxic agents and cells will more frequently die from apoptosis in the absence of Nek1 (Chen et al., 2011). This could be particularly useful in cancer cell lines, which over-express Nek1 and show decreased sensitivity towards DNA damaging agents (Chen et al., 2014). Nevertheless, due to the diverse cellular functions of Nek1 an inhibition could result in severe side effects for healthy tissues. It needs to be investigated how and when such an inhibition would have the greatest therapeutic effect

and therefore it remains elusive, whether Nek1 is a promising candidate for individual human cancer therapy. Rad54 mutations in cancer mainly concern its translocase activity, leading to the accumulation of Rad51 foci, which do not co-localize with DNA damage markers and are therefore called non-damage foci (Mason et al., 2015). Additionally, elevated levels of Rad51 have been found in many tumor cell lines, maybe due to an imbalance of Rad51 and the Rad54 translocase activity (Mason et al., 2015; Richardson et al., 2004). Therefore, Rad51 inhibitors might be a potent tool for cancer therapy, as it was shown, that inhibition of Rad51 can delay cell cycle progression and trigger apoptosis (Jhaveri et al., 2012; Kelley et al., 2014). Considering ATRX for cancer therapy, an inhibition of this HR factor to increase susceptibility for chemotherapeutics would also be possible. However, due to its diverse functions in other cellular processes, the side effects could be dramatic and more research needs to be done to exactly understand how ATRX functions during HR and how it could be inhibited. A more promising approach to use ATRX in cancer therapy however would be targeting ALT-dependent tumor cells. As loss of ATRX was found in most of these cancer cell lines, reintroducing ATRX could prevent the ALT pathway and thereby cause growth suppression (Clynes et al., 2015; Huh et al., 2016). However, only 10% of all cancers depend on the ALT pathway, so the approach to express ATRX in patients with ATRX loss by gene therapy could only be a future scenario for individual tumor therapy. Taken together, all three proteins represent valuable targets for cancer treatment and understanding their exact functions during HR and other cellular processes, will allow suitable application in future therapies.

7 References

Adelman, C.A., Lolo, R.L., Birkbak, N.J., Murina, O., Matsuzaki, K., Horejsi, Z., Parmar, K., Borel, V., Skehel, J.M., Stamp, G., et al. (2013). HELQ promotes RAD51 paralogue-dependent repair to avert germ cell loss and tumorigenesis. Nature *502*, 381–384.

Agarwal, S., van Cappellen, W. a, Guénolé, A., Eppink, B., Linsen, S.E. V, Meijering, E., Houtsmuller, A., Kanaar, R., and Essers, J. (2011). ATP-dependent and independent functions of Rad54 in genome maintenance. J. Cell Biol. *192*, 735–750.

Alexeev, A., Mazin, A., and Kowalczykowski, S.C. (2003). Rad54 protein possesses chromatin-remodeling activity stimulated by the Rad51-ssDNA nucleoprotein filament. Nat Struct Mol Biol *10*, 182–186.

Alexiadis, V., and Kadonaga, J.T. (2002). Strand pairing by Rad54 and Rad51 is enhanced by chromatin. Genes Dev. *16*, 2767–2771.

Amitani, I., Baskin, R.J., and Kowalczykowski, S.C. (2006). Visualization of Rad54, a Chromatin Remodeling Protein, Translocating on Single DNA Molecules. Mol. Cell *23*, 143–148.

Andersen, S.L., and Sekelsky, J. (2010). Meiotic versus mitotic recombination: Two different routes for double-strand break repair. BioEssays *32*, 1058–1066.

van Attikum, H., and Gasser, S.M. (2005). The histone code at DNA breaks: a guide to repair? Nat Rev Mol Cell Biol *6*, 757–765.

Baldeyron, C., Soria, G., Roche, D., Cook, A.J.L., and Almouzni, G. (2011). HP1?? recruitment to DNA damage by p150CAF-1 promotes homologous recombination repair. J. Cell Biol. *193*, 81–95.

Baudat, F., Imai, Y., and de Massy, B. (2013). Meiotic recombination in mammals: localization and regulation. Nat Rev Genet *14*, 794–806.

Baumann, P., Benson, F.E., and West, S.C. (2014). Human Rad51 Protein Promotes ATP-Dependent Homologous Pairing and Strand Transfer Reactions In Vitro. Cell *87*, 757–766.

Bérubé, N.G., Smeenk, C. a, and Picketts, D.J. (2000). Cell cycle-dependent phosphorylation of the ATRX protein correlates with changes in nuclear matrix and chromatin association. Hum. Mol. Genet. *9*, 539–547.

Beucher, A., Birraux, J., Tchouandong, L., Barton, O., Shibata, A., Conrad, S., Goodarzi, A.A., Krempler, A., Jeggo, P.A., and Löbrich, M. (2009). ATM and Artemis promote homologous recombination of radiation-induced DNA double-strand breaks in G2. EMBO J. *28*, 3413–3427.

Bi, X. (2012a). Functions of chromatin remodeling factors in heterochromatin formation and maintenance. Sci. China Life Sci. *55*, 89–96.

Bi, X. (2012b). Functions of chromatin remodeling factors in heterochromatin formation and maintenance. Sci. China Life Sci. *55*, 89–96.

Bolderson, E., Tomimatsu, N., Richard, D.J., Boucher, D., Kumar, R., Pandita, T.K., Burma, S., and Khanna, K.K. (2010). Phosphorylation of Exo1 modulates homologous recombination repair of DNA double-strand breaks. Nucleic Acids Res. *38* , 1821–1831.

Branzei, D., and Foiani, M. (2008). Regulation of DNA repair throughout the cell cycle. Nat Rev Mol Cell Biol *9*, 297–308.

Bruno, M., Flaus, A., Stockdale, C., Rencurel, C., Ferreira, H., and Owen-Hughes, T. (2003). Histone H2A/H2B Dimer Exchange by ATP-Dependent Chromatin Remodeling Activities. Mol. Cell *12*, 1599–1606.

Bugreev, D. V, Mazina, O.M., and Mazin, A. V (2006). Rad54 protein promotes branch migration of Holliday junctions. Nature *442*, 590–593.

Bugreev, D. V., Rossi, M.J., and Mazin, A. V. (2011). Cooperation of RAD51 and RAD54 in regression of a model replication fork. Nucleic Acids Res. *39*, 2153–2164.

Burgess, R.C., Sebesta, M., Sisakova, A., Marini, V.P., Lisby, M., Damborsky, J., Klein, H., Rothstein, R., and Krejci, L. (2013). The PCNA interaction protein box sequence in Rad54 is an integral part of its ATPase domain and is required for efficient DNA repair and recombination. PLoS One *8*.

Cardoso, C., Lutz, Y., Mignon, C., Compe, E., Depetris, D., Mattei, M., Fontes, M., and Colleaux, L. (2000). ATR-X mutations cause impaired nuclear location and altered DNA binding properties of the XNP/ATR-X protein. J. Med. Genet. *37*, 746–751.

Ceballos, S.J., and Heyer, W.-D. (2011). Functions of the Snf2/Swi2 family Rad54 motor protein in homologous recombination. Biochim. Biophys. Acta - Gene Regul. Mech. *1809*, 509–523.

Cesare, A.J., and Reddel, R.R. (2010). Alternative lengthening of telomeres: models, mechanisms and implications. Nat Rev Genet *11*, 319–330.

Chai, B., Huang, J., Cairns, B.R., and Laurent, B.C. (2005). Distinct roles for the RSC and Swi/Snf ATP-dependent chromatin remodelers in DNA double-strand break repair. Genes Dev. *19*, 1656–1661.

Chapman, J.R., Taylor, M.R.G., and Boulton, S.J. (2012). Playing the End Game: DNA Double-Strand Break Repair Pathway Choice. Mol. Cell *47*, 497–510.

Chen, H., and Symington, L.S. (2013). Overcoming the chromatin barrier to end resection. Cell Res. *23*, 317–319.

Chen, Y., Chen, P.-L., Chen, C.-F., Jiang, X., and Riley, D.J. (2008). Never-in-mitosis related Kinase 1 functions in DNA damage response and checkpoint control. Cc *7*, 3194–3201.

Chen, Y., Craigen, W.J., and Riley, D.J. (2009). Nek1 regulates cell death and mitochondrial membrane permeability through phosphorylation of VDAC1. Cc *8*, 257–267.

Chen, Y., Chen, C.-F., Chiang, H.-C., Pena, M., Polci, R., Wei, R.L., Edwards, R. a, Hansel, D.E., Chen, P.-L., and Riley, D.J. (2011). Mutation of NIMA-related kinase 1 (NEK1) leads to chromosome instability. Mol. Cancer *10*, 5.

Chen, Y., Chen, C., Polci, R., Wei, R., Riley, D.J., and Chen, P. (2014). Increased Nek1 expression in Renal Cell Carcinoma cells is associated with decreased sensitivity to DNA-damaging treatment. *1*.

Ciccia, A., and Elledge, S.J. (2010). The DNA Damage Response: Making It Safe to Play with Knives. Mol. Cell *40*, 179–204.

Clapier, C.R., and Cairns, B.R. (2009). The biology of chromatin remodeling complexes. Annu. Rev. Biochem. *78*, 273–304.

Clever, B., Interthal, H., Schmuckli-Maurer, J., King, J., Sigrist, M., and Heyer, W.D. (1997). Recombinational repair in yeast: Functional interactions between Rad51 and Rad54 proteins. EMBO J. *16*, 2535–2544.

Clynes, D., and Gibbons, R.J. (2013). ATRX and the replication of structured DNA. Curr. Opin. Genet. Dev. *23*, 289–294.

Clynes, D., Jelinska, C., Xella, B., Ayyub, H., Taylor, S., Mitson, M., Bachrati, C.Z., Higgs, D.R., and Gibbons, R.J. (2014). ATRX dysfunction induces replication defects in primary mouse cells. PLoS One *9*.

Clynes, D., Jelinska, C., Xella, B., Ayyub, H., Scott, C., Mitson, M., Taylor, S., Higgs, D.R., and Gibbons, R.J. (2015). Suppression of the alternative lengthening of telomere pathway by the chromatin remodelling factor ATRX. Nat. Commun. *6*, 7538.

Conte, D., Huh, M., Goodall, E., Delorme, M., Parks, R.J., and Picketts, D.J. (2012). Loss of Atrx Sensitizes Cells to DNA Damaging Agents through p53-Mediated Death Pathways. PLoS One *7*, 1–9.

Dellaire, G., and Bazett-Jones, D.P. (2004). PML nuclear bodies: dynamic sensors of DNA damage and cellular stress. BioEssays *26*, 963–977.

Deng, Y., Guo, X., Ferguson, D.O., and Chang, S. (2009). Multiple roles for MRE11 at uncapped telomeres. Nature *460*, 914–918.

Dillon, N. (2004). Heterochromatin structure and function. Biol. Cell *96*, 631–637.

Dong, S., Han, J., Chen, H., Liu, T., Huen, M.S.Y., Yang, Y., Guo, C., and Huang, J. (2014). The Human SRCAP Chromatin Remodeling Complex Promotes DNA-End Resection. Curr. Biol. *24*, 2097–2110.

Dürr, H., Flaus, A., Owen-Hughes, T., and Hopfner, K.P. (2006). Snf2 family ATPases and DExx box helicases: Differences and unifying concepts from high-resolution crystal structures. Nucleic Acids Res. *34*, 4160–4167.

Ehrenhofer-Murray, A.E. (2004). Chromatin dynamics at DNA replication, transcription and repair. Eur. J. Biochem. *271*, 2335–2349.

Ensminger, M., Iloff, L., Ebel, C., Nikolova, T., Kaina, B., and Löbrich, M. (2014). DNA breaks and chromosomal aberrations arise when replication meets base excision repair. J. Cell Biol. *206*, 29–43.

Esashi, F., Christ, N., Gannon, J., Liu, Y., Hunt, T., Jasin, M., and West, S.C. (2005). CDK-dependent phosphorylation of BRCA2 as a regulatory mechanism for recombinational repair. Nature *434*, 598–604.

Essers, J., van Steeg, H., de Wit, J., Swagemakers, S.M.A., Vermeij, M., Hoeijmakers, J.H.J., and Kanaar, R. (2000). Homologous and non-homologous recombination differentially affect DNA damage repair in mice. EMBO J. *19*, 1703–1710.

Essers, J., Houtsmuller, A.B., van Veelen, L., Paulusma, C., Nigg, A.L., Pastink, A., Vermeulen, W., Hoeijmakers, J.H.J., and Kanaar, R. (2002). Nuclear dynamics of RAD52 group homologous recombination proteins in response to DNA damage. EMBO J. *21*, 2030–2037.

Esta, A., Ma, E., Dupaigne, P., Maloisel, L., Guerois, R., Le Cam, E., Veaute, X., and Co□c, E. (2013). Rad52 Sumoylation Prevents the Toxicity of Unproductive Rad51 Filaments Independently of the Anti-Recombinase Srs2. PLoS Genet *9*, e1003833.

Eustermann, S., Yang, J.-C., Law, M.J., Amos, R., Chapman, L.M., Jelinska, C., Garrick, D., Clynes, D., Gibbons, R.J., Rhodes, D., et al. (2011). Combinatorial readout of histone H3 modifications specifies localization of ATRX to heterochromatin. Nat. Struct. Mol. Biol. *18*, 777–782.

Feige, E., Shalom, O., Tsuriel, S., Yissachar, N., and Motro, B. (2006). Nek1 shares structural and functional similarities with NIMA kinase. Biochim. Biophys. Acta - Mol. Cell Res. *1763*, 272–281.

Flaus, A., Martin, D.M.A., Barton, G.J., and Owen-Hughes, T. (2006). Identification of multiple distinct Snf2 subfamilies with conserved structural motifs. Nucleic Acids Res. *34*, 2887–2905.

Flott, S., Kwon, Y., Pigli, Y.Z., Rice, P.A., Sung, P., and Jackson, S.P. (2011). Regulation of Rad51 function by phosphorylation. EMBO Rep. *12*, 833–839.

Flynn, R.L., Cox, K.E., Jeitany, M., Wakimoto, H., Bryll, A.R., Ganem, N.J., Bersani, F., Pineda, J.R., Suvà, M.L., Benes, C.H., et al. (2015). Alternative lengthening of telomeres renders cancer cells hypersensitive to ATR inhibitors. Science (80-.). *347*, 273–277.

van Gent, D.C., Hoeijmakers, J.H.J., and Kanaar, R. (2001). Chromosomal stability and the DNA double-stranded break connection. Nat Rev Genet *2*, 196–206.

Geuting, V., Reul, C., and Löbrich, M. (2013). ATM Release at Resected Double-Strand Breaks Provides Heterochromatin Reconstitution to Facilitate Homologous Recombination. PLoS Genet. *9*, e1003667.

Gibbons, R.J., Brueton, L., Buckle, V.J., Burn, J., Clayton-Smith, J., Davison, B.C.C., Gardner, R.J.M., Homfray, T., Kearney, L., Kingston, H.M., et al. (1995). Clinical and hematologic aspects of the X-linked α-thalassemia/mental retardation syndrome (ATR-X). Am. J. Med. Genet. *55*, 288–299.

Gibbons, R.J., McDowell, T.L., Raman, S., O'Rourke, D.M., Garrick, D., Ayyub, H., and Higgs, D.R. (2000). Mutations in ATRX, encoding a SWI/SNF-like protein, cause diverse changes in the pattern of DNA methylation. Nat. Genet. *24*, 368–371.

Gibbons, R.J., Pellagatti, A., Garrick, D., Wood, W.G., Malik, N., Ayyub, H., Langford, C., Boultwood, J., Wainscoat, J.S., and Higgs, D.R. (2003). Identification of acquired somatic mutations in the gene encoding chromatin-remodeling factor ATRX in the [alpha]-thalassemia myelodysplasia syndrome (ATMDS). Nat Genet *34*, 446–449.

Goldberg, A.D., Banaszynski, L.A., Noh, K.-M., Lewis, P.W., Elsaesser, S.J., Stadler, S., Dewell, S., Law, M., Guo, X., Li, X., et al. (2010). Distinct factors control histone variant H3.3 localization at specific genomic regions. Cell *140*, 678–691.

González-Prieto, R., Muñoz-Cabello, A.M., Cabello-Lobato, M.J., and Prado, F. (2013). Rad51 replication fork recruitment is required for DNA damage tolerance. EMBO J. *32*, 1307–1321.

Goodarzi, A.A., Noon, A.T., Deckbar, D., Ziv, Y., Shiloh, Y., Löbrich, M., and Jeggo, P.A. (2008). ATM Signaling Facilitates Repair of DNA Double-Strand Breaks Associated with Heterochromatin. Mol. Cell *31*, 167–177.

Grewal, S.I.S., and Jia, S. (2007). Heterochromatin revisited. Nat Rev Genet *8*, 35–46.

Grewal, S.I.S., and Moazed, D. (2003). Heterochromatin and Epigenetic Control of Gene Expression. Science (80-.). *301*, 798–802.

Helleday, T. (2010). Homologous recombination in cancer development, treatment and development of drug resistance. Carcinog. *31* , 955–960.

Henry-Mowatt, J., Jackson, D., Masson, J.-Y., Johnson, P.A., Clements, P.M., Benson, F.E., Thompson, L.H., Takeda, S., West, S.C., and Caldecott, K.W. (2003). XRCC3 and Rad51 Modulate Replication Fork Progression on Damaged Vertebrate Chromosomes. Mol. Cell *11*, 1109–1117.

Henson, J.D., Neumann, A.A., Yeager, T.R., and Reddel, R.R. (2002). Alternative lengthening of telomeres in mammalian cells. Oncogene *21*, 598–610.

Heyer, W.-D., Li, X., Rolfsmeier, M., and Zhang, X.-P. (2006). Rad54: the Swiss Army knife of homologous recombination? Nucleic Acids Res. *34* , 4115–4125.

Heyer, W.-D., Ehmsen, K.T., and Liu, J. (2010). Regulation of homologous recombination in eukaryotes. Annu. Rev. Genet. *44*, 113–139.

Hildebrandt, F., and Otto, E. (2005). Cilia and centrosomes: a unifying pathogenic concept for cystic kidney disease? Nat Rev Genet *6*, 928–940.

Hilton, L.K., White, M.C., and Quarmby, L.M. (2009). The NIMA-related kinase NEK1 cycles through the nucleus. Biochem. Biophys. Res. Commun. *389*, 52–56.

Hoffmann, R.F., Moshkin, Y.M., Mouton, S., Grzeschik, N.A., Kalicharan, R.D., Kuipers, J., Wolters, A.H.G., Nishida, K., Romashchenko, A. V, Postberg, J., et al. (2016). Guanine quadruplex structures localize to heterochromatin. Nucleic Acids Res. *44*, 152–163.

Huertas, P., and Jackson, S.P. (2009). Human CtIP Mediates Cell Cycle Control of DNA End Resection and Double Strand Break Repair. J. Biol. Chem. *284* , 9558–9565.

Huh, M.S., O'Dea, T.P., Ouazia, D., McKay, B.C., Parise, G., Parks, R.J., Rudnicki, M.A., and Picketts, D.J. (2012). Compromised genomic integrity impedes muscle growth after Atrx inactivation. J. Clin. Invest. *122*, 4412–4423.

Huh, M.S., Ivanochko, D., Hashem, L.E., Curtin, M., Delorme, M., Goodall, E., Yan, K., and Picketts, D.J. (2016). Stalled replication forks within heterochromatin require ATRX for protection. Cell Death Dis. *7*, e2220.

Ishov, A.M., Vladimirova, O. V, and Maul, G.G. (2004). Heterochromatin and ND10 are cell-cycle regulated and phosphorylation-dependent alternate nuclear sites of the transcription repressor Daxx and SWI/SNF protein ATRX. J. Cell Sci. *117*, 3807–3820.

Iwase, S., Xiang, B., Ghosh, S., Ren, T., Lewis, P.W., Cochrane, J.C., Allis, C.D., Picketts, D.J., Patel, D.J., Li, H., et al. (2011). ATRX ADD domain links an atypical histone methylation recognition mechanism to human mental-retardation syndrome. Nat. Struct. Mol. Biol. *18*, 769–776.

Jackson, S.P., and Bartek, J. (2009). The DNA-damage response in human biology and disease. Nature *461*, 1071–1078.

Jaskelioff, M., Van Komen, S., Krebs, J.E., Sung, P., and Peterson, C.L. (2003). Rad54p Is a Chromatin Remodeling Enzyme Required for Heteroduplex DNA Joint Formation with Chromatin. J. Biol. Chem. *278* , 9212–9218.

Jeggo, P.A., and Lobrich, M. DNA double-strand breaks: their cellular and clinical impact? Oncogene *26*, 7717–7719.

Jhaveri, K., Taldone, T., Modi, S., and Chiosis, G. (2012). Advances in the clinical development of heat shock protein 90 (Hsp90) inhibitors in cancers. Biochim. Biophys. Acta *1823*, 742–755.

Karras, G.I., and Jentsch, S. (2010). The RAD6 DNA Damage Tolerance Pathway Operates Uncoupled from the Replication Fork and Is Functional Beyond S Phase. Cell *141*, 255–267.

Kelley, M.R., Logsdon, D., and Fishel, M.L. (2014). Targeting DNA repair pathways for cancer treatment: what's new? Future Oncol. *10*, 1215–1237.

Kingston, R.E., Bunker, C.A., and Imbalzano, A.N. (1996). Repression and activation by multiprotein complexes that alter chromatin structure. Genes Dev. *10* , 905–920.

Kirshner, M., Rathavs, M., Nizan, A., Essers, J., Kanaar, R., Shiloh, Y., and Barzilai, A. (2009). Analysis of the relationships between ATM and the Rad54 paralogs involved in homologous recombination repair. DNA Repair (Amst). *8*, 253–261.

Krejci, L., Altmannova, V., Spirek, M., and Zhao, X. (2012). Homologous recombination and its regulation. Nucleic Acids Res. *40*, 5795–5818.

Kwon, Y., Chi, P., Roh, D.H., Klein, H., and Sung, P. (2007). Synergistic action of the Saccharomyces cerevisiae homologous recombination factors Rad54 and Rad51 in chromatin remodeling. DNA Repair (Amst). *6*, 1496–1506.

De La Fuente, R., Baumann, C., and Viveiros, M.M. (2015). ATRX contributes to epigenetic asymmetry and silencing of major satellite transcripts in the maternal genome of the mouse embryo. Development *142*, 1806–1817.

de la Torre-Ruiz, M.-A., and Lowndes, N.F. (2000). The Saccharomyces cerevisiae DNA damage checkpoint is required for efficient repair of double strand breaks by non-homologous end joining. FEBS Lett. *467*, 311–315.

Lamarche, B.J., Orazio, N.I., and Weitzman, M.D. (2010). The MRN complex in Double-Strand Break Repair and Telomere Maintenance. FEBS Lett. *584*, 3682–3695.

Lans, H., Marteijn, J.A., and Vermeulen, W. (2012a). ATP-dependent chromatin remodeling in the DNA-damage response. Epigenetics Chromatin *5*, 1–14.

Lans, H., Marteijn, J.A., and Vermeulen, W. (2012b). ATP-dependent chromatin remodeling in the DNA-damage response. Epigenetics Chromatin *5*, 4.

Law, M.J., Lower, K.M., Voon, H.P.J., Hughes, J.R., Garrick, D., Viprakasit, V., Mitson, M., De Gobbi, M., Marra, M., Morris, A., et al. (2010). ATR-X Syndrome Protein Targets Tandem Repeats and Influences Allele-Specific Expression in a Size-Dependent Manner. Cell *143*, 367–378.

Lawrence, J.G., and Retchless, A.C. (2009). The Interplay of Homologous Recombination and Horizontal Gene Transfer in Bacterial Speciation BT - Horizontal Gene Transfer: Genomes in Flux. M.B. Gogarten, J.P. Gogarten, and L.C. Olendzenski, eds. (Totowa, NJ: Humana Press), pp. 29–53.

Lee, H.-S., Park, J.-H., Kim, S.-J., Kwon, S.-J., and Kwon, J. (2010). A cooperative activation loop among SWI/SNF, gamma-H2AX and H3 acetylation for DNA double-strand break repair. EMBO J. *29*, 1434–1445.

Leung, J.W.C., Ghosal, G., Wang, W., Shen, X., Wang, J., Li, L., and Chen, J. (2013). Alpha thalassemia/mental retardation syndrome X-linked gene product ATRX is required for proper replication restart and cellular resistance to replication stress. J. Biol. Chem. *288*, 6342–6350.

Li, X., and Heyer, W.-D. (2008). Homologous recombination in DNA repair and DNA damage tolerance. Cell Res. *18*, 99–113.

Li, X., Zhang, X.-P., Solinger, J.A., Kiianitsa, K., Yu, X., Egelman, E.H., and Heyer, W.-D. (2007). Rad51 and Rad54 ATPase activities are both required to modulate Rad51-dsDNA filament dynamics. Nucleic Acids Res. *35* , 4124–4140.

Li, X., Stith, C.M., Burgers, P.M., and Heyer, W.-D. (2009). PCNA Is Required for Initiation of Recombination-Associated DNA Synthesis by DNA Polymerase δ. Mol. Cell *36*, 704–713.

Liu, Y., and West, S.C. (2004). Happy Hollidays: 40th anniversary of the Holliday junction. Nat Rev Mol Cell Biol *5*, 937–944.

Liu, S., Ho, C.K., Ouyang, J., and Zou, L. (2013). Nek1 kinase associates with ATR-ATRIP and primes ATR for efficient DNA damage signaling. Proc. Natl. Acad. Sci. U. S. A. *110*, 2175–2180.

Lorch, Y., Zhang, M., and Kornberg, R.D. (1999). Histone Octamer Transfer by a Chromatin-Remodeling Complex. Cell *96*, 389–392.

Lord, C.J., and Ashworth, A. (2012). The DNA damage response and cancer therapy. Nature *481*, 287–294.

Lovejoy, C.A., Li, W., Reisenweber, S., Thongthip, S., Bruno, J., de Lange, T., De, S., Petrini, J.H.J., Sung, P.A., Jasin, M., et al. (2012). Loss of ATRX, genome instability, and an altered DNA damage response are hallmarks of the alternative lengthening of Telomeres pathway. PLoS Genet. *8*, 12–15.

Luciani, J.J., Depetris, D., Usson, Y., Metzler-Guillemain, C., Mignon-Ravix, C., Mitchell, M.J., Megarbane, A., Sarda, P., Sirma, H., Moncla, A., et al. (2006). PML nuclear bodies are highly organised DNA-protein structures with a function in heterochromatin remodelling at the G2 phase. J. Cell Sci. *119*, 2518–2531.

Luijsterburg, M.S., de Krijger, I., Wiegant, W.W., Shah, R.G., Smeenk, G., de Groot, A.J., Pines, A., Vertegaal, A.C., Jacobs, J.J., Shah, G.M., et al. (2016). PARP1 Links CHD2-Mediated Chromatin Expansion and H3.3 Deposition to DNA Repair by Non-homologous End-Joining. Mol. Cell *61*, 547–562.

Lydeard, J.R., Lipkin-Moore, Z., Sheu, Y.-J., Stillman, B., Burgers, P.M., and Haber, J.E. (2010). Break-induced replication requires all essential DNA replication factors except those specific for pre-RC assembly. Genes Dev. *24* , 1133–1144.

Machida, S., Takaku, M., Ikura, M., Sun, J., Suzuki, H., Kobayashi, W., Kinomura, A., Osakabe, A., Tachiwana, H., Horikoshi, Y., et al. (2014). Nap1 stimulates homologous recombination by RAD51 and RAD54 in higher-ordered chromatin containing histone H1. Sci. Rep. *4*, 4863.

Martens, J.A., and Winston, F. (2003). Recent advances in understanding chromatin remodeling by Swi/Snf complexes. Curr. Opin. Genet. Dev. *13*, 136–142.

Mason, J.M., Dusad, K., Wright, W.D., Grubb, J., Budke, B., Heyer, W.-D., Connell, P.P., Weichselbaum, R.R., and Bishop, D.K. (2015). RAD54 family translocases counter genotoxic effects of RAD51 in human tumor cells. Nucleic Acids Res. .

Matos, J., and West, S.C. (2014). Holliday junction resolution: Regulation in space and time. DNA Repair (Amst). *19*, 176–181.

Matsuda, M., Miyagawa, K., Takahashi, M., Fukuda, T., Kataoka, T., Asahara, T., Inui, H., Watatani, M., Yasutomi, M., Kamada, N., et al. (1999). Mutations in the RAD54 recombination gene in primary cancers. Oncogene *18*, 3427–3430.

Matulova, P., Marini, V., Burgess, R.C., Sisakova, A., Kwon, Y., Rothstein, R., Sung, P., and Krejci, L. (2009). Cooperativity of Mus81·Mms4 with Rad54 in the Resolution of Recombination and Replication Intermediates. J. Biol. Chem. *284*, 7733–7745.

Mazin, A. V, Alexeev, A.A., and Kowalczykowski, S.C. (2003). A Novel Function of Rad54 Protein: STABILIZATION OF THE Rad51 NUCLEOPROTEIN FILAMENT . J. Biol. Chem. *278* , 14029–14036.

Mazin, A. V, Mazina, O.M., Bugreev, D. V, and Rossi, M.J. (2010). Rad54, the motor of homologous recombination. DNA Repair (Amst). *9*, 286–302.

Mazina, O.M., and Mazin, A. V (2008). Human Rad54 protein stimulates human Mus81–Eme1 endonuclease. Proc. Natl. Acad. Sci. *105* , 18249–18254.

Minocherhomji, S., Ying, S., Bjerregaard, V.A., Bursomanno, S., Aleliunaite, A., Wu, W., Mankouri, H.W., Shen, H., Liu, Y., and Hickson, I.D. (2015). Replication stress activates DNA repair synthesis in mitosis. Nature *528*, 286–290.

Mirkin, E. V, and Mirkin, S.M. (2007). Replication Fork Stalling at Natural Impediments. Microbiol. Mol. Biol. Rev. *71*, 13–35.

Mito, Y., Henikoff, J.G., and Henikoff, S. (2007). Histone Replacement Marks the Boundaries of cis-Regulatory Domains. Science (80-.). *315*, 1408–1411.

Mizuguchi, G., Shen, X., Landry, J., Wu, W.-H., Sen, S., and Wu, C. (2004). ATP-Driven Exchange of Histone H2AZ Variant Catalyzed by SWR1 Chromatin Remodeling Complex. Science (80-.). *303*, 343–348.

Moniz, L., Dutt, P., Haider, N., and Stambolic, V. (2011). Nek family of kinases in cell cycle, checkpoint control and cancer. Cell Div. *6*, 18.

Moura, D.J., Castilhos, B., Immich, B.F., Cañedo, A.D., Henriques, J. a P., Lenz, G., and Saffi, J. (2010). Kin3 protein, a NIMA-related kinase of Saccharomyces cerevisiae, is involved in DNA adduct damage response. Cell Cycle *9*, 2220–2229.

Moynahan, M.E., and Jasin, M. (2010). Mitotic homologous recombination maintains genomic stability and suppresses tumorigenesis. Nat Rev Mol Cell Biol *11*, 196–207.

Nakamura, K., Kato, A., Kobayashi, J., Yanagihara, H., Sakamoto, S., Oliveira, D. V, Shimada, M., Tauchi, H., Suzuki, H., and Tashiro, S. (2011). Regulation of homologous recombination by RNF20-dependent H2B ubiquitination. Mol Cell *41*.

North, J.A., Amunugama, R., Klajner, M., Bruns, A.N., Poirier, M.G., and Fishel, R. (2013). ATP-dependent nucleosome unwrapping catalyzed by human RAD51. Nucleic Acids Res. *41*, 7302–7312.

Nussenzweig, A., and Nussenzweig, M.C. (2010). Origin of chromosomal translocations in lymphoid cancer. Cell *141*, 27–38.

O'Connor, M.J. (2016). Targeting the DNA Damage Response in Cancer. Mol. Cell *60*, 547–560.

Pâques, F., and Haber, J.E. (1999). Multiple Pathways of Recombination Induced by Double-Strand Breaks in Saccharomyces cerevisiae. Microbiol. Mol. Biol. Rev. *63*, 349–404.

Pelegrini, A.L., Moura, D.J., Brenner, B.L., Ledur, P.F., Maques, G.P., Henriques, J.A.P., Saffi, J., and Lenz, G. (2010). Nek1 silencing slows down DNA repair and blocks DNA damage-induced cell cycle arrest. Mutagen. *25* , 447–454.

Polci, R., Peng, A., Chen, P., Riley, D.J., and Chen, Y. (2004). NIMA-Related Protein Kinase 1 Is Involved Early in the Ionizing Radiation-Induced DNA Damage Response. 8800–8803.

Polo, S.E., and Jackson, S.P. (2011). Dynamics of DNA damage response proteins at DNA breaks: a focus on protein modifications. Genes Dev. *25* , 409–433.

Ratnakumar, K., and Bernstein, E. (2013). ATRX: The case of a peculiar chromatin remodeler. Epigenetics *8*, 3–9.

Renkawitz, J., Lademann, C.A., and Jentsch, S. (2014). Mechanisms and principles of homology search during recombination. Nat Rev Mol Cell Biol *15*, 369–383.

Riballo, E., Kühne, M., Rief, N., Doherty, A., Smith, G.C.M., Recio, M.-J., Reis, C., Dahm, K., Fricke, A., Krempler, A., et al. (2004). A Pathway of Double-Strand Break Rejoining Dependent upon ATM, Artemis, and Proteins Locating to γ-H2AX Foci. Mol. Cell *16*, 715–724.

Richardson, C., Stark, J.M., Ommundsen, M., and Jasin, M. Rad51 overexpression promotes alternative double-strand break repair pathways and genome instability. Oncogene *23*, 546–553.

Ritchie, K., Seah, C., Moulin, J., Isaac, C., Dick, F., and B??rub??, N.G. (2008). Loss of ATRX leads to chromosome cohesion and congression defects. J. Cell Biol. *180*, 315–324.

Saito, Y., Zhou, H., and Kobayashi, J. (2015). Chromatin modification and NBS1: their relationship in DNA double-strand break repair. Genes Genet. Syst. *90*, 195–208.

San Filippo, J., Sung, P., and Klein, H. (2008). Mechanism of eukaryotic homologous recombination. Annu. Rev. Biochem. *77*, 229–257.

Sancar, A., Lindsey-Boltz, L. a, Unsal-Kaçmaz, K., and Linn, S. (2004). Molecular mechanisms of mammalian DNA repair and the DNA damage checkpoints. Annu. Rev. Biochem. *73*, 39–85.

Sartori, A.A., Lukas, C., Coates, J., Mistrik, M., Fu, S., Bartek, J., Baer, R., Lukas, J., and Jackson, S.P. (2007). Human CtIP promotes DNA end resection. Nature *450*, 509–514.

Schlacher, K., Christ, N., Siaud, N., Egashira, A., Wu, H., and Jasin, M. (2011). Double-Strand Break Repair-Independent Role for BRCA2 in Blocking Stalled Replication Fork Degradation by MRE11. Cell *145*, 529–542.

Sebesta, M., Burkovics, P., Juhasz, S., Zhang, S., Szabo, J.E., Lee, M.Y.W.T., Haracska, L., and Krejci, L. (2013). Role of PCNA and TLS polymerases in D-loop extension during homologous recombination in humans. DNA Repair (Amst). *12*, 691–698.

Shahar, O.D., Ram, E.V.S.R., Shimshoni, E., Hareli, S., Meshorer, E., and Goldberg, M. (2012). Live imaging of induced and controlled DNA double-strand break formation reveals extremely low repair by homologous recombination in human cells. Oncogene *31*, 3495–3504.

Shay, J.W., and Bacchetti, S. (1997). A survey of telomerase activity in human cancer. Eur. J. Cancer *33*, 787–791.

Shinohara, M., Shita-Yamaguchi, E., Buerstedde, J.M., Shinagawa, H., Ogawa, H., and Shinohara, A. (1997). Characterization of the Roles of the Saccharomyces Cerevisiae Rad54 Gene and a Homologue of Rad54, Rdh54/Tid1, in Mitosis and Meiosis. Genetics *147*, 1545–1556.

Sigurdsson, S., Van Komen, S., Petukhova, G., and Sung, P. (2002). Homologous DNA Pairing by Human Recombination Factors Rad51 and Rad54. J. Biol. Chem. *277* , 42790–42794.

Smeenk, G., Wiegant, W.W., Marteijn, J.A., Luijsterburg, M.S., Sroczynski, N., Costelloe, T., Romeijn, R.J., Pastink, A., Mailand, N., Vermeulen, W., et al. (2013). Poly(ADP-ribosyl)ation links the chromatin remodeler SMARCA5/SNF2H to RNF168-dependent DNA damage signaling. J. Cell Sci. *126*, 889–903.

Sneeden, J.L., Grossi, S.M., Tappin, I., Hurwitz, J., and Heyer, W.-D. (2013). Reconstitution of recombination-associated DNA synthesis with human proteins. Nucleic Acids Res. *41*, 4913–4925.

Solinger, J. a, Kiianitsa, K., and Heyer, W.-D. (2002). Rad54, a Swi2/Snf2-like recombinational repair protein, disassembles Rad51:dsDNA filaments. Mol. Cell *10*, 1175–1188.

Sørensen, C.S., Hansen, L.T., Dziegielewski, J., Syljuåsen, R.G., Lundin, C., Bartek, J., and Helleday, T. (2005). The cell-cycle checkpoint kinase Chk1 is required for mammalian homologous recombination repair. Nat. Cell Biol. *7*, 195–201.

Sung, P., and Klein, H. (2006). Mechanism of homologous recombination: mediators and helicases take on regulatory functions. Nat Rev Mol Cell Biol *7*, 739–750.

Surpili, M.J., Delben, T.M., and Kobarg, J. (2003). Identification of Proteins That Interact with the Central Coiled-Coil Region of the Human Protein Kinase NEK1†. Biochemistry *42*, 15369–15376.

Symington, L.S. (2002). Role of RAD52 Epistasis Group Genes in Homologous Recombination and Double-Strand Break Repair. Microbiol. Mol. Biol. Rev. *66*, 630–670.

Symington, L.S., and Gautier, J. (2011). Double-strand break end resection and repair pathway choice. Annu. Rev. Genet. *45*, 247–271.

Tan, T.L.R., Essers, J., Citterio, E., Swagemakers, S.M.A., de Wit, J., Benson, F.E., Hoeijmakers, J.H.J., and Kanaar, R. (1999). Mouse Rad54 affects DNA conformation and DNA-damage-induced Rad51 foci formation. Curr. Biol. *9*, 325–328.

Tang, J., Wu, S., Liu, H., Stratt, R., Barak, O.G., Shiekhattar, R., Picketts, D.J., and Yang, X. (2004). A Novel Transcription Regulatory Complex Containing Death Domain-associated Protein and the ATR-X Syndrome Protein. J. Biol. Chem. *279*, 20369–20377.

Terasawa, M., Ogawa, H., Tsukamoto, Y., Shinohara, M., Shirahige, K., Kleckner, N., and Ogawa, T. (2007). Meiotic recombination-related DNA synthesis and its implications for cross-over and non-cross-over recombinant formation. Proc. Natl. Acad. Sci. *104* , 5965–5970.

Thangavel, S., Berti, M., Levikova, M., Pinto, C., Gomathinayagam, S., Vujanovic, M., Zellweger, R., Moore, H., Lee, E.H., Hendrickson, E.A., et al. (2015). DNA2 drives processing and restart of reversed replication forks in human cells. J. Cell Biol. *208* , 545–562.

Thiel, C., Kessler, K., Giessl, A., Dimmler, A., Shalev, S. a., Von Der Haar, S., Zenker, M., Zahnleiter, D., St??ss, H., Beinder, E., et al. (2011). NEK1 mutations cause short-rib polydactyly syndrome type majewski. Am. J. Hum. Genet. *88*, 106–114.

Thomä, N.H., Czyzewski, B.K., Alexeev, A. a, Mazin, A. V, Kowalczykowski, S.C., and Pavletich, N.P. (2005). Structure of the SWI2/SNF2 chromatin-remodeling domain of eukaryotic Rad54. Nat. Struct. Mol. Biol. *12*, 350–356.

Ting, N.S.Y., and Lee, W.-H. (2004). The DNA double-strand break response pathway: becoming more BRCAish than ever. DNA Repair (Amst). *3*, 935–944.

Toiber, D., Erdel, F., Bouazoune, K., Silberman, D.M., Zhong, L., Mulligan, P., Sebastian, C., Cosentino, C., Martinez-Pastor, B., Giacosa, S., et al. (2013). SIRT6 recruits SNF2H to sites of DNA breaks, preventing genomic instability through chromatin remodeling. Mol. Cell *51*, 454–468.

Tsuzuki, T., Fujii, Y., Sakumi, K., Tominaga, Y., Nakao, K., Sekiguchi, M., Matsushiro, A., Yoshimura, Y., and MoritaT (1996). Targeted disruption of the Rad51 gene leads to lethality in embryonic mice. Proc. Natl. Acad. Sci. U. S. A. *93*, 6236–6240.

Upadhya, P., Birkenmeier, E.H., Birkenmeier, C.S., and Barker, J.E. (2000). Mutations in a NIMA-related kinase gene, Nek1, cause pleiotropic effects including a progressive polycystic kidney disease in mice. Proc. Natl. Acad. Sci. U. S. A. *97*, 217–221.

Veaute, X., Jeusset, J., Soustelle, C., Kowalczykowski, S.C., Le Cam, E., and Fabre, F. (2003). The Srs2 helicase prevents recombination by disrupting Rad51 nucleoprotein filaments. Nature *423*, 309–312.

Vidi, P.-A., Liu, J., Salles, D., Jayaraman, S., Dorfman, G., Gray, M., Abad, P., Moghe, P. V, Irudayaraj, J.M., Wiesmüller, L., et al. (2014). NuMA promotes homologous recombination repair by regulating the accumulation of the ISWI ATPase SNF2h at DNA breaks. Nucleic Acids Res. *42*, 6365–6379.

Villard, L., Lossi, A.-M., Cardoso, C., Proud, V., Chiaroni, P., Colleaux, L., Schwartz, C., and Fontés, M. (1997). Determination of the Genomic Structure of the XNP/ATRX Gene Encoding a Potential Zinc Finger Helicase. Genomics *43*, 149–155.

Voon, H.P.J., and Wong, L.H. (2016). New players in heterochromatin silencing: histone variant H3.3 and the ATRX/DAXX chaperone. Nucleic Acids Res. *44*, 1496–1501.

Wang, X., Ira, G., Tercero, J.A., Holmes, A.M., Diffley, J.F.X., and Haber, J.E. (2004). Role of DNA Replication Proteins in Double-Strand Break-Induced Recombination in Saccharomyces cerevisiae. Mol. Cell. Biol. *24*, 6891–6899.

Watson, L.A., Solomon, L.A., Li, J.R., Jiang, Y., Edwards, M., Shin-ya, K., Beier, F., and Bérubé, N.G. (2013). Atrx deficiency induces telomere dysfunction, endocrine defects, and reduced life span . J. Clin. Invest. *123*, 2049–2063.

Wesoly, J., Agarwal, S., Sigurdsson, S., Komen, S. Van, Qin, J., Steeg, H. Van, Benthem, J. Van, Wassenaar, E., Baarends, W.M., Ghazvini, M., et al. (2006). Differential Contributions of Mammalian Rad54 Paralogs to Recombination , DNA Damage Repair , and Meiosis Differential Contributions of Mammalian Rad54 Paralogs to Recombination , DNA Damage Repair , and Meiosis †.

White, M.C., and Quarmby, L.M. (2008). The NIMA-family kinase, Nek1 affects the stability of centrosomes and ciliogenesis. BMC Cell Biol. *9*, 29.

White, D., Rafalska-Metcalf, I.U., Ivanov, a. V., Corsinotti, a., Peng, H., Lee, S.-C., Trono, D., Janicki, S.M., and Rauscher, F.J. (2012). The ATM Substrate KAP1 Controls DNA Repair in Heterochromatin: Regulation by HP1 Proteins and Serine 473/824 Phosphorylation. Mol. Cancer Res. *10*, 401–414.

Whitehouse, I., Flaus, A., Cairns, B.R., White, M.F., Workman, J.L., and Owen-Hughes, T. (1999). Nucleosome mobilization catalysed by the yeast SWI/SNF complex. Nature *400*, 784–787.

Willers, H., Xia, F., and Powell, S.N. (2002). Recombinational DNA Repair in Cancer and Normal Cells: The Challenge of Functional Analysis. J. Biomed. Biotechnol. *2*, 86–93.

Wolner, B., and Peterson, C.L. (2005). ATP-dependent and ATP-independent Roles for the Rad54 Chromatin Remodeling Enzyme during Recombinational Repair of a DNA Double Strand Break. J. Biol. Chem. *280* , 10855–10860.

Wu, L., and Hickson, I.D. (2003). The Bloom's syndrome helicase suppresses crossing over during homologous recombination. Nature *426*, 870–874.

Xue, Y., Gibbons, R., Yan, Z., Yang, D., McDowell, T.L., Sechi, S., Qin, J., Zhou, S., Higgs, D., and Wang, W. (2003). The ATRX syndrome protein forms a chromatin-remodeling complex with Daxx and localizes in promyelocytic leukemia nuclear bodies. Proc. Natl. Acad. Sci. U. S. A. *100*, 10635–10640.

Yang, H., Jeffrey, P.D., Miller, J., Kinnucan, E., Sun, Y., Thomä, N.H., Zheng, N., Chen, P.-L., Lee, W.-H., and Pavletich, N.P. (2002). BRCA2 Function in DNA Binding and Recombination from a BRCA2-DSS1-ssDNA Structure. Sci. *297* , 1837–1848.

Yata, K., Lloyd, J., Maslen, S., Bleuyard, J.-Y., Skehel, M., Smerdon, S.J., and Esashi, F. (2012). Plk1 and CK2 Act in Concert to Regulate Rad51 during DNA Double Strand Break Repair. Mol. Cell *45*, 371–383.

Yeung, P.L., Denissova, N.G., Nasello, C., Hakhverdyan, Z., Chen, J.D., and Brenneman, M.A. (2012). Promyelocytic leukemia nuclear bodies support a late step in DNA double-strand break repair by homologous recombination. J. Cell. Biochem. *113*, 1787–1799.

Ying, S., Minocherhomji, S., Chan, K.L., Palmai-Pallag, T., Chu, W.K., Wass, T., Mankouri, H.W., Liu, Y., and Hickson, I.D. (2013). MUS81 promotes common fragile site expression. Nat Cell Biol *15*, 1001–1007.

Yoder, B.K. (2007). Role of Primary Cilia in the Pathogenesis of Polycystic Kidney Disease. J. Am. Soc. Nephrol. *18* , 1381–1388.

Yun, M.H., and Hiom, K. (2009). CtIP-BRCA1 modulates the choice of DNA double-strand break repair pathway throughout the cell cycle. Nature *459*, 460–463.

Zellweger, R., Dalcher, D., Mutreja, K., Berti, M., Schmid, J.A., Herrador, R., Vindigni, A., and Lopes, M. (2015). Rad51-mediated replication fork reversal is a global response to genotoxic treatments in human cells. J. Cell Biol. *208*, 563–579.

Zou, L., and Elledge, S.J. (2003). Sensing DNA Damage Through ATRIP Recognition of RPA-ssDNA Complexes. Science (80-.). *300*, 1542–1548.

8 Appendix

8.1 Curriculum vitae

Name **Anja Waizenegger**
Date of birth: August 10th 1986
Place of birth: Tuttlingen
Nationality: German

Education

PhD Thesis:

09/2012 – 06/2016 University of Technology Darmstadt
Radiation Biology and DNA Repair, Prof. Dr. Markus Löbrich
Titel: "Factors involved in late stages of homologous recombination"

Studies:

10/2009 – 03/2012 University of Constance
Master of Sciences (Biology)
Molecular Toxicology, Prof. Dr. Alexander Bürkle
Grade 2.4

10/2005 – 05/2008 University of Constance
Bachelor of Sciences (Biology)
Cell Biology, Prof. Dr. Helmut Plattner
Grade 1.5

High School:

09/1996 – 06/2005 Immanuel-Kant Gymnasium, Tuttlingen, Germany
Abitur, Grade: 2,2

Experience abroad

08/2010 – 11/2010 **Research Assistant**
Institute for Ageing and Health, Dr. Gabriele Saretzki, Newcastle, UK

06/2009 – 10/2009 **Research Assistant**
Institute for Molecular Oncology, Dr. Ian Spendlove, Nottingham, UK

01/2009 – 05/2009 **Volunteer, English teacher**
Orphanage in Nongkhai, Thailand

8.2 Publications

Spies J., Waizenegger A., Barton O., Sürder M., Wright W. D., Heyer W.-D., Löbrich M. (2016). Nek1 Regulates Rad54 to Orchestrate Homologous Recombination and Replication Fork Stability. Molecular Cell 62, 1-15; June 16, 2016
http://dx.doi.org/10.1016/j.molcel.201604.032

Manuscript:

Waizenegger A., Spies J., Löbrich M. (2016). Involvement of ATRX in Homologous Recombination Repair.

8.2.1 Poster presentations

18th Annual Conference, Gesellschaft für Biologische Strahlenforschung, Dresden, Germany, 09/2015, poster presentation

13th Biennial Conference of the DGDR (German Society for Research on DNA Repair), Mainz, Germany, 09/2014, poster presentation

8.2.2 Awards

18th Annual Conference, Gesellschaft für Biologische Strahlenforschung, Dresden, Germany, 09/2015, poster presentation (Travel Award)

8.3 Acknowledgement

Mein Dank gilt Herrn Prof. Dr. Markus Löbrich für die Möglichkeit meine Dissertation in seiner Arbeitsgruppe anfertigen zu dürfen und für die Betreuung während dieser Zeit.

Mein besonderer Dank geht an Herrn Prof. Dr. Paul Layer und Frau Prof. Dr. Cristina Cardoso für die spontane, bereitwillige Übernahme des Erst-, und Zweitgutachtens.

Ein großes Dankeschön geht an die gesamte AG Löbrich mit allen ehemaligen und momentanen Mitgliedern. Ich habe mich dank euch in Darmstadt gleich sehr wohl gefühlt und die vielen Gespräche im Seminarraum und auch außerhalb der Arbeit sehr genossen. Wissenschaftlich möchte ich mich vor allem bei Julian Spies und Olivia Barton bedanken, von denen ich sehr viele Methoden gelernt habe. Vielen Dank auch fürs Korrekturlesen meiner Arbeit, ganz besonders mein Betreuer Julian hat viel Zeit investiert, aber auch Szilivi, Johanna, Michi und Ratna waren daran beteiligt. Vielen vielen Dank euch allen!!!

Bedanken möchte ich mich vor allem auch bei all meinen meiner Familie und meinen Freunden, die mich die letzten Jahre über unterstützt haben und mich immer wieder ermutigt und aufgebaut haben. Ohne euch hätte ich diese Arbeit wahrscheinlich nicht zu Ende gebracht, und die letzten Wochen/ Monate waren bestimmt auch für euch nicht einfach ☺